AD-A269 752

Technical Report ITL-92-12
August 1993

US Army Corps
of Engineers
Waterways Experiment
Station

Computer-Aided Structural Engineering (CASE) Project

Computer-Aided, Field-Verified Structural Evaluation

Report 4
Field Test and Analysis Correlation at Red River Lock and Dam No. 1

by *Brett C. Commander, Jeff X. Schulz, George G. Goble, Eric Hanson*
Bridge Diagnostics, Inc.

Cameron P. Chasten
Information Technology Laboratory

DTIC
S ELECTE D
SEP 24 1993
E

WES

Approved For Public Release; Distribution Is Unlimited

93-22183

93 9 22 001

Prepared for Headquarters, U.S. Army Corps of Engineers

The contents of this report are not to be used for advertising, publication, or promotional purposes. Citation of trade names does not constitute an official endorsement or approval of the use of such commercial products.

PRINTED ON RECYCLED PAPER

Computer-Aided Structural Engineering (CASE) Project

Technical Report ITL-92-12
August 1993

Computer-Aided, Field-Verified Structural Evaluation

Report 4
Field Test and Analysis Correlation at Red River Lock and Dam No. 1

by Brett C. Commander, Jeff X. Schulz, George G. Goble, Eric Hanson

Bridge Diagnostics, Inc.
5398 Manhattan Circle, Suite 280
Boulder, CO 80303

Cameron P. Chasten
Information Technology Laboratory

U.S. Army Corps of Engineers
Waterways Experiment Station
3909 Halls Ferry Road
Vicksburg, MS 39180-6199

Accesion For	
NTIS CRA&I	☒
DTIC TAB	☐
Unannounced	☐
Justification	
By	
Distribution /	
Availability Codes	
Dist	Avail and / or Special
A-1	

Report 4 of a series

Approved for public release; distribution is unlimited

DTIC QUALITY INSPECTED 1

Prepared for U.S. Army Corps of Engineers
Washington, DC 20314-1000

Under Contract No. DACW39-91-C-0102

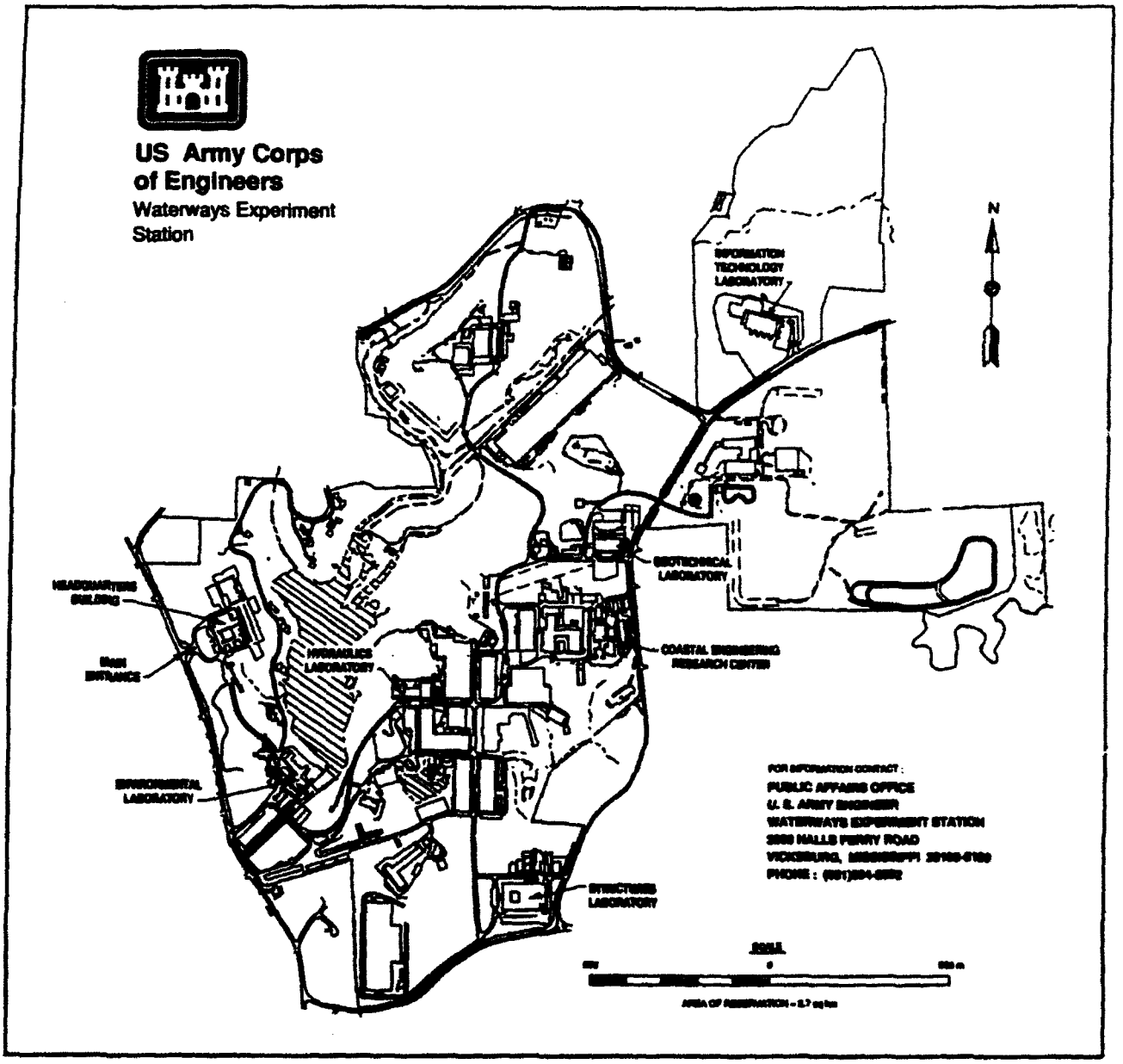

Waterways Experiment Station Cataloging-In-Publication Data

Computer-aided, field-verified structural evaluation. Report 4, Field test and analysis correlation at Red River Lock and Dam No. 1 / by Brett C. Commander ... [et al.] ; prepared for Department of the Army, US Army Corps of Engineers.

62 p. : ill. ; 28 cm. — (Technical report ; ITL-92-12 rept. 4)

Includes bibliographical references.

1. Hydraulic gates — Computer simulation. 2. Locks (Hydraulic engineering) — Evaluation — Data processing. 3. Structural analysis (Engineering) — Data processing. 4. Locks (Hydraulic engineering) — Red River (Tex.-La) I. Commander, Brett C. II. United States. Army. Corps of Engineers. III. U.S. Army Engineer Waterways Experiment Station. IV. Computer-aided Structural Engineering Project. V. Title: Field test and analysis correlation at Red River Lock and Dam No. 1. VI. Series: Technical report (U.S. Army Engineer Waterways Experiment Station) ; ITL-92-12 rept. 4.

TA7 W34 no.ITL-92-12 rept.4

Contents

Preface vii

Conversion Factors, Non-SI to SI Units of Measurement ix

1—Introduction 1

2—Field Test 3

Structural Description 3
Test Procedures 3
Head differential tests 7
Gate operation tests 8
Field Test Conclusions 8

3—Structural Analysis and Data Comparison 10

Model Description 10
Data Comparison 12
Analysis Results 13
Original model 14
Modified model 17
Discussion of results 19

4—Conclusions 21

References 22

Appendix A: Head Differential Test Data A1

Appendix B: Gate Operation Opening Test Data B1

Field Data B1
Pintle Torque Comparison with Model Studies B1

Appendix C: Gate Operation Closing Test Data C1

Field Data C1
Pintle Torque Comparison with Model Studies C1

SF 298

List of Figures

Figure 1. Downstream elevation: landside leaf of the lower gate of Red River Lock No. 1 4

Figure 2. Plan view of a typical horizontal girder 5

Figure 3. Downstream elevation of gate leaf with transducer locations. 6

Figure 4. Girder cross sections with transducer placement. 7

Figure 5. Computer-generated display of gate leaf. 11

Figure 6. Calculated (original model) and measured strain comparisons for G3 15

Figure 7. Calculated (original model) and measured strain comparisons for G4 15

Figure 8. Calculated (original model) and measured strain comparisons for G5 16

Figure 9. Calculated (modified model) and measured strain comparisons for G3 17

Figure 10. Calculated (modified model) and measured strain comparisons for G4 18

Figure 11. Calculated (modified model) and measured strain comparisons for G5 18

Figure A1. Head differential test strain: G1 midspan A1

Figure A2. Head differential test strain: G2 midspan A2

Figure A3. Head differential test strain: G3 quoin end A2

Figure A4. Head differential test strain: G3 midspan A3

Figure A5. Head differential test strain: G3 miter end A3

Figure A6. Head differential test strain: G4 quoin end A4

Figure A7. Head differential test strain: G4 midspan A4

Figure A8. Head differential test strain: G4 miter end A5

Figure A9. Head differential test strain: G5 quoin end A5

Figure A10. Head differential test strain: G5 midspan A6

Figure A11. Head differential test strain: G5 miter end A6

Figure A12. Head differential test strain: diaphragm 3 . . . . . A7

Figure A13. Head differential test strain: diaphragm 2 . . . . . A7

Figure A14. Head differential test strain: diaphragm 1 . . . . . A8

Figure A15. Head differential test strain: diagonal 2 . . . . . A8
Figure A16. Head differential test strain: diagonal 1 . . . . . A9
Figure B1. Gate operation opening test strain: G1 midspan B2
Figure B2. Gate operation opening test strain: operating strut B3
Figure B3. Gate operation opening test strain: G3 quoin end B4
Figure B4. Gate operation opening test strain: G3 midspan B5
Figure B5. Gate operation opening test strain: G3 miter end B6
Figure B6. Gate operation opening test strain: G4 quoin end B7
Figure B7. Gate operation opening test strain: G4 midspan B8
Figure B8. Gate operation opening test strain: G4 miter end B9
Figure B9. Gate operation opening test strain: G5 quoin end B10
Figure B10. Gate operation opening test strain: G5 midspan B11
Figure B11. Gate operation opening test strain: G5 miter end B12
Figure B12. Gate operation opening test strain: diaphragm 3 . . . . . B13
Figure B13. Gate operation opening test strain: diaphragm 2 . . . . . B14
Figure B14. Gate operation opening test strain: diaphragm 1 . . . . . B15
Figure B15. Gate operation opening test strain: diagonal 2 . . . . . B16
Figure B16. Gate operation opening test strain: diagonal 1 . . . . . B17
Figure B17. Modified Ohio River linkage geometry B18
Figure B18. Gate operation opening test: operating strut force B19
Figure B19. Gate operation opening test: pintle torque B20
Figure C1. Gate operation closing test strain: G1 midspan C2
Figure C2. Gate operation closing test strain: operating strut C3
Figure C3. Gate operation closing test strain: G3 quoin end C4
Figure C4. Gate operation closing test strain: G3 midspan C5
Figure C5. Gate operation closing test strain: G3 miter end C6
Figure C6. Gate operation closing test strain: G4 quoin end C7
Figure C7. Gate operation closing test strain: G4 midspan C8
Figure C8. Gate operation closing test strain: G4 miter end C9
Figure C9. Gate operation closing test strain: G5 quoin end C10
Figure C10. Gate operation closing test strain: G5 midspan C11
Figure C11. Gate operation closing test strain: G5 miter end C12
Figure C12. Gate operation closing test strain: diaphragm 3 . . . . . C13

Figure C13. Gate operation closing test strain: diaphragm 2 . . . . . C14
Figure C14. Gate operation closing test strain: diaphragm 1 . . . . . C15
Figure C15. Gate operation closing test strain: diagonal 2 . . . . . C16
Figure C16. Gate operation closing test strain: diagonal 1 . . . . . C17
Figure C17. Gate operation closing test: operating strut force C18
Figure C18. Gate operation closing test: pintle torque C19

Preface

This report is the fourth and final report of a series that describes the research conducted as part of a Computer-Aided Structural Engineering (CASE) Project effort entitled "Computer-Aided, Field-Verified Structural Evaluation." The primary goal of this project is to develop a simple system that can be used to evaluate the structural integrity of miter gates through a combination of experimental and analytical techniques. A major task of this project is to perform field testing and mathematical analysis for miter lock gates. The objectives of this task are to obtain measured data that describe the behavior of miter lock gates in service, develop and subsequently verify analytical modeling procedures, and evaluate the field testing system. Each report of the Computer-Aided, Field-Verified Structural Evaluation project discusses these objectives in detail.

During this study, three field tests of miter lock gates were conducted to obtain experimental data. Miter gates at the John Hollis Bankhead Lock and Dam, Black Warrior River; the Emsworth Lock and Dam, Ohio River; and the Red River Lock and Dam No. 1 were tested under normal operating conditions. This report describes the field testing and analytical work conducted for a horizontally framed miter gate at Red River Lock and Dam No. 1. In Report 1, general modeling procedures for analyzing horizontally and vertically framed miter lock gates were described. The development and verification of the proposed models were based on limited experimental data from two case studies. Report 2 described experimental and analytical studies conducted for a horizontally framed miter gate at John Hollis Bankhead Lock and Dam. Four modeling approaches, each involving various geometric simulations, were described in Reports 1 and 2. These included three finite element grid models of various geometry and complexity, and a three-dimensional finite element model. Based on overall accuracy and simplicity of model development, a grid model that simulates out-of-plane geometry with eccentric frame elements is recommended for modeling of both horizontally and vertically framed miter gates. Report 3 described experimental and analytical work performed for a vertically framed miter gate at the Emsworth Lock and Dam. Although the primary goal of this work was to further verify the proposed analytical modeling procedures, this case provided an excellent example of structural evaluation. Based on an onsite review of experimental measurements, it was determined that one of the diagonal members was slack. After the testing, the structure was analyzed with the simple grid model (hybrid grid model) and the

structural effect of the loose diagonal was assessed by examining experimental and analytical data.

The CASE Project is managed by the Scientific and Engineering Applications Center (S&EAC) of the Computer-Aided Engineering Division (CAED), Information Technology Laboratory (ITL), U.S. Army Engineer Waterways Experiment Station (WES), Vicksburg, MS. The CASE Project is funded by the Civil Works Directorate of Headquarters, U.S. Army Corps of Engineers. Mr. Cameron P. Chasten, ITL, was Project Manager under the general supervision of Mr. H. Wayne Jones, Chief, S&EAC, Dr. Reed L. Mosher, Chief, CAED, and Dr. N. Radhakrishnan, Director, ITL.

The work was performed by Bridge Diagnostics, Incorporated (BDI), under Contract No. DACW39-91-C-0102. The report was prepared by Mr. Brett C. Commander, Mr. Jeff X. Schulz, Dr. George G. Goble, and Mr. Eric Hanson, BDI, and Mr. Chasten, ITL, under the general supervision of Mr. Jones, ITL. Acknowledgement is expressed to Mr. Robert Coco, Lockmaster at Red River Lock and Dam No. 1, for providing arrangements for and assisting in the field testing.

At the time of publication of this report, Director of WES was Dr. Robert W. Whalin. Commander was COL Bruce K. Howard, EN.

Conversion Factors, Non-SI to SI Units of Measurement

Non-SI units of measurement used in this report can be converted to SI units as follows:

Multiply	By	To Obtain
degrees (angle)	0.01745329	radians
feet	0.3048	meters
inches	0.0254	meters
kip-feet	1355.818	newton-meters
kips (force)	4.448222	kilonewtons
kips (force) per square inch	6894.757	kilopascals
square inches	0.0006451	square meters

1 Introduction

The primary goal of the Computer-Aided, Field-Verified Structural Evaluation Project is to develop a simple system that can be used to evaluate the structural integrity of miter gates through a combination of experimental and analytical techniques. A major task of this project is to perform field testing and mathematical analysis for miter lock gates. The objectives of this task are to obtain measured data that describe the behavior of miter lock gates in service, develop and subsequently verify analytical modeling procedures, and evaluate the field testing system. During this study, three cases of miter lock gates were considered. Miter gates at the John Hollis Bankhead Lock and Dam, Black Warrior River; the Emsworth Lock and Dam, Ohio River; and the Red River Lock and Dam No. 1 were tested under normal operating conditions and subsequently analyzed.

Prior to any field studies, general modeling procedures for analyzing horizontally and vertically framed miter lock gates were developed based on limited experimental data from two previous studies (Commander et al. 1992a). These procedures were verified and further developed using experimental data that were obtained through the first case, a field test of a horizontally framed miter gate at John Hollis Bankhead Lock and Dam (Commander et al. 1992b). Four modeling approaches, each involving various geometric simulations, included three finite element grid models of various geometry and complexity, and a three-dimensional finite element model were proposed. Based on overall accuracy and simplicity of model development, a simple grid model that simulates out-of-plane geometry with eccentric frame elements was recommended for modeling of both horizontally and vertically framed miter gates. This model incorporates a unique beam element that includes eccentricity of the member neutral axis with respect to the end nodes of the element.

Experimental and analytical work performed for the second case, a vertically framed miter gate at Emsworth Lock and Dam, is reported in Commander et al. (1992c). This case provided an excellent example of structural evaluation. Based on an onsite review of experimental measurements, it was determined that one of the diagonal members was slack. After the testing, the structure was analyzed with the recommended simple grid model, and the structural effect of the loose diagonal was assessed by examining experimental and analytical data.

This report describes analytical and experimental studies conducted for a horizontally framed miter gate at Red River Lock and Dam No. 1 located in Catahoula Parish, Louisiana. The main lock chamber is 84 ft wide and 685 ft long,[1] with horizontally framed miter gates located at both ends. The lock was opened in 1984, so the gates are relatively new and have not experienced any significant damage. A structurally sound gate is desirable for testing since the primary goal of the testing is to evaluate the modeling and analysis procedures. A more reliable evaluation of the procedures is possible when a minimum of unknown quantities (effects of damage or deterioration) is present. Strain measurements were recorded at 32 locations on the miter gate under normal operating conditions as described in Chapter 2. An analytical model using the recommended simple grid approach was developed, a linear elastic analysis performed, and the results compared with those obtained in the field. Chapter 3 describes the modeling procedures and analysis, and a detailed examination of the correlation between the field and analytical data is presented. Chapter 4 provides general conclusions of this Red River Lock and Dam No. 1 case. Appendixes A through C present strain history graphs of the experimental data.

[1] A table of factors for converting non-SI units of measurement to SI units is presented on page ix.

2 Field Test

Instrumentation and field testing of the landside leaf of the downstream horizontally framed miter gate at Red River Lock and Dam No. 1 were performed on August 17, 1992. Due to the geometric symmetry of a miter gate structure, only one gate leaf was tested. This assumed symmetry has been verified by previous field tests (Chasten and Ruf 1992), and the sound condition of the gates did not cause reason to suspect otherwise.

Structural Description

Each leaf of the downstream gate is approximately 65 ft in height and spans 48 ft, 8 in. between the miter and quoin contact points. Each leaf contains one pair of diagonal members located on the downstream face, fourteen horizontal girders, and four vertical diaphragms. Vertical intercostals spanning between the girders stiffen the skin plate. The gate is designed for a lift (pool differential) of approximately 36 ft. Figure 1 shows the downstream elevation of the landside leaf, and Figure 2 shows a plan view describing the geometry of the girders.

Test Procedures

Similar to previous tests (Commander et al. 1992b, 1992c), the landside leaf was monitored under two loading conditions:

a. Hydrostatic head differential load. With the gate in the mitered position, head differential loads were applied by raising the lock chamber water elevation from the lower pool elevation to the upper pool elevation.

b. Gate operating load. With the lock chamber water elevation at the lower pool elevation (zero head differential), the landside leaf was swung open and closed. Loads applied to the leaf were the force of the operating strut and the inertial resistance of water on the submerged portion of the leaf.

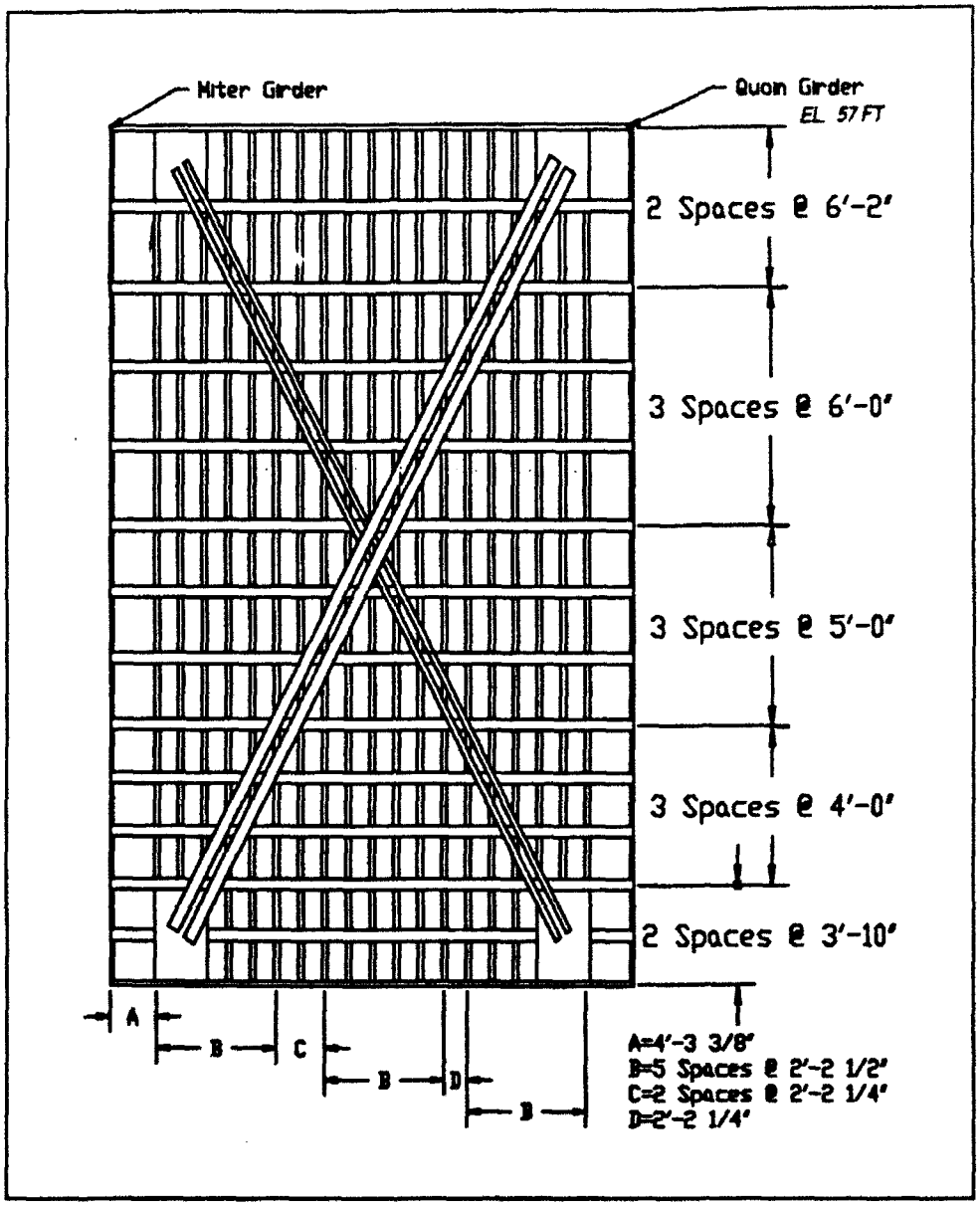

Figure 1. Downstream elevation: landside leaf of the lower gate of Red River Lock No. 1

Two tests were conducted for each loading condition.

Instrumentation consisted of steel strain transducers, a position indicator, and a 32-channel data acquisition system (DAS). (A more complete description of the testing system is in Commander et al. (1992b, 1992c).) Prior to testing, 32 strain transducers were mounted (bolted or clamped) at various locations on girders, diaphragms, and diagonal members. Since longitudinal stresses were of primary interest, the transducers were oriented in the longitudinal direction of the structural components. For girder and diaphragm members, transducers were placed on both the upstream and downstream flanges at

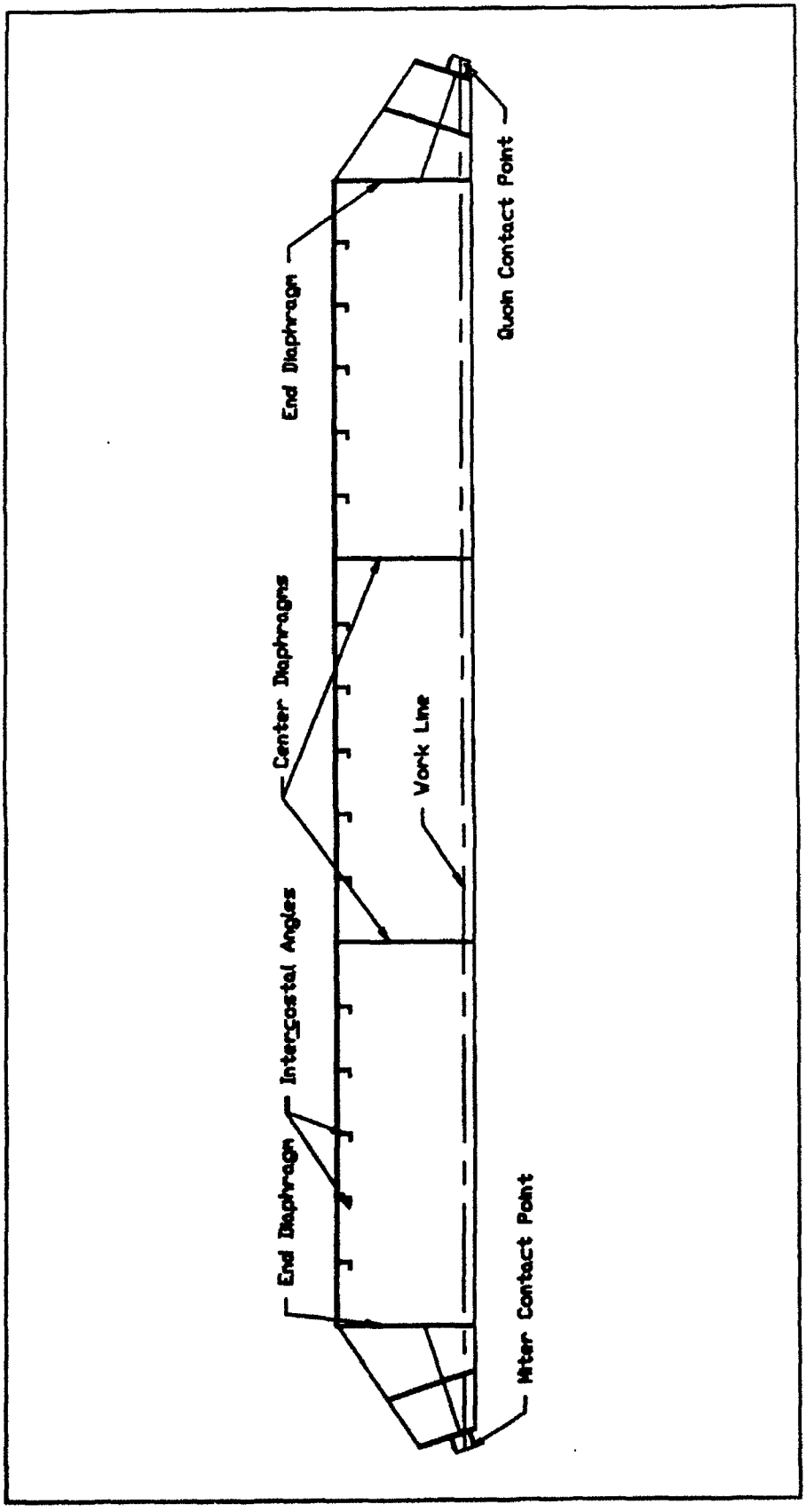

Figure 2. Plan view of a typical horizontal girder

common cross sections in order to obtain data for both axial and flexural behavior. Figure 3 shows the location of the transducers and identifies girder and diaphragm numbering. Each circled location includes two transducers numbered by corresponding DAS channel number. At each girder or diaphragm location, the upper number refers to a transducer located on the upstream flange, and the lower number refers to a transducer located on the downstream flange. The transducers for the girders were located on the flanges as shown by Figure 4.

The location of transducers was identical for both load conditions with the exception that the transducers for DAS channels 3 and 4 were located on girder G2 for the head differential tests, and on the operating strut for the gate operation tests. For each test, strains were digitally recorded at a rate of 32 Hz from each of the 32 transducers. Instrumentation and testing of the structure required approximately 8 hr with a three-man crew.

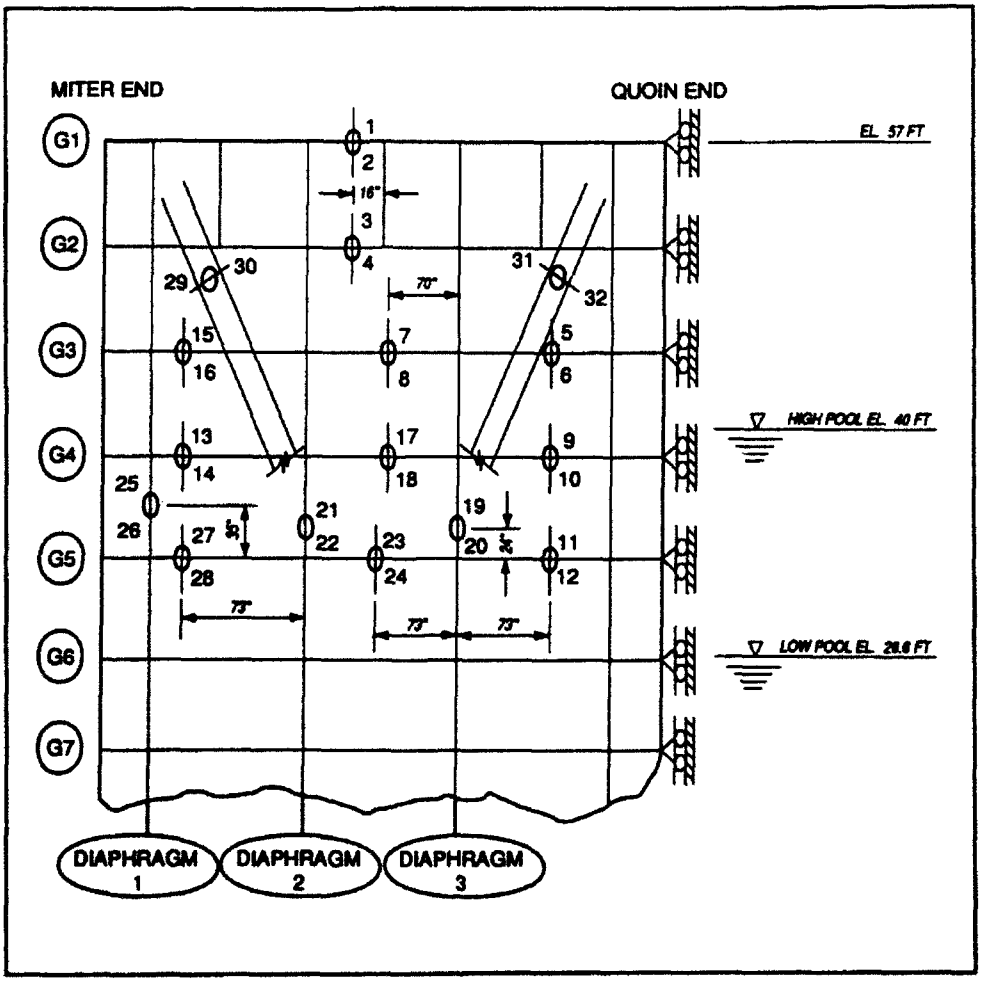

Figure 3. Downstream elevation of gate leaf with transducer locations

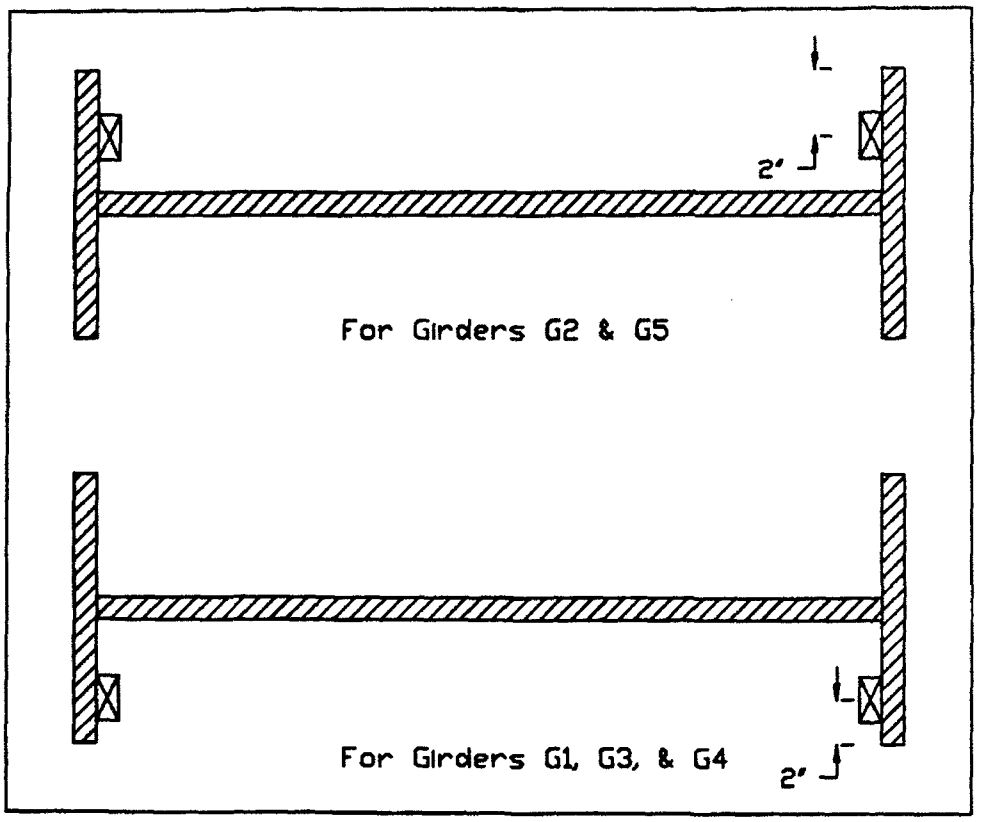

Figure 4. Girder cross sections with transducer placement

Head differential tests

The two head differential tests consisted of monitoring strain (measured by the 32 transducers) as the water level in the lock chamber was raised from lower pool elevation to upper pool elevation. The maximum pool differential (lift) at Red River Lock and Dam No. 1 is approximately 36 ft; however, on August 17, 1992, the lift was 13.4 ft with the lower pool elevation at 26.6 ft and the upper pool elevation at 40 ft. For both tests, the datum for strain measurement was established by setting all of the strain readings to zero (balancing) while the gate was mitered and the chamber pool level was at the lower pool elevation (zero head differential). Strains were monitored and recorded continuously as the lock chamber was filled. The chamber pool elevation was monitored using the lock wall elevation markers, and the position indicator was activated (a signal was recorded by the DAS along with the strain data) at 1-ft intervals of increasing chamber pool level. This allowed for the strain data to be identified as a function of head differential. Data from the second head differential test are shown in Appendix A (results of the first test were very similar). These data were used for comparison with analytical data.

Gate operation tests (opening - closing)

After the head differential tests, strain transducers numbered 3 and 4 were moved from girder G2 to the operating strut. Two gate operation tests were conducted: (1) moving the leaf from miter position to recess position (opening), and (2) moving the leaf from recess position to miter position (closing). For each gate operation test, the riverside leaf was held stationary in the miter position. Strains were monitored continuously as the landside leaf was swung open or closed under zero head differential. For the gate opening test, the datum for strain readings was established by balancing the transducers while the gate was in the miter position with zero head differential on the leaf. Recording of data began just prior to gate operation and continued until the gate leaf was in the open (recess) position. The gate closing test was performed in the same manner, except that it started with the gate leaf in the recess position and ended in the closed (mitered) position. The leaf position was monitored as a function of its angle with respect to the lock wall. The gate angle was recorded by activating the position indicator at 10-deg increments. Data for the gate opening and closing tests are included in Appendixes B and C, respectively. Also included in Appendixes B and C are comparisons of measured response to scale model studies of operating forces on miter gates (U.S. Army Engineer Waterways Experiment Station 1964).

Field Test Conclusions

Appendix A shows plots of measured strain as a function of head differential for all transducer locations. The low head differential condition and location of many of the transducers resulted in very low magnitude strains. (The maximum head differential was 13.4 ft compared with the 36-ft design level, and ten transducers were located on girders G1, G2, and G3, which were above the upper pool elevation as shown by Figure 3.) The maximum measured strain on the structure was approximately 120 micro-strains ($\mu\varepsilon$) (3.6 ksi), and for many of the locations, the maximum strain was between 20 and 40 $\mu\varepsilon$ (0.6 to 0.8 ksi). With such low levels of recorded strain, only a small fraction of the structure's capacity was monitored. Additionally, even a small error in measurement (due to electrical noise for example) can have a large effect on the measured strain. Future head differential tests should be conducted at a time when the environmental conditions will yield close to the maximum design head differential. This will enable the structure to be evaluated at conditions close to its capacity.

Transducers were placed near the zero moment region (inflection point) on the girders. In the future, strain transducers should not be located in this region since the moment induced by the eccentricity of the axial load is equal and opposite to the flexural load induced by the uniform water pressure load on the skin plate. Any small error in the transducer location on the member could result in calculated strains that would indicate curvature opposite in sign

from the actual curvature. Even though the flexural curvature near the inflection point is very small, a small difference in transducer placement can cause a complete sign reversal in the compared flexural response. Difference in strain of opposite sign will not have a large effect on the absolute or percentage error calculations; however, the correlation factor can be significantly altered since it is based strictly on the shape of the strain response as a function of head differential (see Chapter 3, pg 12, for a description of error calculations).

3 Structural Analysis and Data Comparison

General modeling procedures for miter gates have been developed in previous phases of this project (Commander et al. 1992a, 1992b). A grid model incorporating plate-membrane elements (to represent skin plates) and eccentric frame elements (to represent girders, diaphragms, and diagonal members) has been recommended for modeling of vertically and horizontally framed miter gates (Commander et al. 1992b). This model was implemented in the Emsworth Lock and Dam study (Commander et al. 1992c) and is used in this study to model the Red River Lock No. 1 miter gate leaf. The advantage of this grid model is that a relatively detailed geometric representation of the gate can be defined with a minimum number of nodes and degrees of freedom (dof). This simplifies the effort required for model generation and minimizes the computer run time. Structural analysis is performed using the simple finite element program Structural Analysis and Correlation (SAC) which has been customized for miter gate modeling and analysis.

The plate-membrane elements in SAC include five degrees of freedom per node; resistance to membrane forces along two in-plane axes, an out-of-plane force normal to the plate, and two bending moments about the two in-plane axes are accounted for. Eccentric frame elements are space frame elements for which the flexural neutral axis (NA) (centroidal axis) is eccentric to the end nodal points (Commander et al. 1992b). Use of these elements greatly simplifies the model generation procedure for two-dimensional analysis of miter gates. For example, common nodes can be utilized by skin plate elements and girder elements where the girder NA is eccentric to the skin plate.

Model Description

The gate leaf is modeled as a grid of eccentric frame elements and rectangular plate-membrane elements in a three-dimensional Cartesian coordinate system. The y-axis is aligned vertically along the miter contact surface, and the x-axis is parallel to the plane of the leaf and is located at the elevation of the bottom girder web. The z-axis is perpendicular to the plane of the leaf. The reference plane, at which Z equals zero, is defined as a vertical plane

containing the top girder work line. The work line for miter gates is an imaginary line that connects the quoin and miter contact points of the girders (U.S. Army Corps of Engineers 1984).

The grid model is defined in three general segments as shown by Figure 5. The center segment represents the portion of the leaf between end diaphragms, and the outer segments represent the portions between the end diaphragms and the miter and quoin contacts. Nodal points locating the miter and quoin contact points of each girder, the pintle support, and the boundaries of the skin plate are defined according to the actual geometry of the leaf. The nodes of the model for the center segment have z-coordinates equal to the actual distance between the work line (Z = 0) and the skin plate, and x- and y-coordinates correspond to the intersection of the vertical members (intercostals and diaphragms) and the horizontal girders.

The skin plate is represented by plate-membrane elements having the properties of Young's modulus, thickness, and Poisson's ratio. The girders, diaphragms, diagonals, and intercostals are all represented by eccentric frame elements. These elements are assigned an eccentricity in the z-direction equal to the distance between the center of the skin plate thickness (location of the

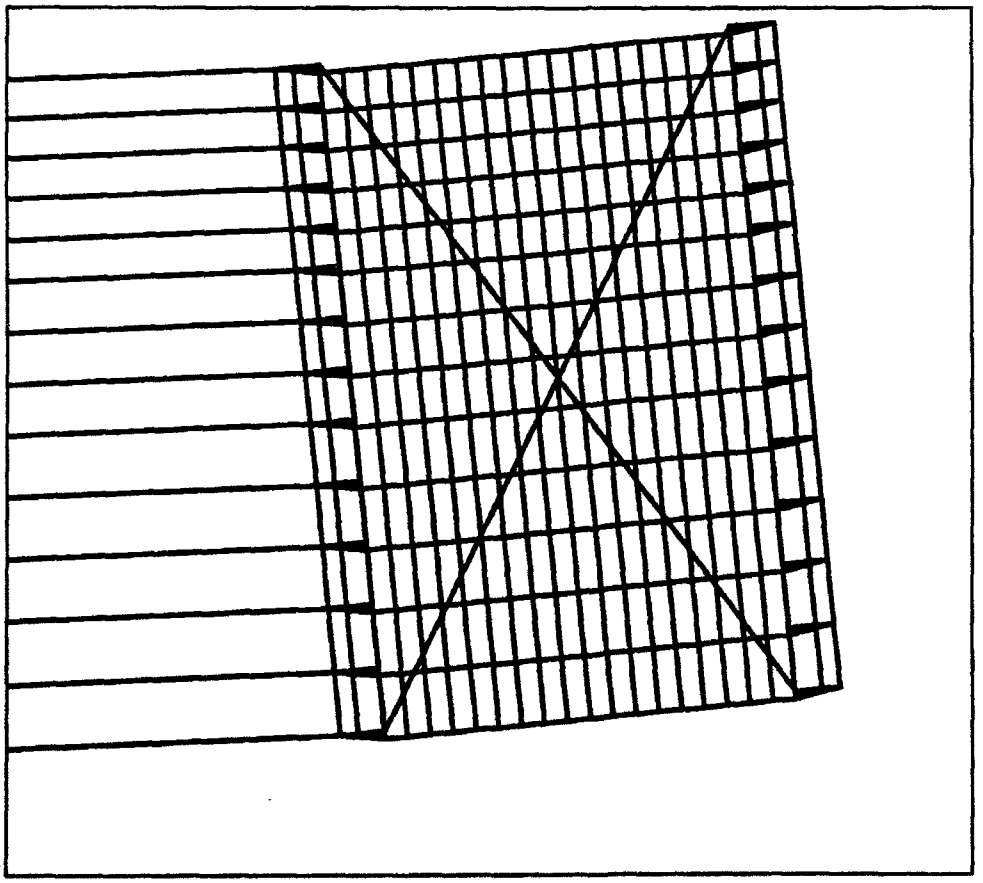

Figure 5. Computer-generated display of gate leaf

nodes) and the principal NA of the represented member. The section properties of each element correspond to the actual properties of the represented members and are calculated with respect to the flexural NA. The eccentricity of the frame elements are not displayed in Figure 5, but the general layout of the nodal coordinates and element connectivity is shown.

Boundary conditions (BC) for the leaf are defined by truss elements at the miter end of the leaf and restrained nodal dof at the quoin end. Nodal dof for the displacement in the x-, y-, and z-directions are restrained for the node representing the pintle support. Nodal dof for displacement in the x- and z-directions are restrained for the nodes representing the quoin contact points. Nodes representing the miter contact points are connected to horizontal truss elements (lines extending from the left side of the model in Figure 5) inclined at the appropriate angle of the opposing leaf.

Data Comparison

To verify or check the analytical model, comparison of analytical and experimental data is required. In this study, comparisons are performed only for the head differential tests since the hydrostatic loads are well defined and easily modeled; for the gate operation tests, an accurate load model of the leaf moving through the water is not well defined. For the head differential tests, measured data consist of strain at each transducer location as a function of head differential. Therefore, comparisons of measured and calculated strain as a function of head differential are used to evaluate the analytical model. In SAC, strain can be calculated directly at any specified location.

Although strain is the only physical comparison quantity, several means of comparing measured and computed strain are utilized. Data are compared using a graphical approach and various numerical comparison quantities. Graphical comparisons provide an excellent intuitive perspective. Analytical and experimental data can be plotted as a function of head differential on the same graph, and the overall accuracy of analytical data can be evaluated. Results from locations at common cross sections can be presented on the same graph to evaluate axial and bending effects conceptually.

Numerical comparison quantities include absolute error, percent error, and correlation factor. The absolute error E_{abs} provides a means of comparing the accuracy of one model with another or evaluating the improvement of a model during parameter optimization (Commander et al. 1992a). The E_{abs} is the summation of the absolute values of the strain differences (difference in measured and calculated strain for a given location) for each location and load case considered. The percentage error E_{per} is calculated by dividing the summation of the strain differences squared by the summation of the measured strains squared. The terms are squared so that the error terms are always positive and so that the locations producing the largest strain magnitudes have the greatest effect on the error calculation. The correlation factor CF is a measure of how

strongly two variables are linearly related or how closely the shapes of the measured and analytical response curves match. The error functions can be computed for individual gauge locations as well. This allows determinations to be made as to which locations on the structure produce good agreements between the computed and measured results and which locations do not. The error quantities are calculated by the following equations.

$$E_{abs} = \sum_{i=1}^{n} |\varepsilon_{f_i} - \varepsilon_{c_i}| \tag{1}$$

$$E_{per} = \frac{\sum_{i=1}^{n} (\varepsilon_{f_i} - \varepsilon_{c_i})^2}{\sum_{i=1}^{n} \varepsilon_{f_i}^2} \times 100 \tag{2}$$

$$CF = \frac{\frac{1}{n} \sum_{i=1}^{n} (\varepsilon_{f_i} - \overline{\varepsilon_f})(\varepsilon_{c_i} - \overline{\varepsilon_c})}{\sigma_{\varepsilon f}\, \sigma_{\varepsilon c}} \tag{3}$$

where:

ε_{f_i} = Field strain measurement of a single transducer for a given head differential load.

ε_{c_i} = Computed strain corresponding to ε_{f_i}.

n = Number of transducers times the number of applied load cases (total number of different strain readings).

$\overline{\varepsilon_f}$ = Mean value of measured strains.

$\overline{\varepsilon_c}$ = Mean value of computed strains.

$\sigma_{\varepsilon f}$ = Sample standard deviation of measured strains.

$\sigma_{\varepsilon c}$ = Sample standard deviation of computed strains.

Analysis Results

Analytical simulation of the field test was challenging in several respects. Because of the low level of applied head differential, only a small part the structure's capacity was tested. Many of the recorded strains were of very low magnitude, in some cases close to the resolution of the data acquisition system (due to the low level of loading and location of transducers as explained in

Chapter 2). It is difficult to compare analytical and experimental data for a very low magnitude of strain because a very small (and acceptable) error in experimental measurement has a large effect on the measured values. Additionally, the strain data at some locations showed an unexpected bilinear response as a function of head differential.

However, analyses were performed and results were compared with the measured test data in order to evaluate the analytical model and to study the unexpected behavior. To evaluate the analytical model, the measured strain (using results of the second head differential test) and computed strain were compared graphically as a function of head differential, and by the error quantities described in the previous section. The following sections describe comparisons utilizing the original analytical model (described in the Model Description section) and a modified analytical model. The comparisons for the original model were very poor, and a modified analytical model was developed in an attempt to study the unexpected behavior. For each model, analyses were conducted for six levels of head differential in 2-ft increments (in order to obtain data as a function of changing head differential).

Original model

Figures 6-8 show analytical (for the original model) and measured strain as a function of head differential at locations on the downstream flanges of girders G3 (transducer Nos. 16 and 6), G4 (transducer Nos. 14 and 10), and G5 (transducer Nos. 28 and 12), respectively. In each of these figures, data are presented for transducers located symmetrically at equal distances from the centerline of the leaf near the miter and quoin ends. (See Figure 3 for transducer locations.) The overall comparisons between the measured and computed strain are very poor. The graphical comparisons (Figures 6-8) show significant differences in measured and computed strain for corresponding locations. Table 1 shows the error quantities E_{abs}, E_{per} = 38.9 percent, and CF = 0.79. In comparison, previous studies (Commander et al. 1992b, 1992c) resulted in E_{per} of less than 10 percent, and CF values greater than 0.95.

Since the applied loads, structural geometry, and BC are essentially symmetric about the centerline of the leaf, strain at symmetric locations on the girders should be approximately equal. The analytical data for symmetric locations near the miter and quoin ends for girders G3, G4, and G5 are nearly equal as shown by Figures 6-8. However, the measured data for the symmetric locations are significantly different. Furthermore, the analytical data for each location show a near-linear response, while the measured strain responses obtained from the miter ends of girders are highly nonlinear. The measured strain as a function of head differential for locations near the miter end of girders G4 (transducer No. 14) and G5 (transducer No. 28) is essentially bilinear with near-zero values for head differential levels up to approximately 7 ft.

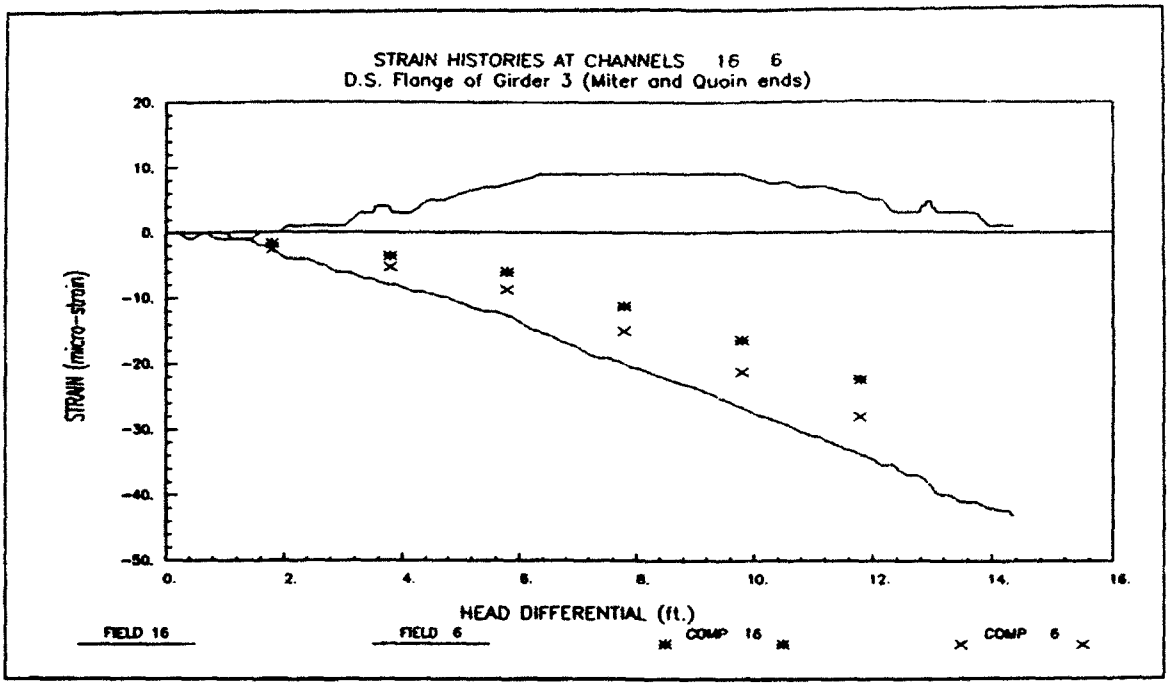

Figure 6. Calculated (original model) and measured strain comparisons for G3

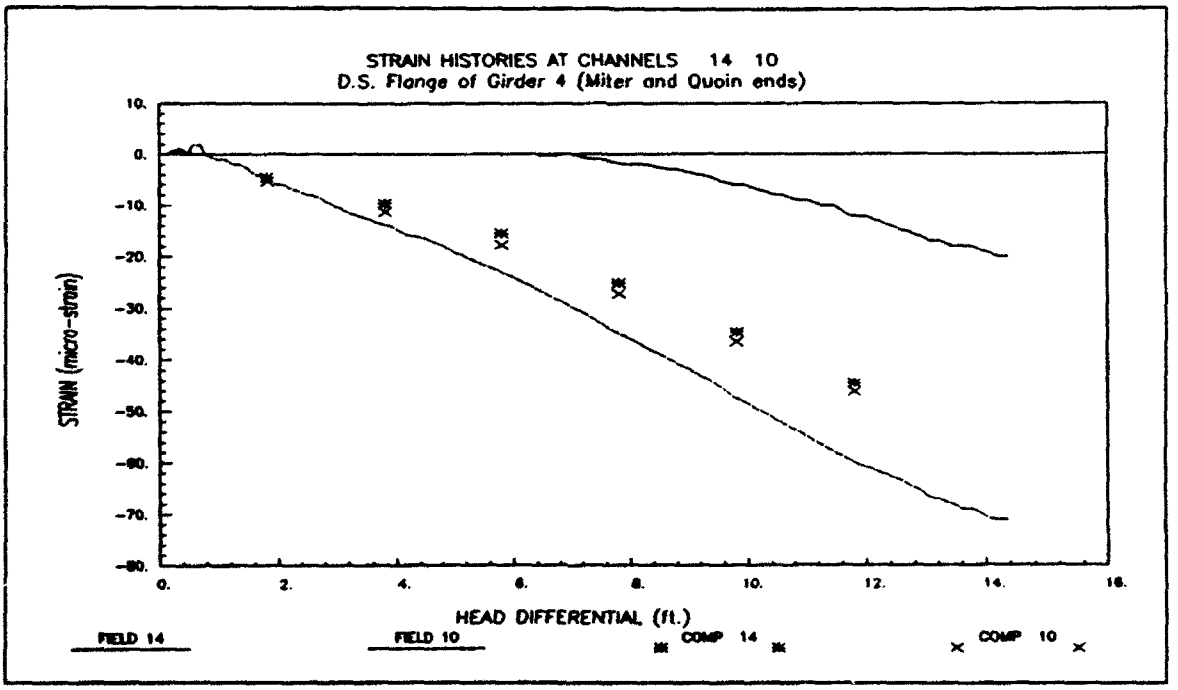

Figure 7. Calculated (original model) and measured strain comparisons for G4

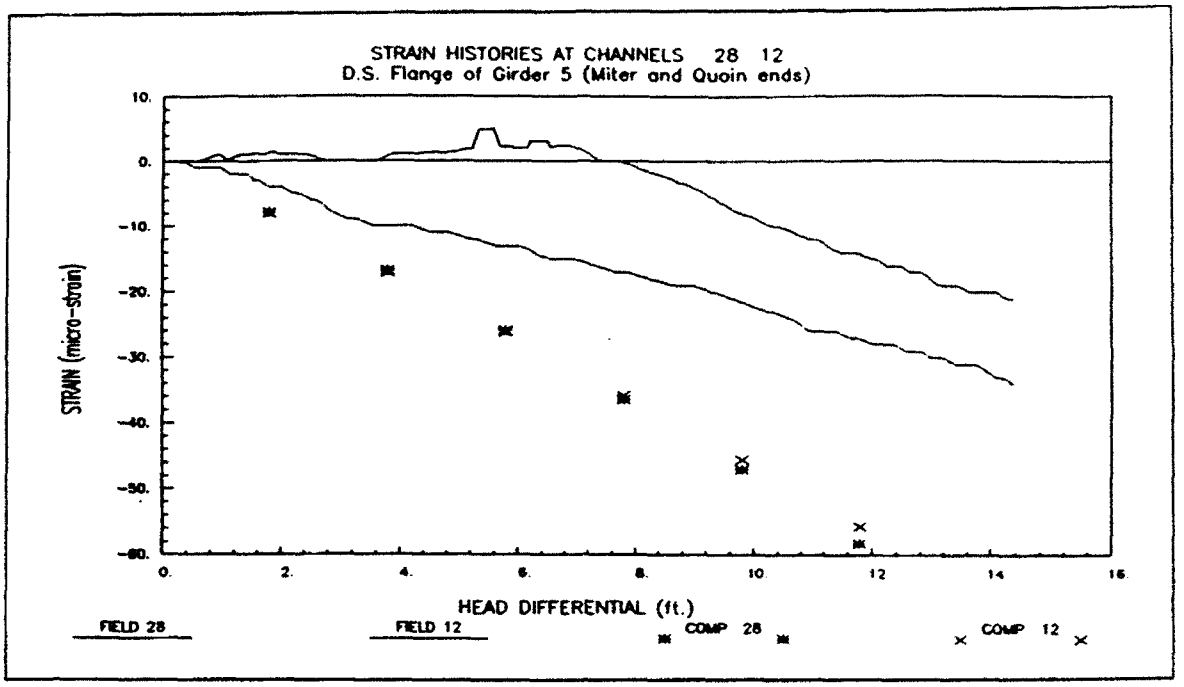

Figure 8. Calculated (original model) and measured strain comparisons for G5

Table 1
Error quantity calculations for original and modified models

Model	E_{abs} (με)[1]	E_{per}	*CF*
Original	2009	38.9 %	0.79
Modified BC	1625	21.7 %	0.89

[1] E_{abs} was computed for 32 transducers and 6 load cases. Average error per location would be equal to $E_{abs}/(32\times6)$.

Due to significant differences in measured and calculated data, and since the loading and structural geometry are well defined, it is likely that the BC of the original model do not represent those of the actual structure. The computed strain histories presented in Figures 6-8 were based on the assumption that the miter ends of all girders were in full contact with their respective counterparts. However, for head differential less than approximately 7 ft, the near-zero measured strain at the locations near the miter end indicates that the girders were not completely mitered at the initial stage of the test (with no support from the opposing gate leaf, very little load would be transferred to the miter ends of the girders). Asymmetrical BC resulting from the lack of contact at the miter end provide an explanation for the near-zero level of strain near the miter end for head differential less than 7 ft, and the differences in strain records at symmetric locations. Based on these results, the original

model was modified by changing the BC at the miter ends of girders G1 through G6.

Modified model

In an attempt to test the hypothesis that certain girders were not initially mitered, and to more closely predict the measured results, the original model was revised several times. Various combinations of the inclined support elements (that represent the support of the adjacent leaf) were eliminated from the miter contact points of girders G1 through G6. When this was done, the correlations between analytical and measured data improved significantly. Results are presented here for the modified model with inclined support elements of girders G1 through G5 eliminated.

Table 1 shows that each of the numerical comparison quantities improved. E_{abs} reduced to 0.8 times that of the original model, E_{per} is approximately half that of the original model, and *CF* improved from 0.79 to 0.89. Figures 9-11 show the computed (modified model) and measured strain histories at locations on the downstream flanges of girders G3 (transducer Nos. 16 and 6), G4 (transducer Nos. 14 and 10), and G5 (transducer Nos. 28 and 12), respectively. The analytical data for symmetric locations near the miter and quoin ends for girders G3, G4, and G5 vary significantly indicating the effect of the altered BC. Although the bilinear behavior at the miter ends of the girders is not

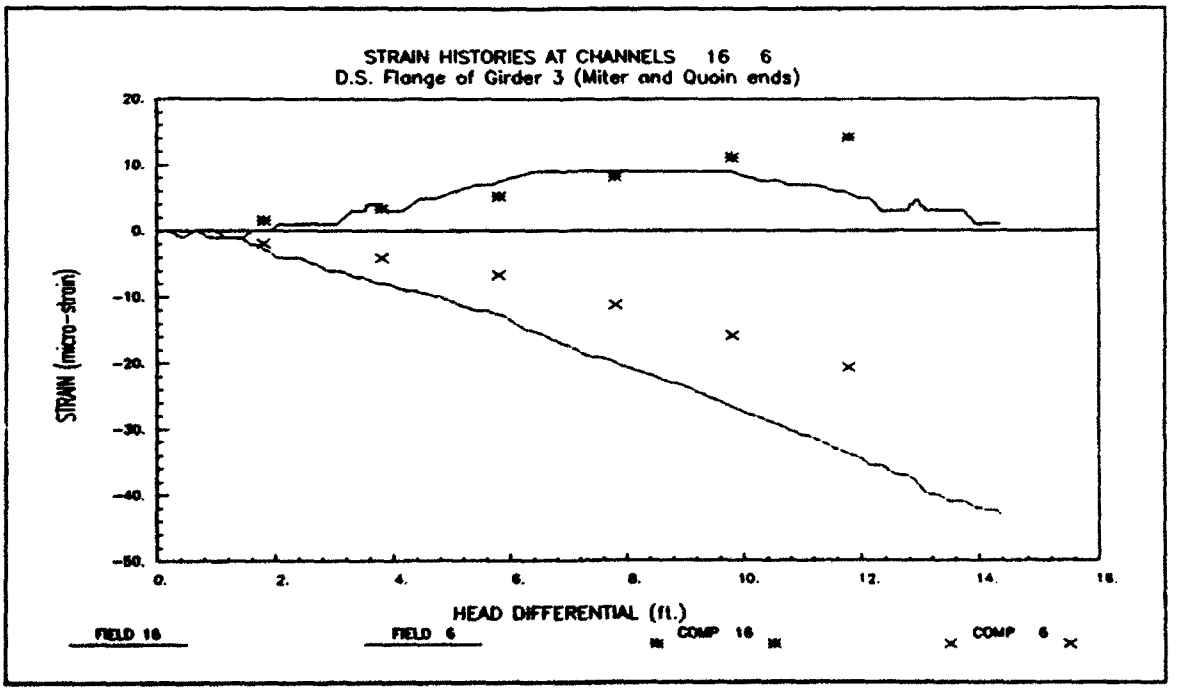

Figure 9. Calculated (modified model) and measured strain comparisons for G3

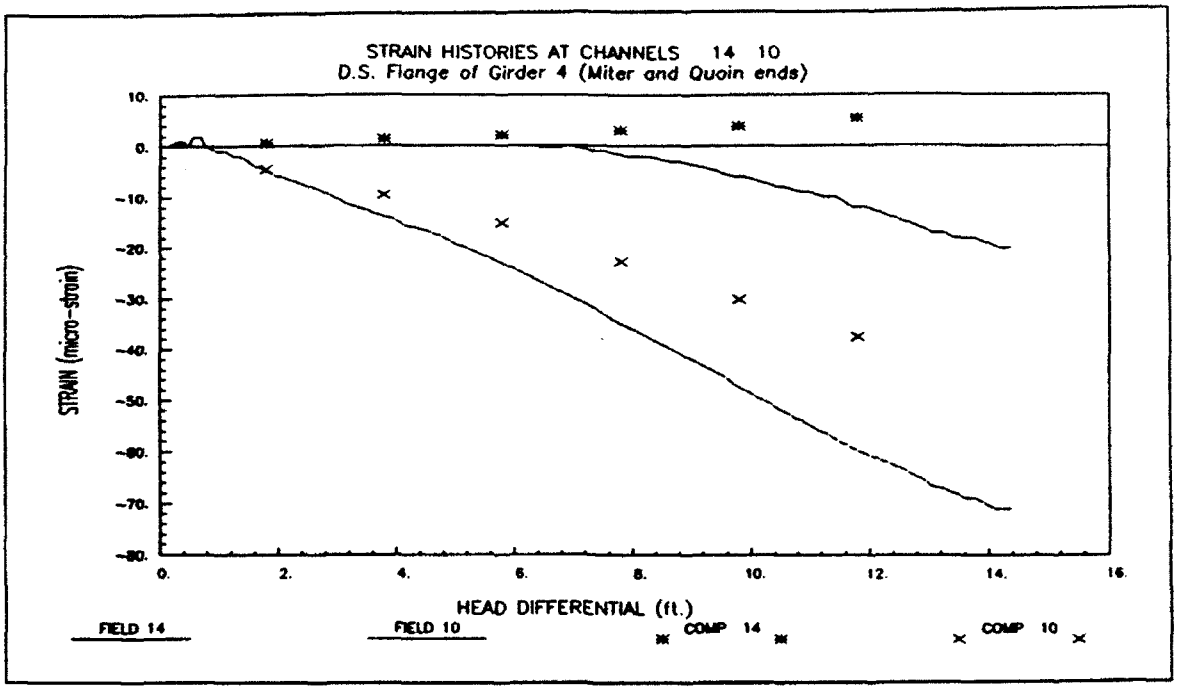

Figure 10. Calculated (modified model) and measured strain comparisons for G4

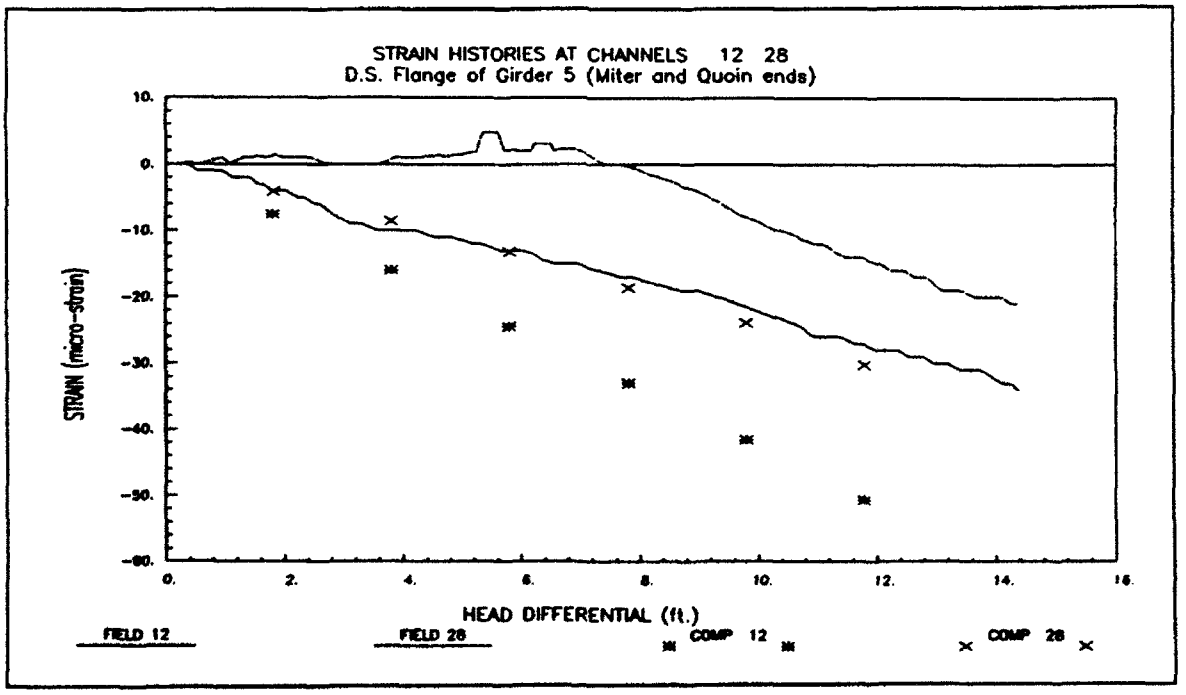

Figure 11. Calculated (modified model) and measured strain comparisons for G5

captured, the computed results for initial levels of head differential in this case show a much better comparison with the measured results, especially for girders G3 and G4.

Discussion of results

At the miter ends of the girders, the bilinear behavior indicated by the measured strain histories (see data for transducer No. 14, Figure 10, and No. 28, Figure 11) was caused by the change in BC of several girder ends as the head differential increased. The miter ends that were initially free to displace became supported by the opposing gate leaf when there was sufficient pressure to push the girder ends together. The measured strain for transducer No. 14 and No. 28 is near zero for head differential below approximately 7 ft (free miter end) and increases for head differential greater than 7 ft (supported miter end). Accurate representation of the changing BC would require a relatively complicated nonlinear analysis program, and would involve a substantial amount of computer run time. Simulating this condition would also require knowledge of when each girder becomes supported.

For this case, further analysis would be trivial since the behavior that was measured is not reason for concern. As stated earlier, the maximum level of head differential loading for this test was much less than the design load. The increase in strain for the locations near the miter end occurred at very low levels of loading, which indicates that the initial displacement from full miter contact was small, most likely within fabrication tolerances. At the low levels of loading considered, this type of behavior is likely to occur for any miter gate simply due to fabrication tolerances, and is not considered to be a concern.

The correlations between analytical and measured data were significantly better for the modified model compared with the original model. This indicates that there was some inconsistency in the originally assumed BC and that this inconsistency was in the miter end BC. It was not attempted to model the change in BC with increasing head differential, and therefore, the measured behavior was not simulated with great accuracy, even with the modified model. One way to verify the model would be to compare the results for head differential loading above that which resulted in full contact of the miter girders (at this point the miter end BC are known). This would be possible if the particular level at which the contact occurs were known, and if there would have been enough data remaining with which to make a reasonable comparison. The strain measured for transducer No. 14 (G4) and No. 28 (G5) varies with increasing head differential at a rate similar to that predicted by the original model at head differential levels above approximately 7 ft (indicating contact for G4 and G5 occurs at approximately 7 ft). However, there is not a distinct indication shown by strain data for transducer No. 16 (G3).

A similar bilinear response due to head differential loading was measured at several locations on a vertically framed miter gate at the Emsworth Lock and

Dam (Commander et al. 1992c). This was shown to be a result of changing BC as the head differential increased. The Emsworth miter gate was warped such that the lower girder was not in contact with the sill under zero head differential. As head differential was applied, the leaf deflected such that the lower girder was pushed back against the bottom sill. Therefore, the BC at the lower girder changed from no support (free) to full support of the sill (fixed) with increasing head differential. For the Emsworth study, the miter gate was loaded to near its design load and a much larger range of strain data was available for comparison purposes. The nonlinear behavior occurred at very low levels of loading, and linear results were available for a large range of head differential. Therefore, in the Emsworth case, the model could be verified by comparing results at head differential levels after which the lower girder was in full contact with the sill.

4 Conclusions

In future testing of miter gates, tests should be conducted when the pool levels are such that a significant head differential load can be applied. In this study, the low pool was higher than the level considered for design, and only the upper portion of the leaf could be instrumented. The maximum head differential at the time of testing was only 13.4 ft compared with the design condition of 36 ft. Therefore, very low magnitudes of strain were induced, and as described in Chapter 3, it was difficult to model the structural behavior under these conditions. Additionally, transducers should be placed along the length of girders at regions away from the zero moment region (see Chapter 2, pg 8).

The analysis, as performed for this study, was not capable of representing the nonlinear responses that were measured during the head differential tests due to unknown BC (as described in Chapter 3). However, the modeling procedures proved to be beneficial. It was shown that having the capability to load a structure to a significant level is an important aspect in a structural evaluation. Additionally, although the behavior of the tested leaf could not be modeled with desired accuracy, the modeling procedure was used to understand what was occurring in the field (i.e., some of the girder ends were not initially in full contact with the opposing leaf).

The overall goal of this project was to develop a system that incorporates field testing and analytic computer methods to evaluate structural performance. As for the evaluation of the Emsworth lock and dam (Commander et al. 1992c), a structural irregularity was detected in the Red River miter gate by reviewing the results of the field test. In this case, the structural irregularity was a BC at the miter end that was not consistent with design assumptions. Through examination of the measured data and comparison with computed data, the inconsistent BC was identified, and its effect on structural behavior was determined. Although the inconsistent BC does not jeopardize the performance of this structure, this case shows the value of the developed procedures in a structural evaluation.

References

Chasten, C. P., and Ruf, T. (1992). "Miter Gate Barge Impact Testing, Locks and Dam 26, Mississippi River." *Corps of Engineers Structural Engineering Conference*, published by U.S. Army Engineer Waterways Experiment Station, Vicksburg, MS.

Commander, B. C., Schulz, J. X., Goble, G. G., and Chasten, C. P. (1992a). "Computer-aided, field-verified, structural evaluation; Report 1, Development of computer modeling techniques for miter lock gates," Technical Report ITL-92-12, U.S. Army Engineer Waterways Experiment Station, Vicksburg, MS.

_____ (1992b). "Computer-aided, field-verified, structural evaluation; Report 2, Field test and analysis correlation at John Hollis Bankhead Lock and Dam," Technical Report ITL-92-12, U.S. Army Engineer Waterways Experiment Station, Vicksburg, MS.

_____ (1992c). "Computer-aided, field-verified, structural evaluation; Report 3, Field testing and analysis correlation of a vertically framed miter gate at the Emsworth Lock and Dam," Technical Report ITL-92-12, U.S. Army Engineer Waterways Experiment Station, Vicksburg, MS.

U.S. Army Corps of Engineers. (1984). "Engineering and design, lock gates and operating equipment," Engineer Manual 1110-2-2703, Washington DC.

U.S. Army Engineer Waterways Experiment Station. (1964). "Operating forces on miter-type lock gates," Technical Report No. 2-651, Vicksburg, MS.

Appendix A
Head Differential Test Data

The appendix includes figures that show graphs displaying the measured strain data as a function of head differential. In each figure, the data presented are labeled in the plot legends by the term FIELD No., where No. identifies the transducer (see Figure 3) from which the data were recorded.

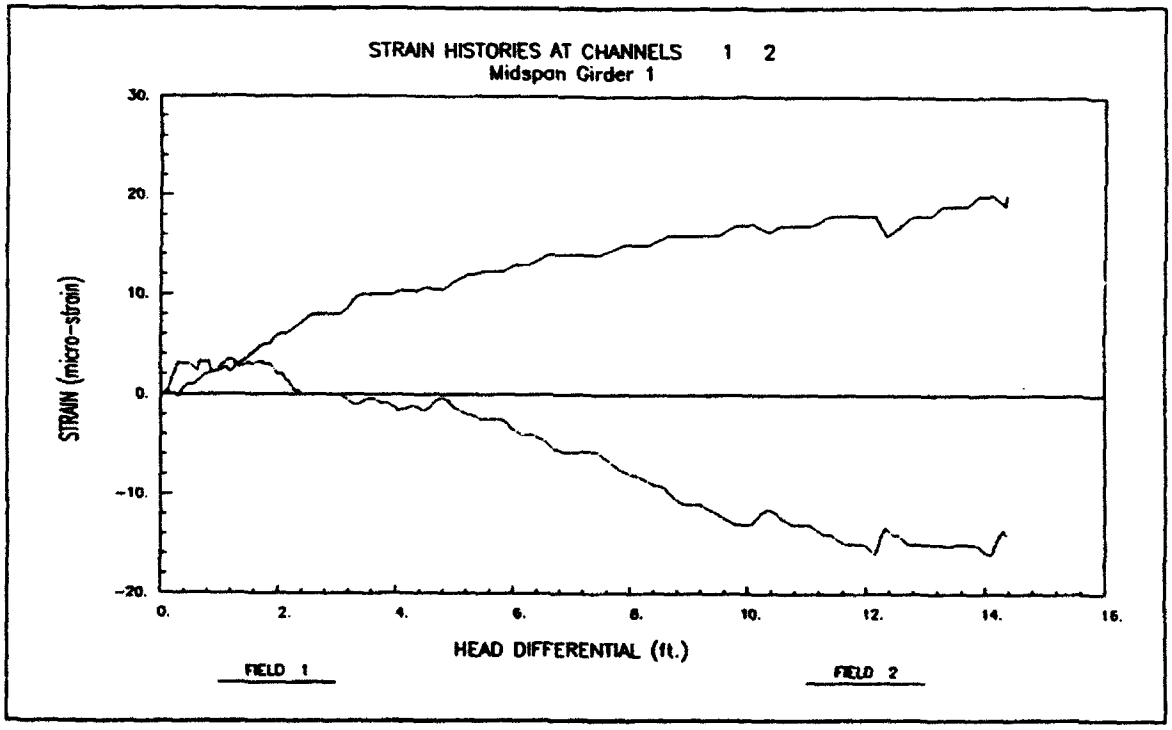

Figure A1. Head differential test strain: G1 midspan

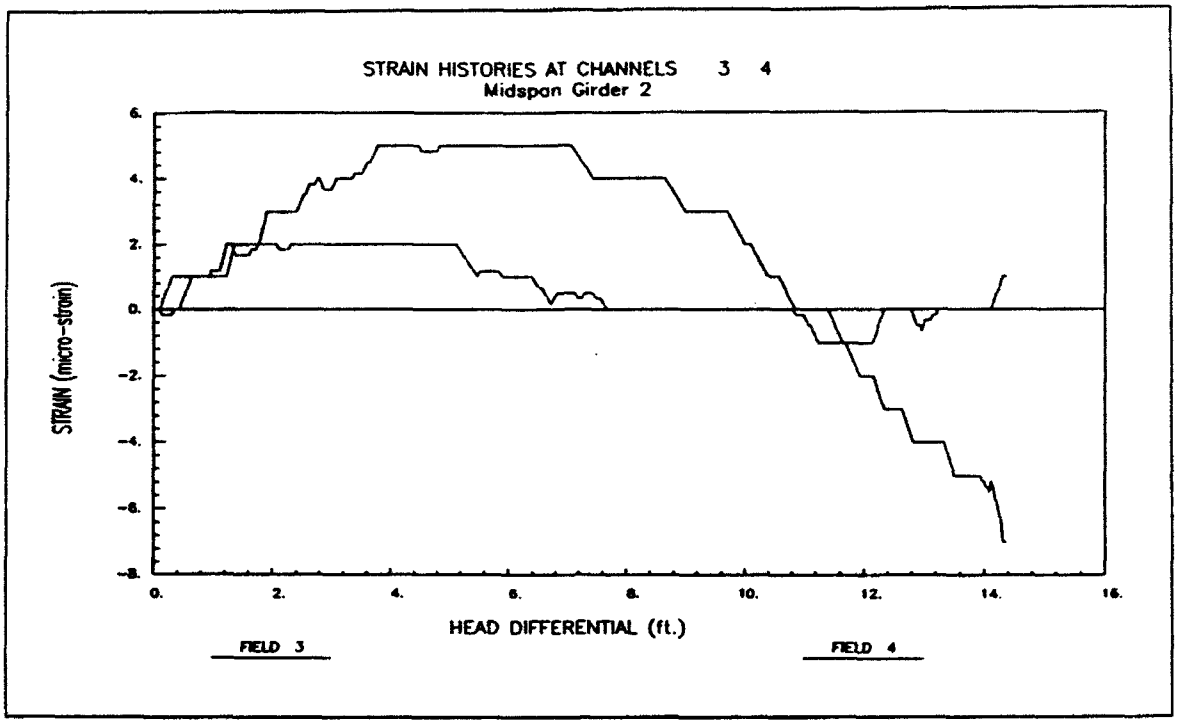

Figure A2. Head differential test strain: G2 midspan

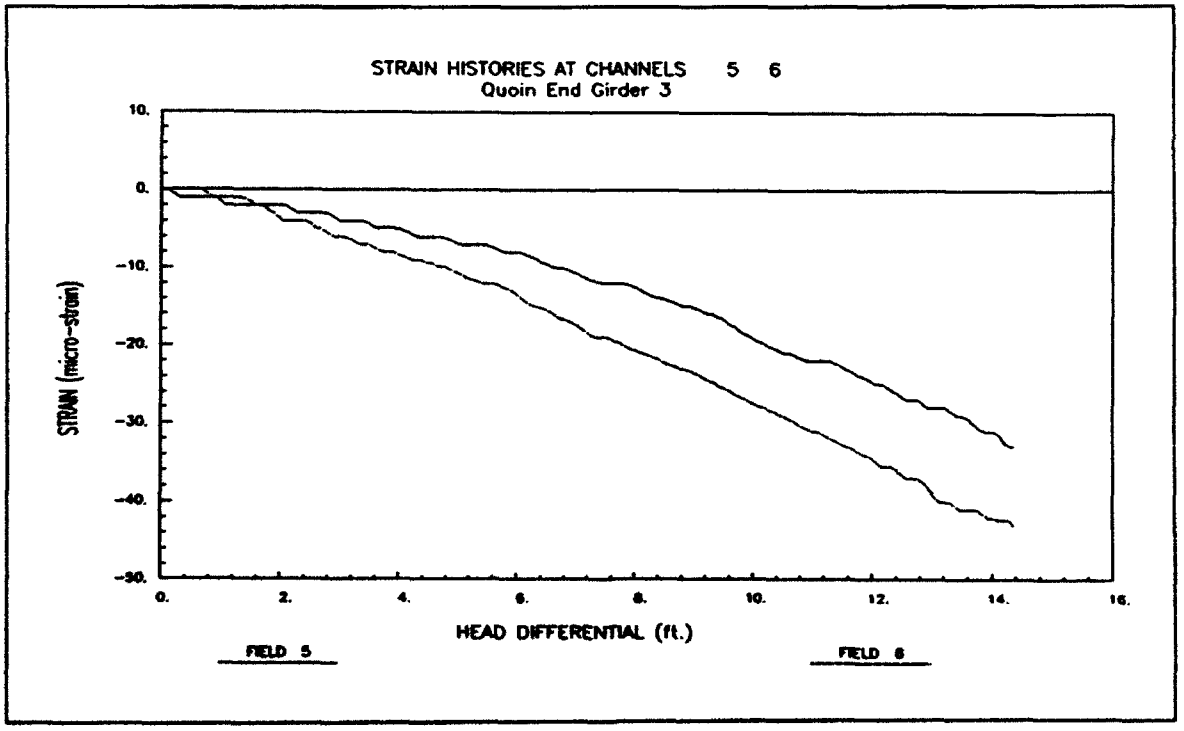

Figure A3. Head differential test strain: G3 quoin end

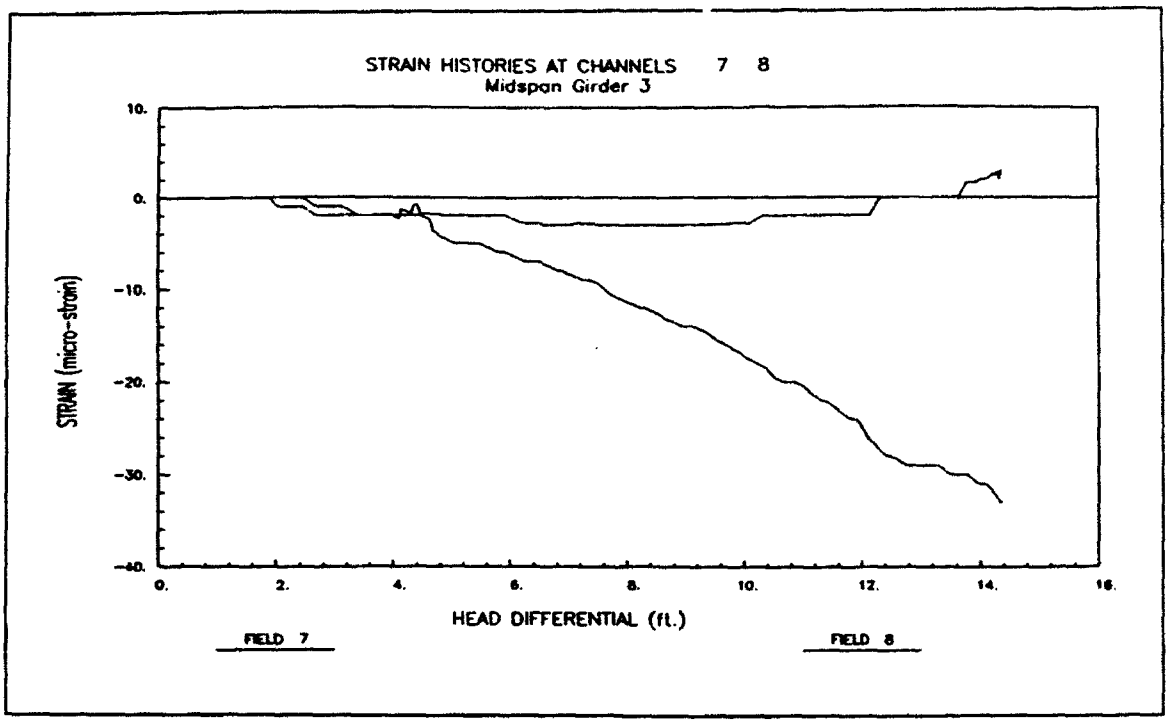

Figure A4. Head differential test strain: G3 midspan

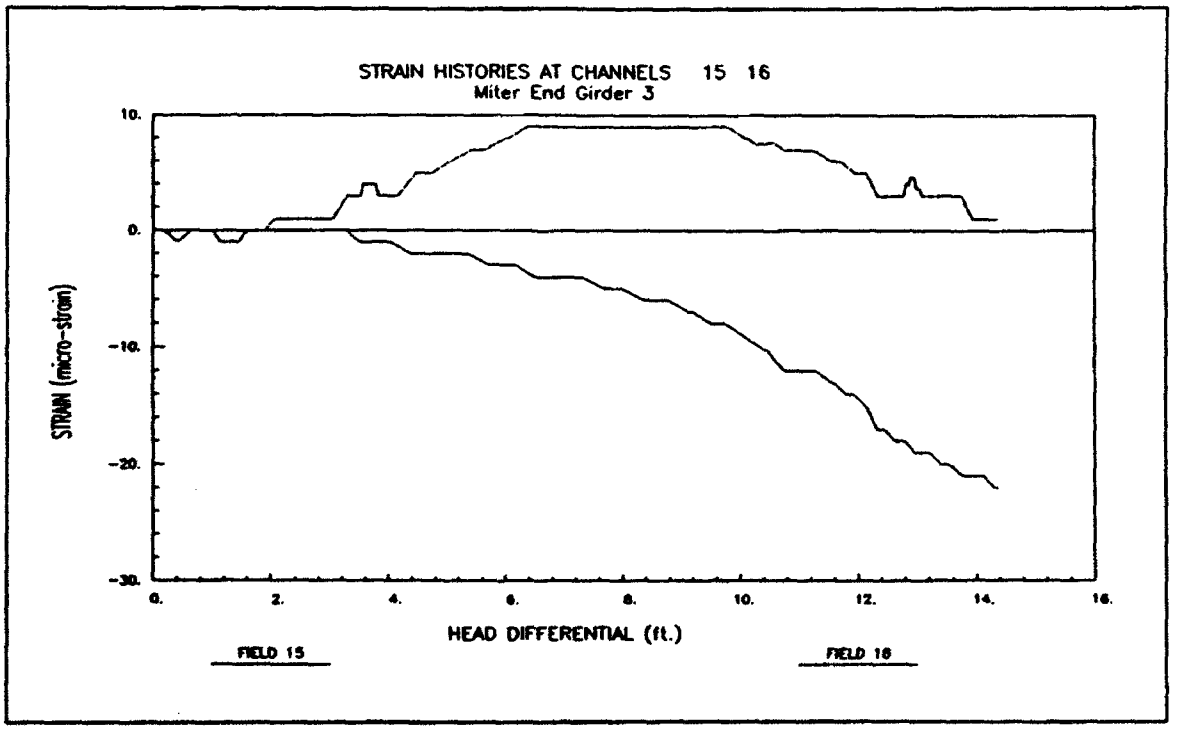

Figure A5. Head differential test strain: G3 miter end

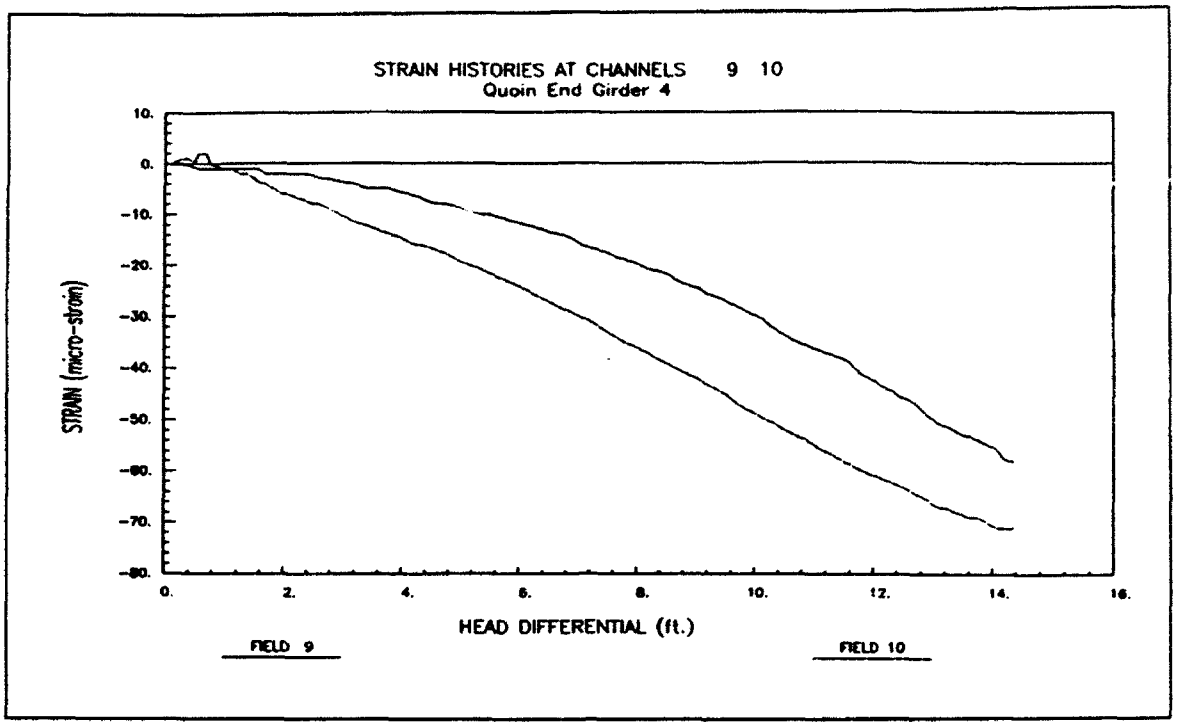

Figure A6. Head differential test strain: G4 quoin end

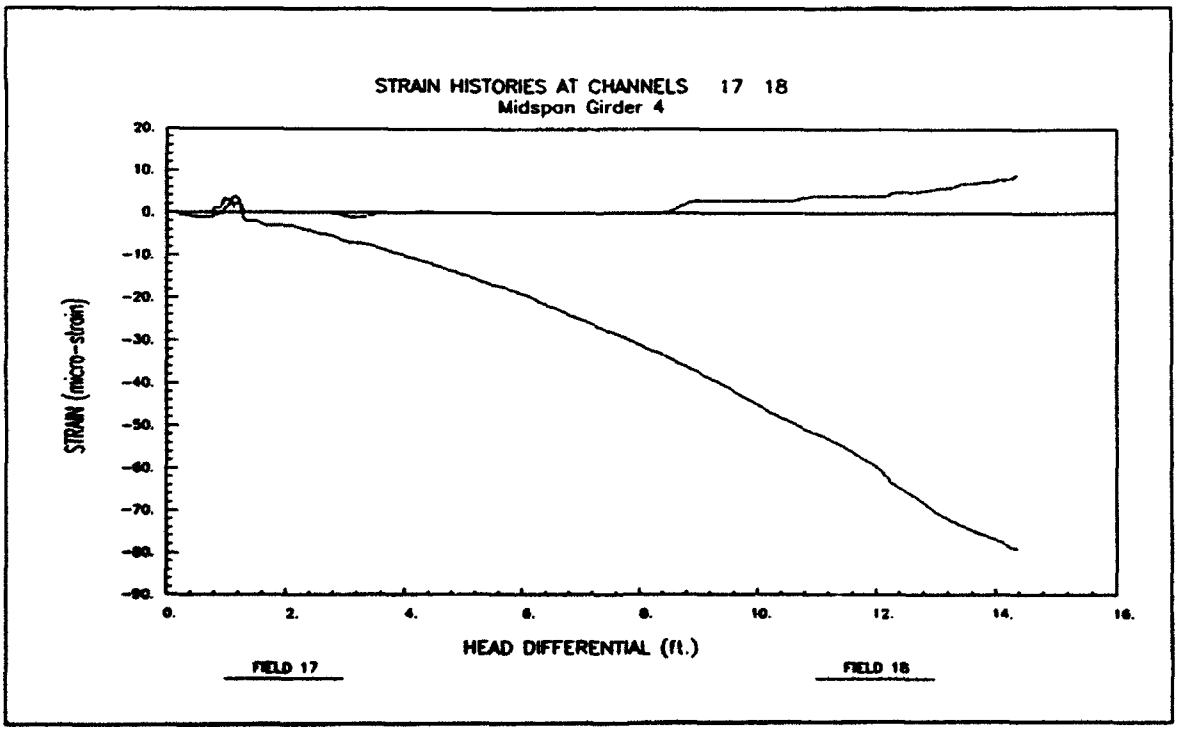

Figure A7. Head differential test strain: G4 midspan

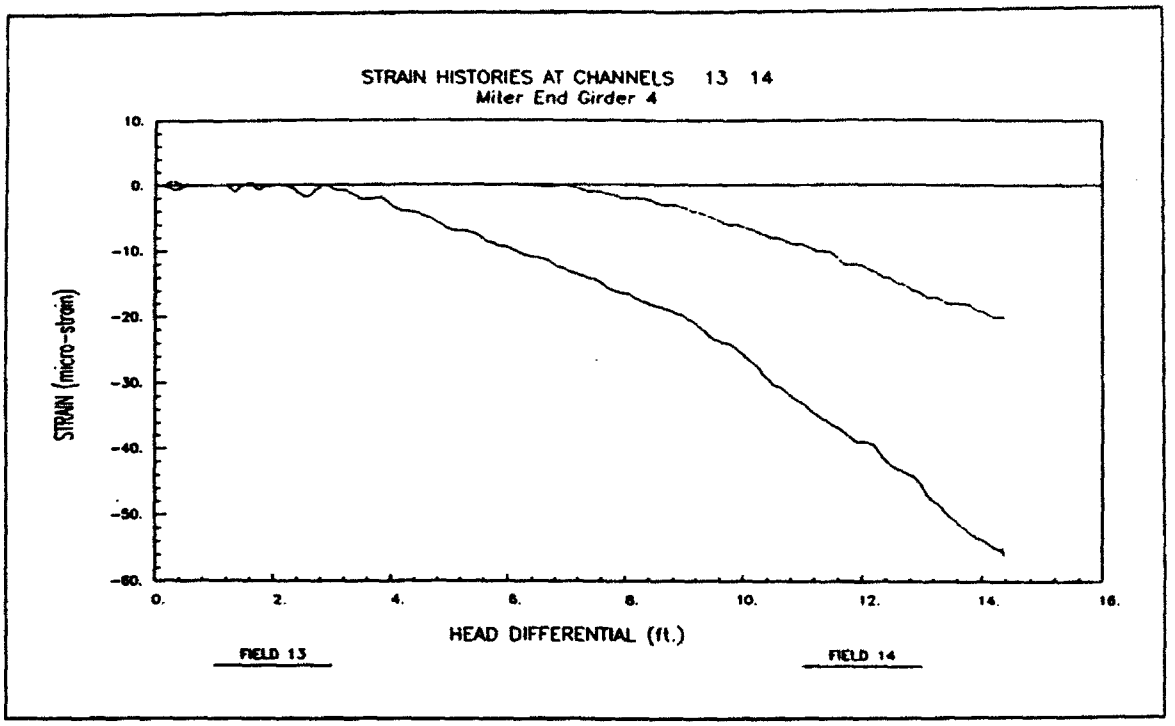

Figure A8. Head differential test strain: G4 miter end

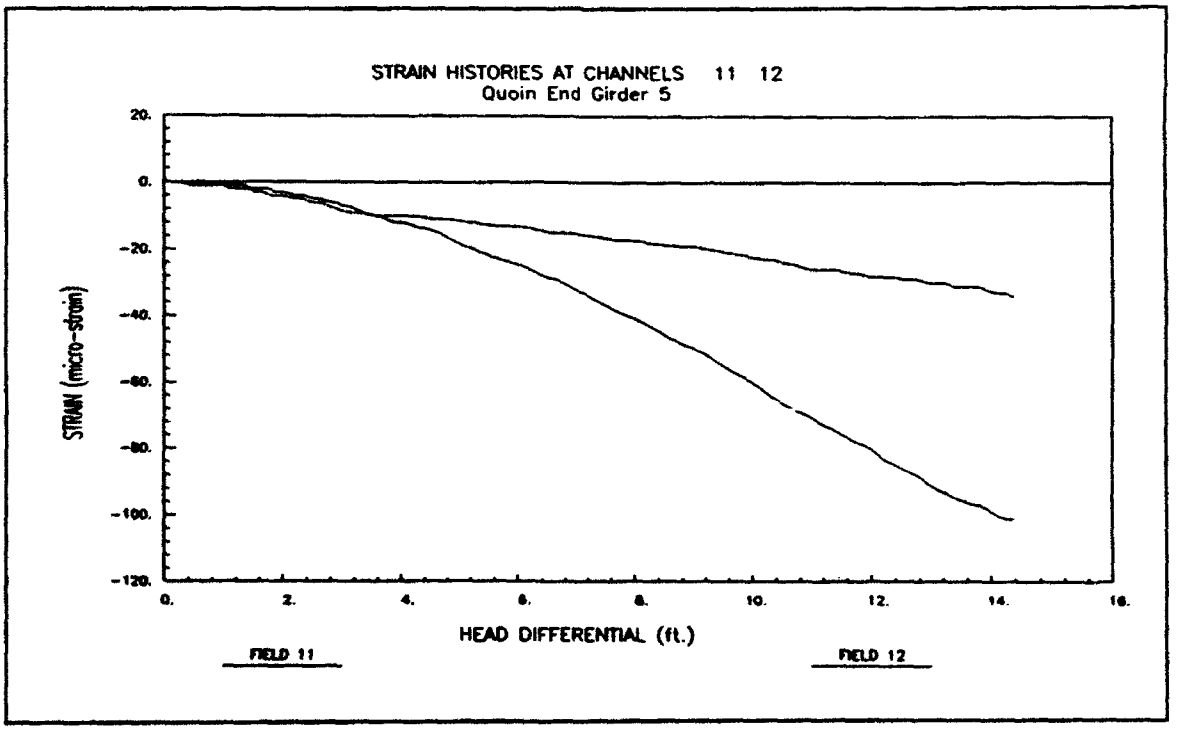

Figure A9. Head differential test strain: G5 quoin end

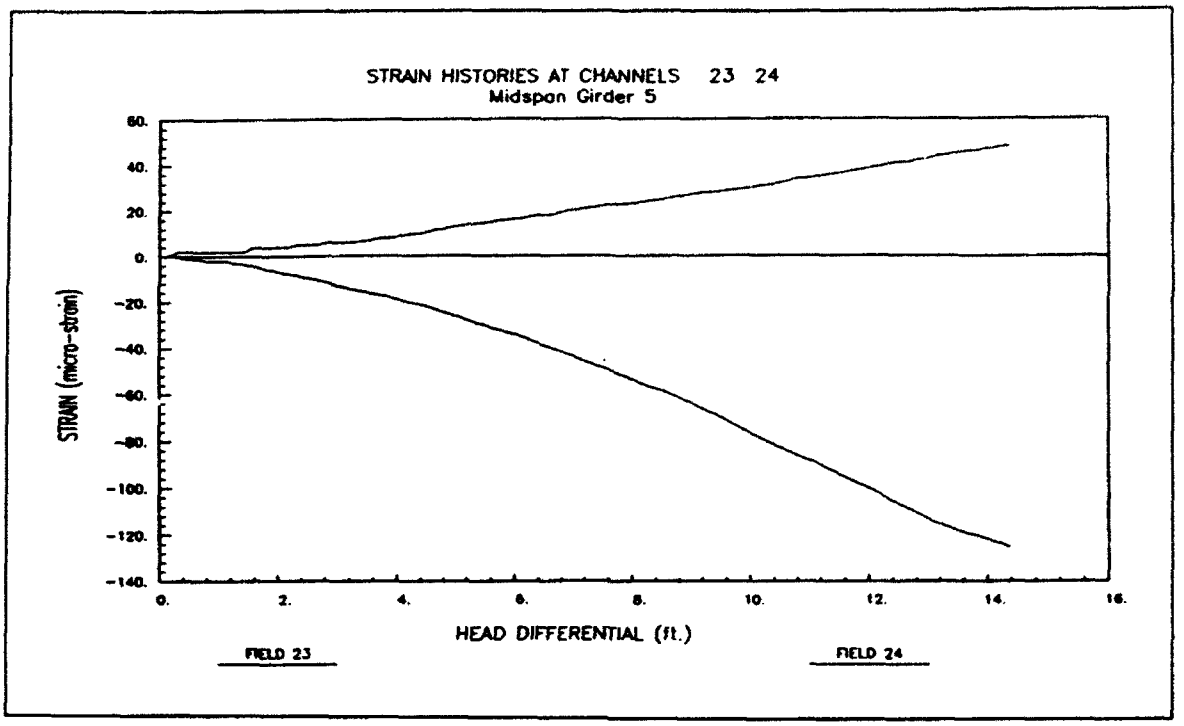

Figure A10. Head differential test strain: G5 midspan

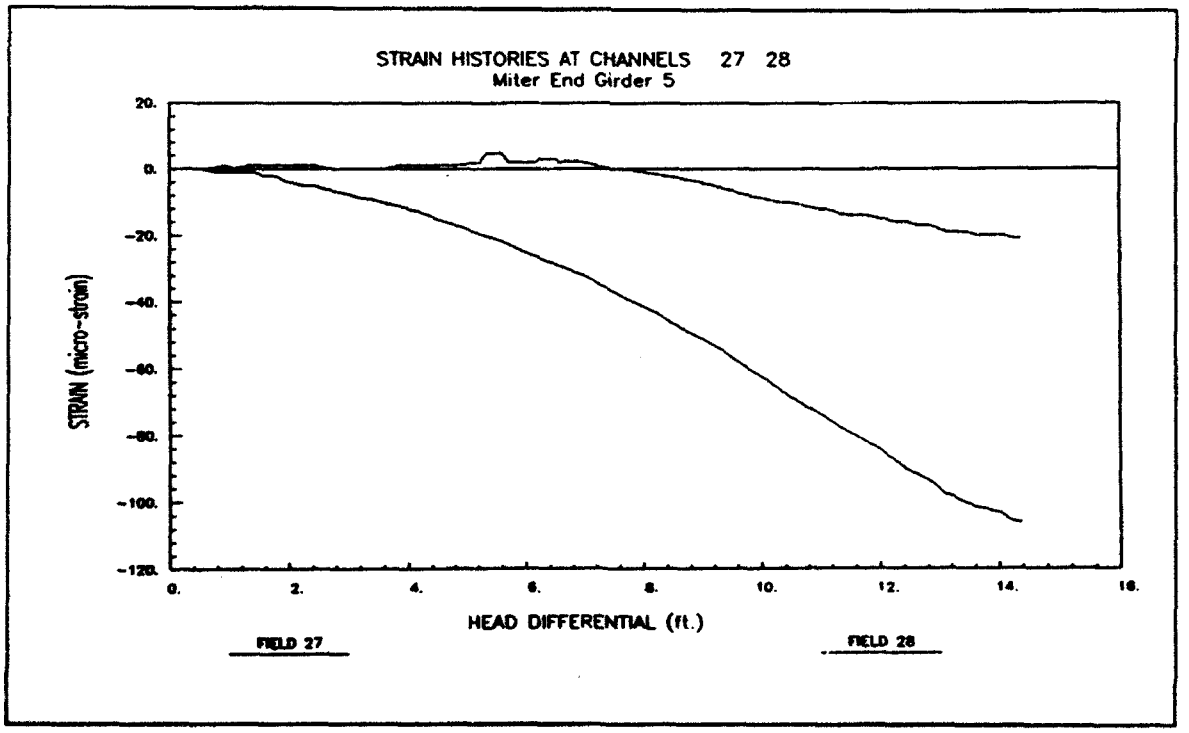

Figure A11. Head differential test strain: G5 miter end

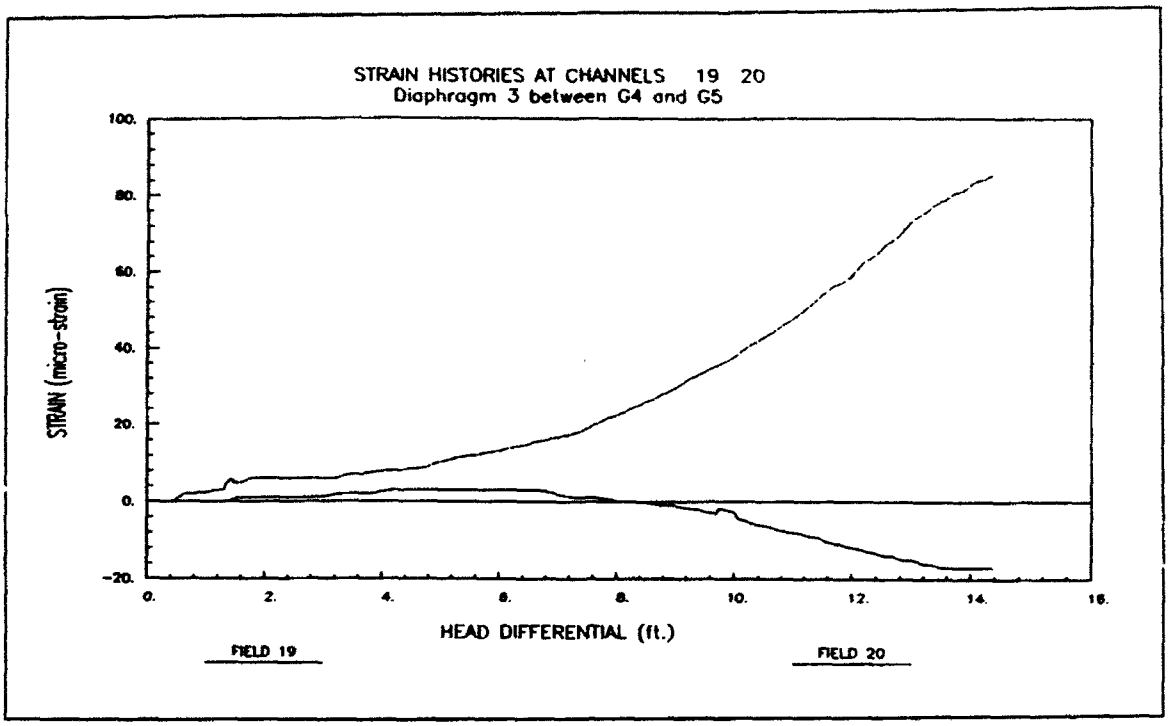

Figure A12. Head differential test strain: diaphragm 3

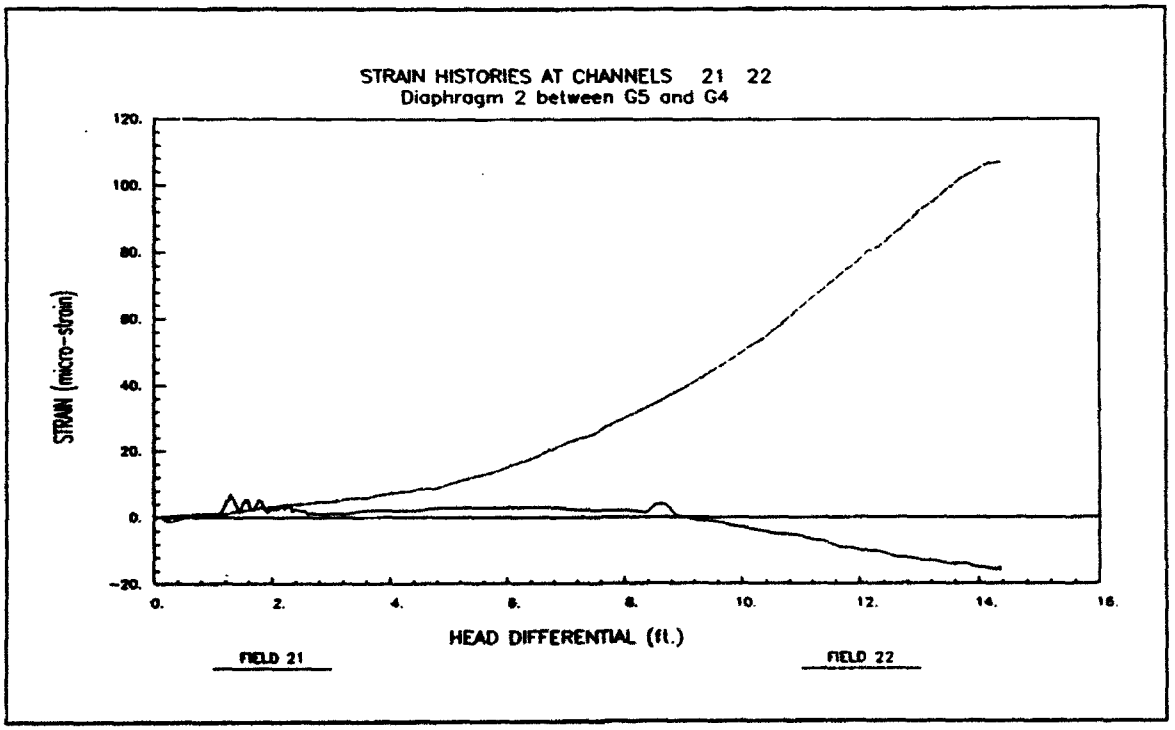

Figure A13. Head differential test strain: diaphragm 2

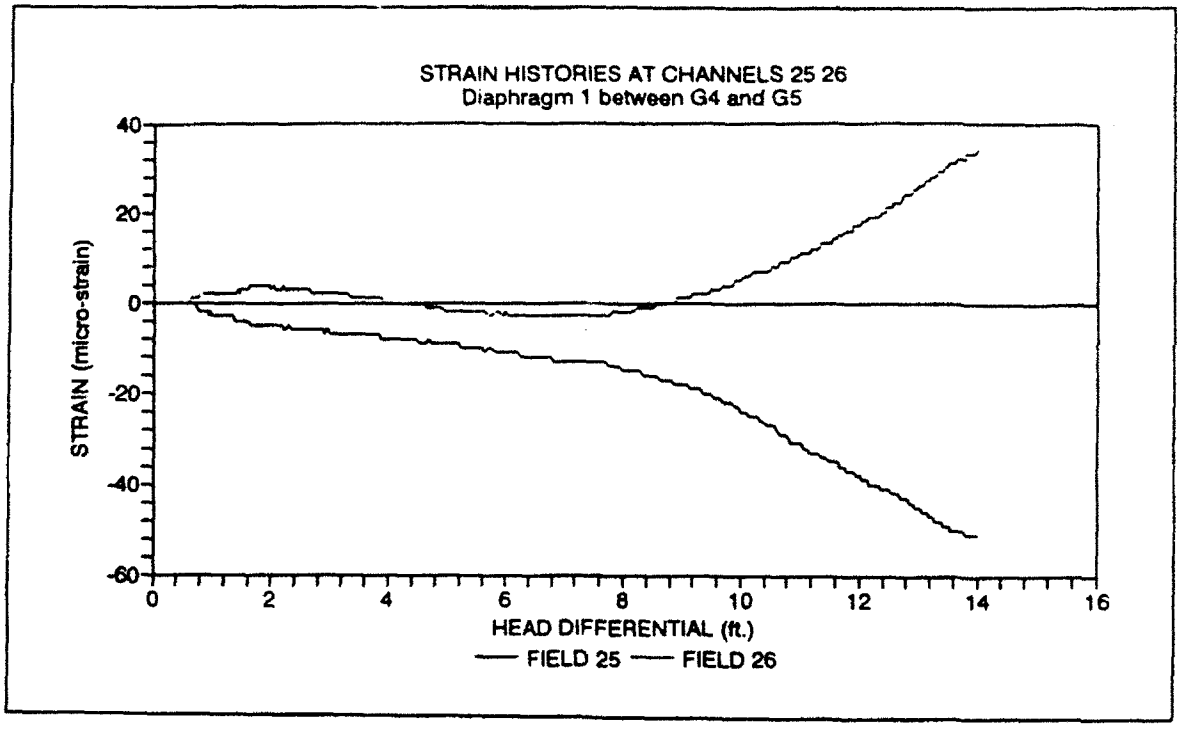

Figure A14. Head differential test strain: diaphragm 1

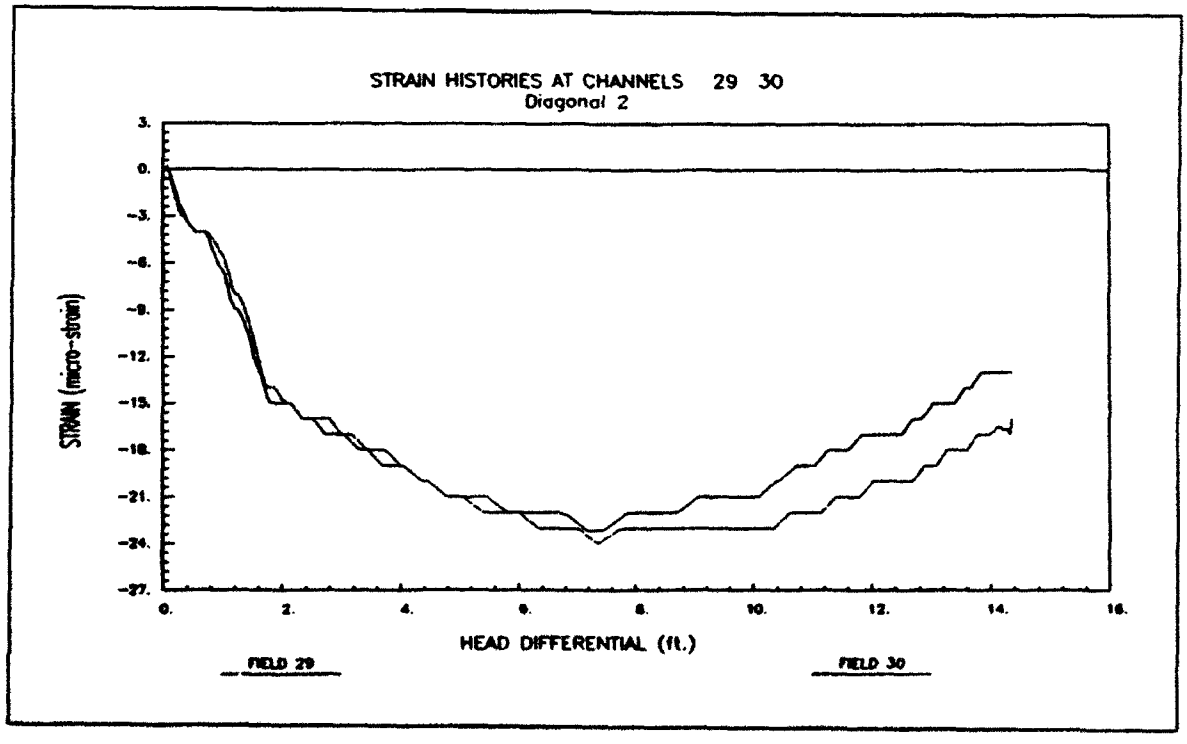

Figure A15. Head differential test strain: diagonal 2

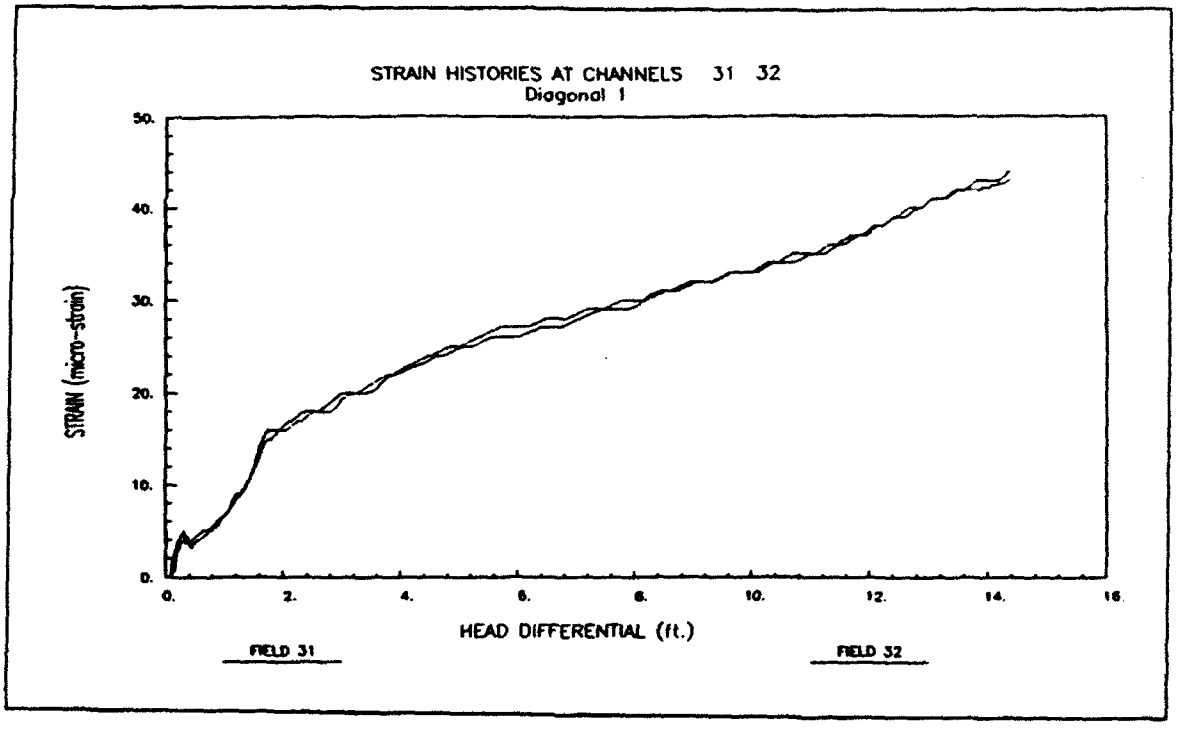

Figure A16. Head differential test strain: diagonal 1

Appendix B
Gate Operation Opening Test Data

Field Data

This appendix provides data obtained for the gate operation opening test. Figures B1-B16 graphically display the measured strain data as a function of the leaf angle with respect to the lock wall (beginning at 72 deg and opening to 0 deg). In Figures B1-B16, the data presented are labeled by the number of the corresponding transducer from which the data were recorded (See Figure 3 for location and numbering of transducers).

Pintle Torque Comparison with Model Studies

Extensive model studies determining operating forces on miter lock gates have been conducted at the U.S. Army Engineer Waterways Experiment Station (WES) (U.S. Army Engineer Waterways Experiment Station 1964).[1] EM 1110-2-2703 provides the WES model results for pintle torque T (torque applied about the pintle by the operating strut) and outlines the approach to estimate T for any given lock gate (on the basis of the scalar ratio between the model and the given lock gate). Values for T for the Red River leaf are calculated and are compared with estimated results based on the WES model studies as described in the following paragraphs.

The Red River Lock and Dam No. 1 miter gates are equipped with Modified Ohio River linkage. The geometry of this type of linkage at an arbitrary leaf angle is shown in Figure B17. The pintle torque is the moment applied by the operating strut about the pintle:

[1] References cited are listed at the end of the main text.

$$T = Fa \tag{B1}$$

where

F = axial force in the operating strut

a = perpendicular distance from the strut to the pintle as defined by Figure B17.

The axial force in the operating strut F is determined directly from the strain measurements of transducer No. 3 (ε_3) and No. 4 (ε_4). F is calculated as the product of the average of ε_3 and ε_4, Young's modulus E, and the cross-sectional area (assuming that uniform strain occurs at the monitored cross section). The cross-sectional area of the operating strut at the location of transducer Nos. 3 and 4 is 78 in^2. With E = 29,500 ksi, F is determined by the following equation:

$$F = \frac{EA}{2}(\varepsilon_3 + \varepsilon_4) = 1.15 \times 10^6(\varepsilon_3 + \varepsilon_4) \tag{B2}$$

Figure B18 shows the operating strut force calculated as a function of leaf angle for the leaf opening test (beginning position is at 72 deg).

Figure B19 shows the comparison of the measured T and that determined based on the WES model studies. The measured T was calculated as a function of leaf angle by Equation B1, and T based on WES data was determined by the procedure outlined in paragraph 2-4.d of EM 1110-2-2703. Figure B19 shows that the measured and WES model results are not even comparable. The measured torque is significantly larger than that determined by the WES model results. One explanation for the large measured T is that the leaf was opened as it was restrained at the bottom by accumulated silt or some other obstruction. The accumulation of silt has been a concern in the past at locks on the Red River.

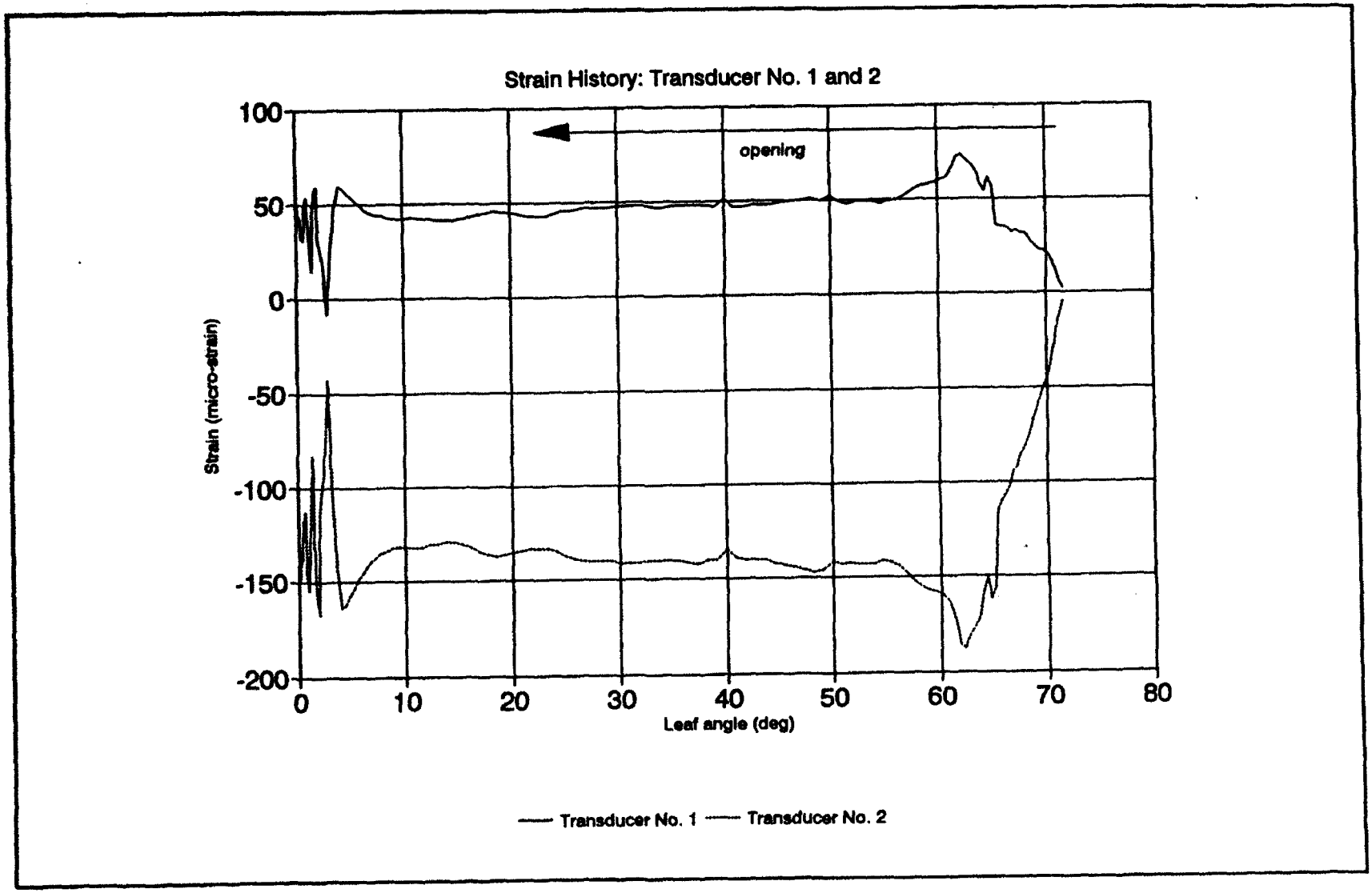

Figure B1. Gate operation opening test strain: G1 midspan

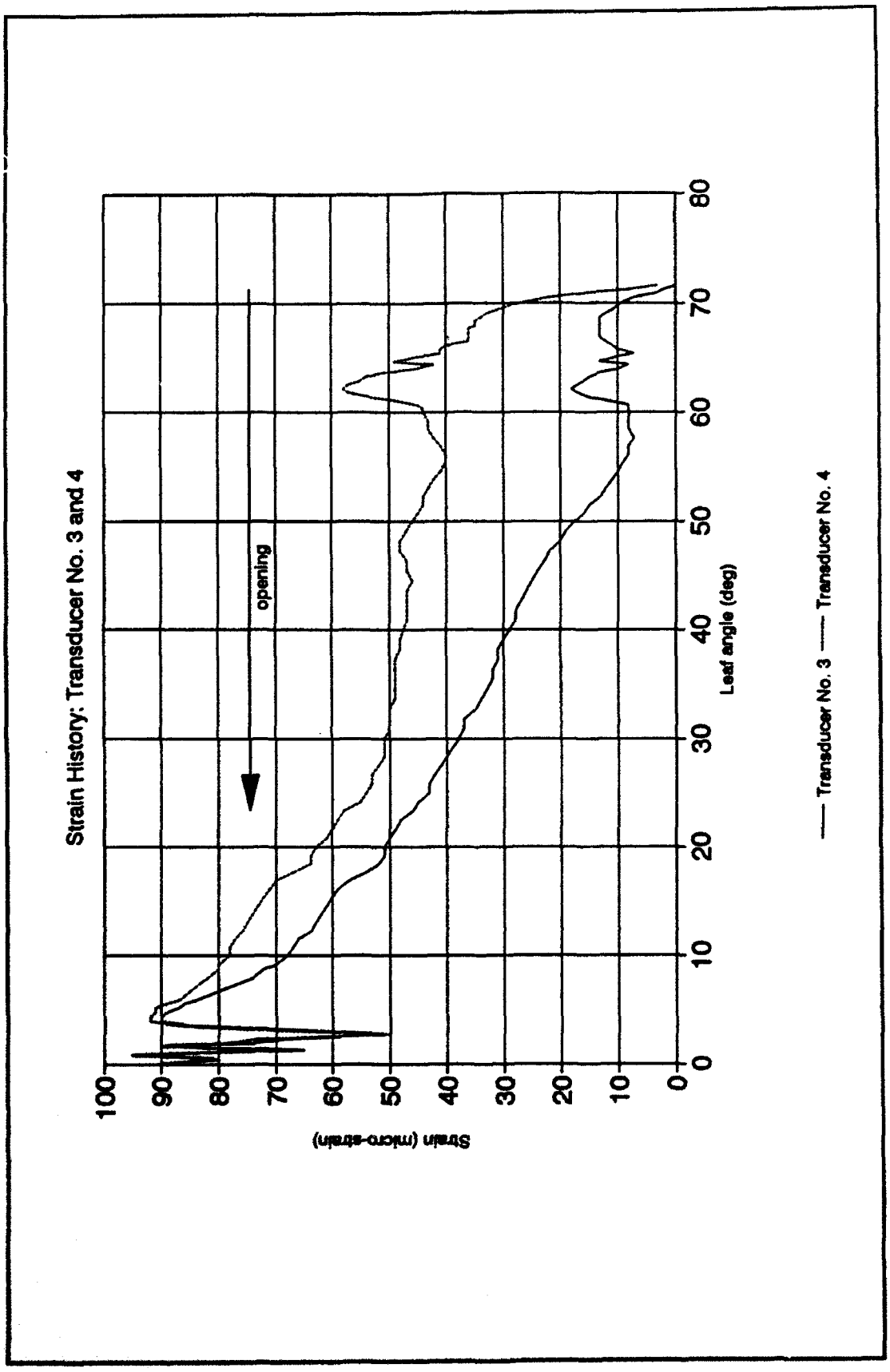

Figure B2. Gate operation opening test strain: operating strut

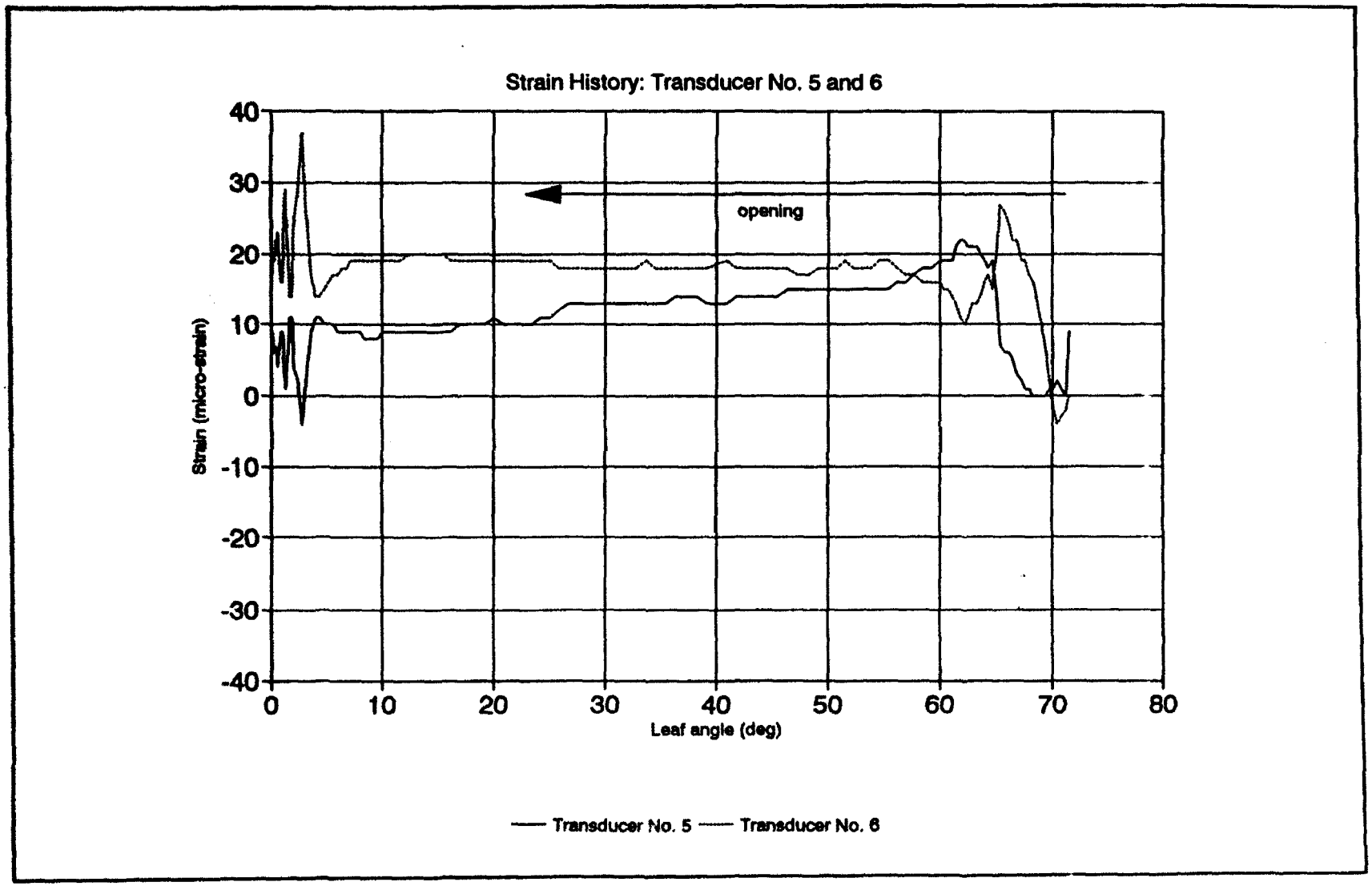

Figure B3. Gate operation opening test strain: G3 quoin end

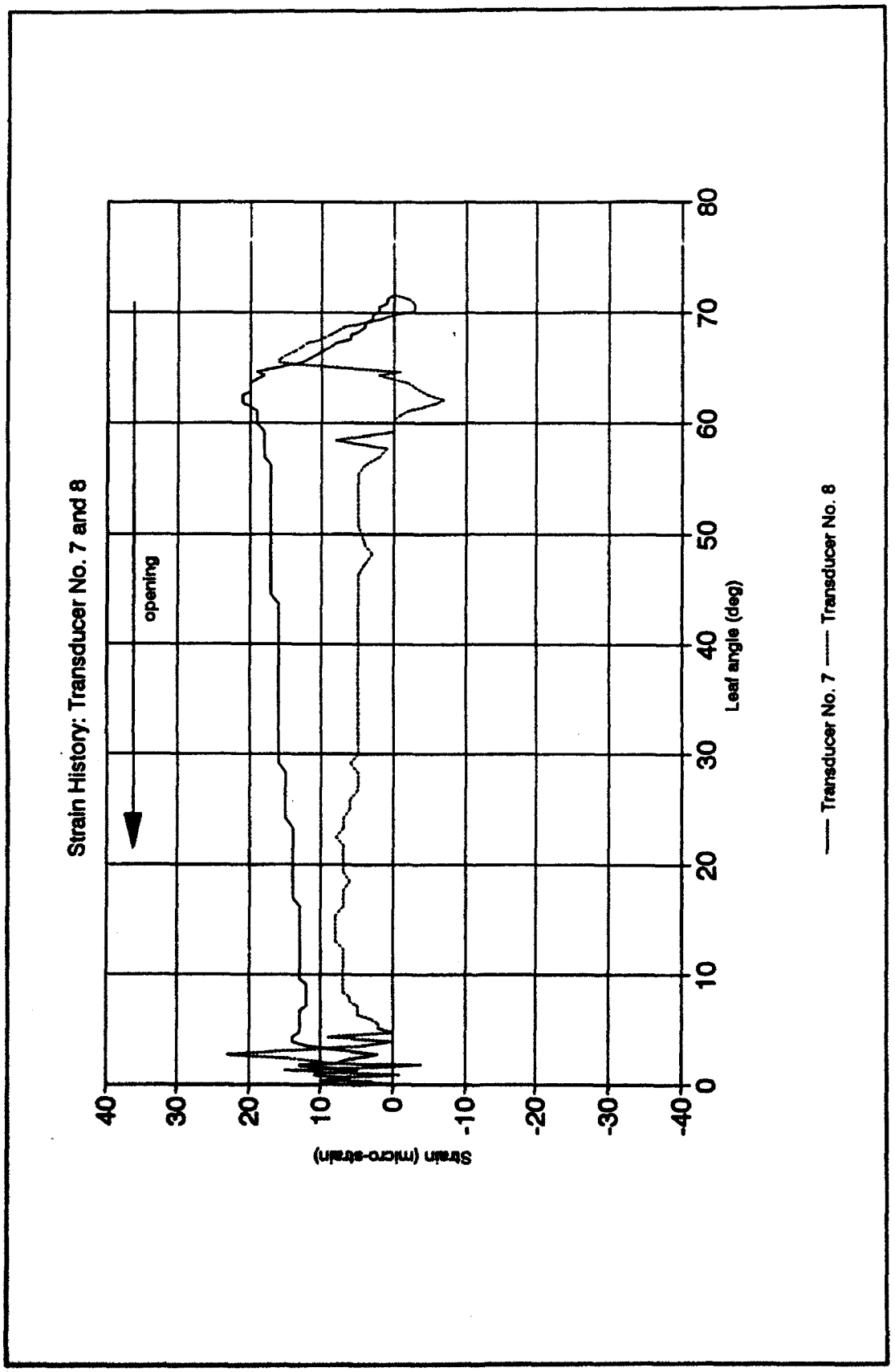

Figure B4. Gate operation opening test strain: G3 midspan

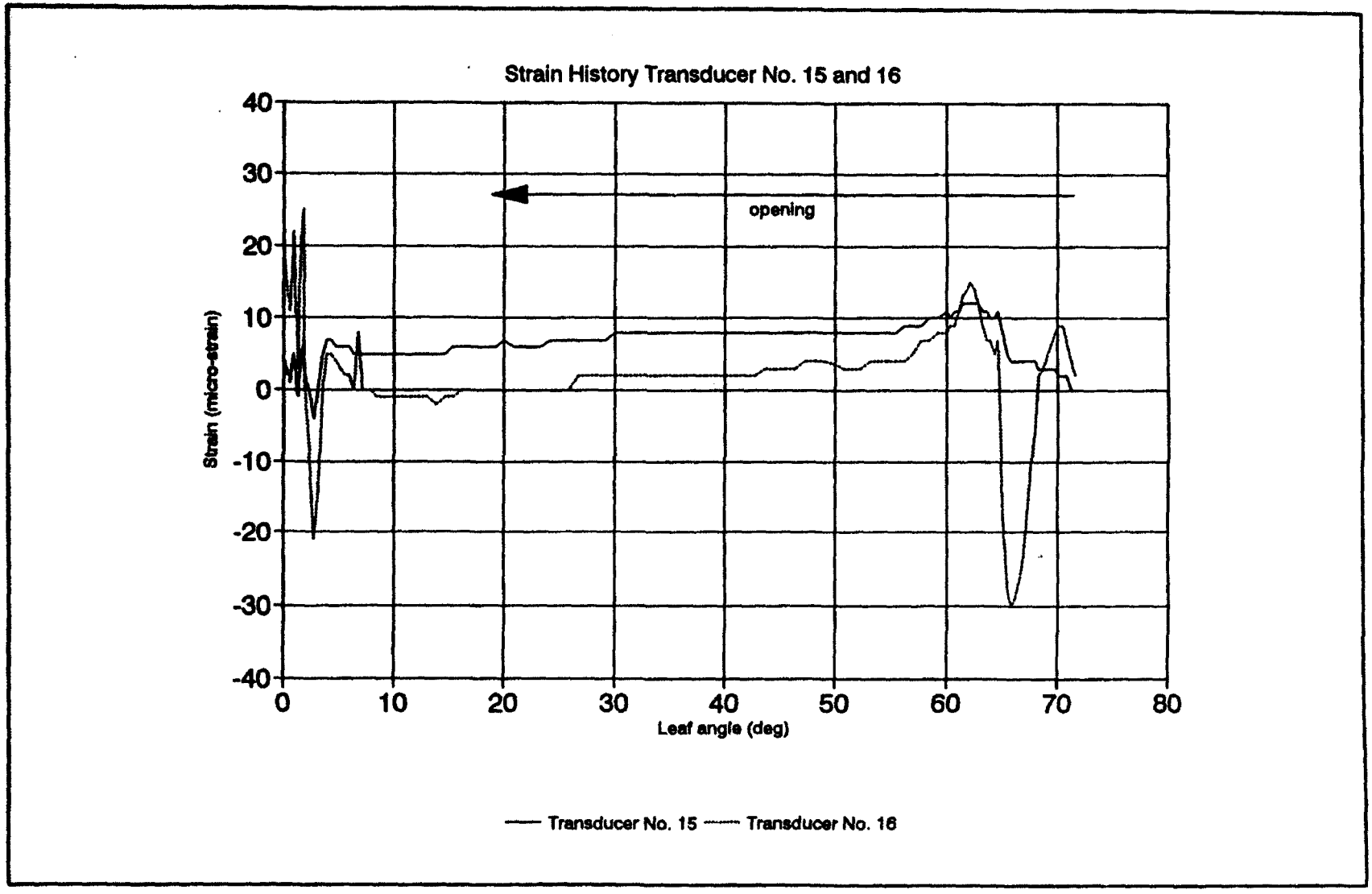

Figure B5. Gate operation opening test strain: G3 miter end

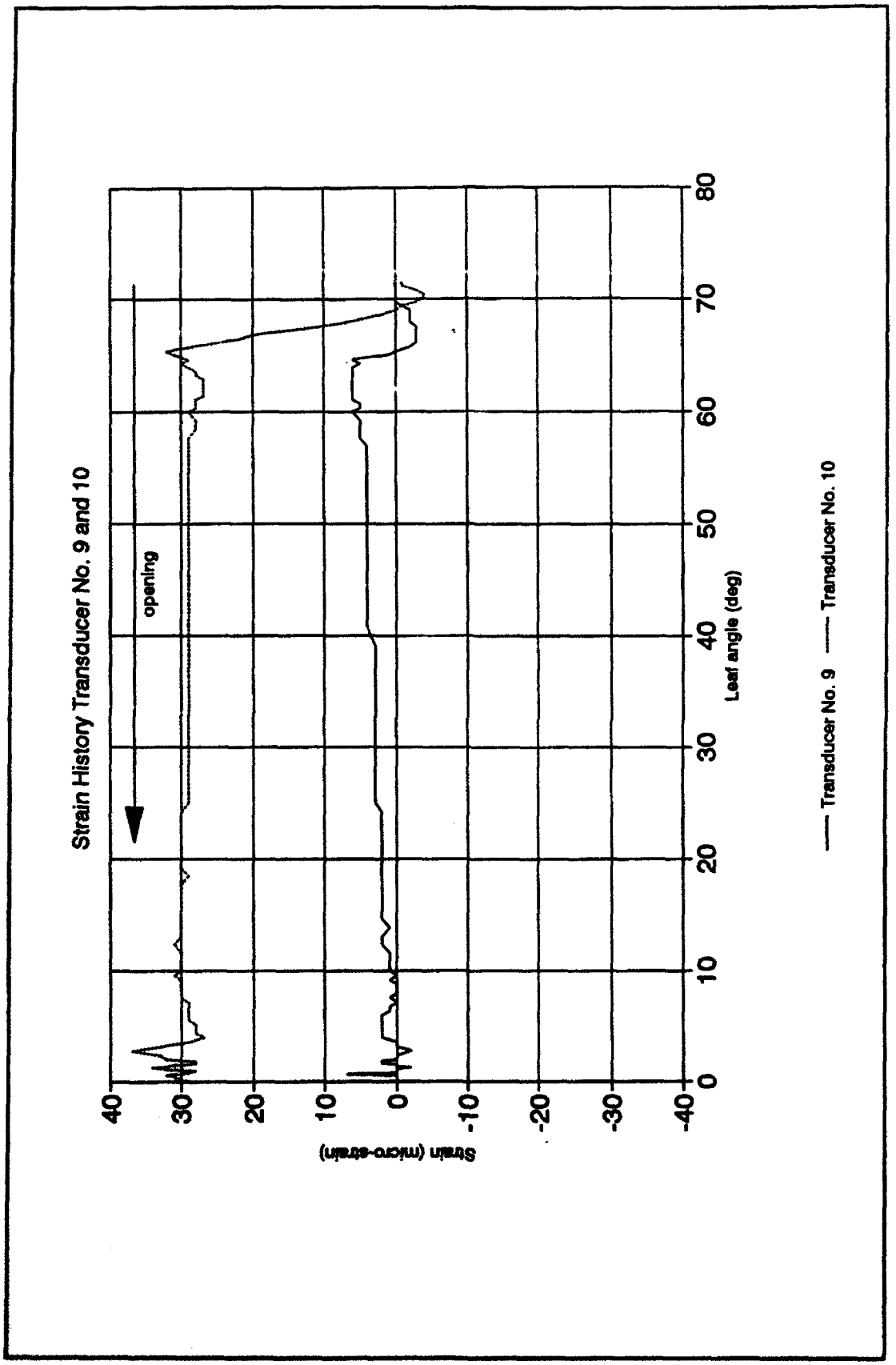

Figure B6. Gate operation opening test strain: G4 quoin end

Figure B7. Gate operation opening test strai G4 midspan

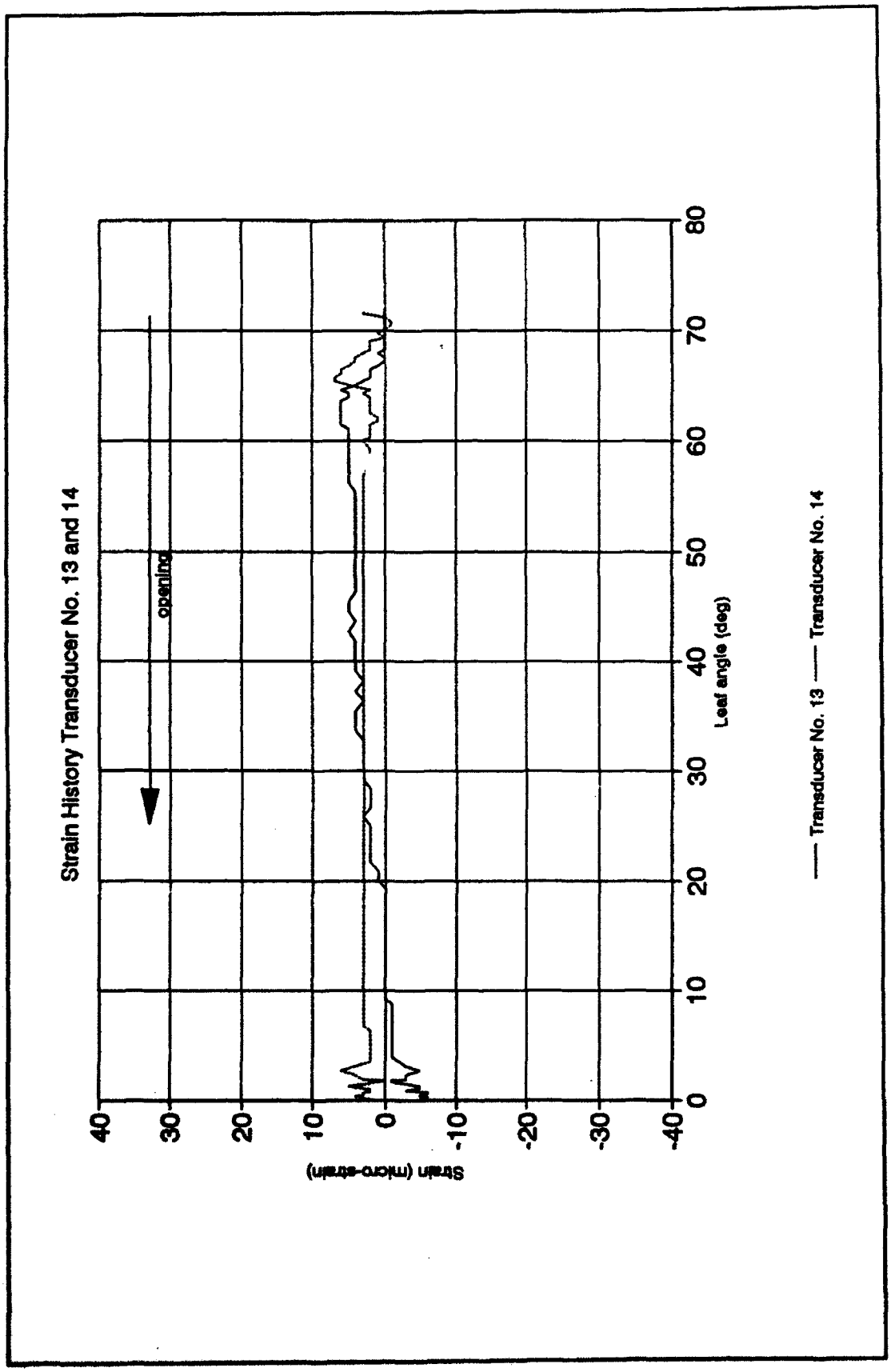

Figure B8. Gate operation opening test strain: G4 miter end

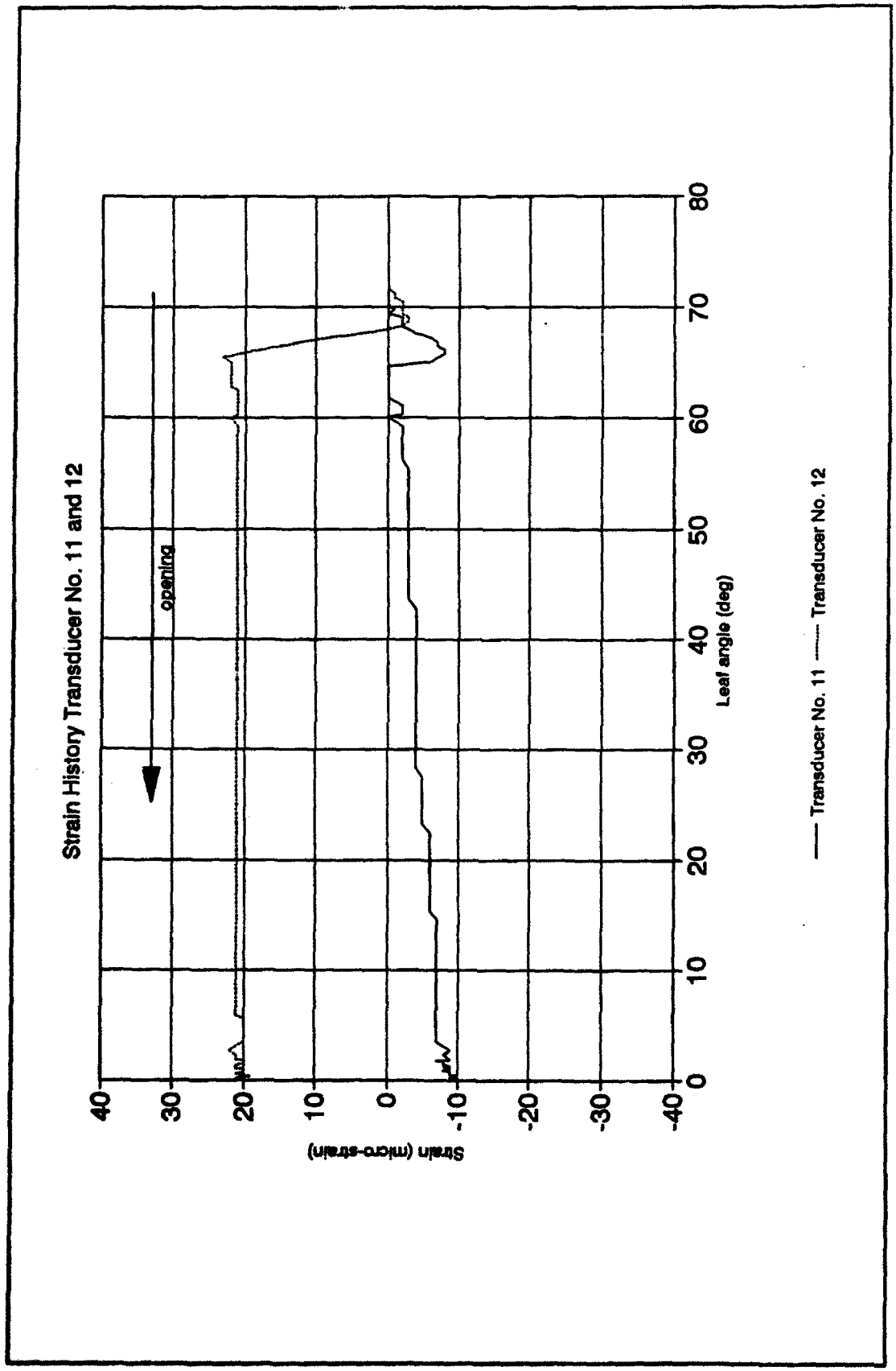

Figure B9. Gate operation opening test strain: G5 quoin end

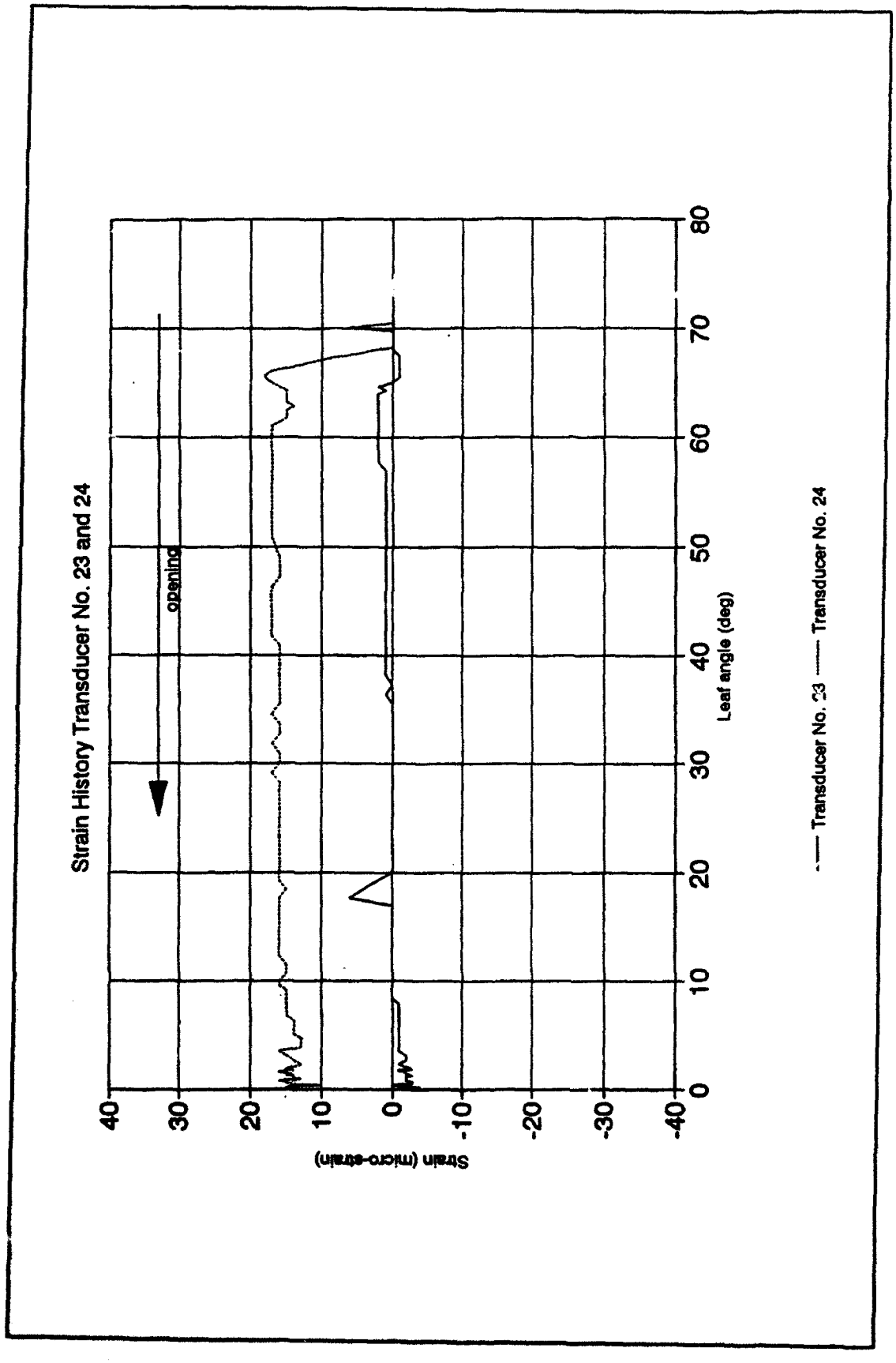

Figure B10. Gate operation opening test strain: G5 midspan

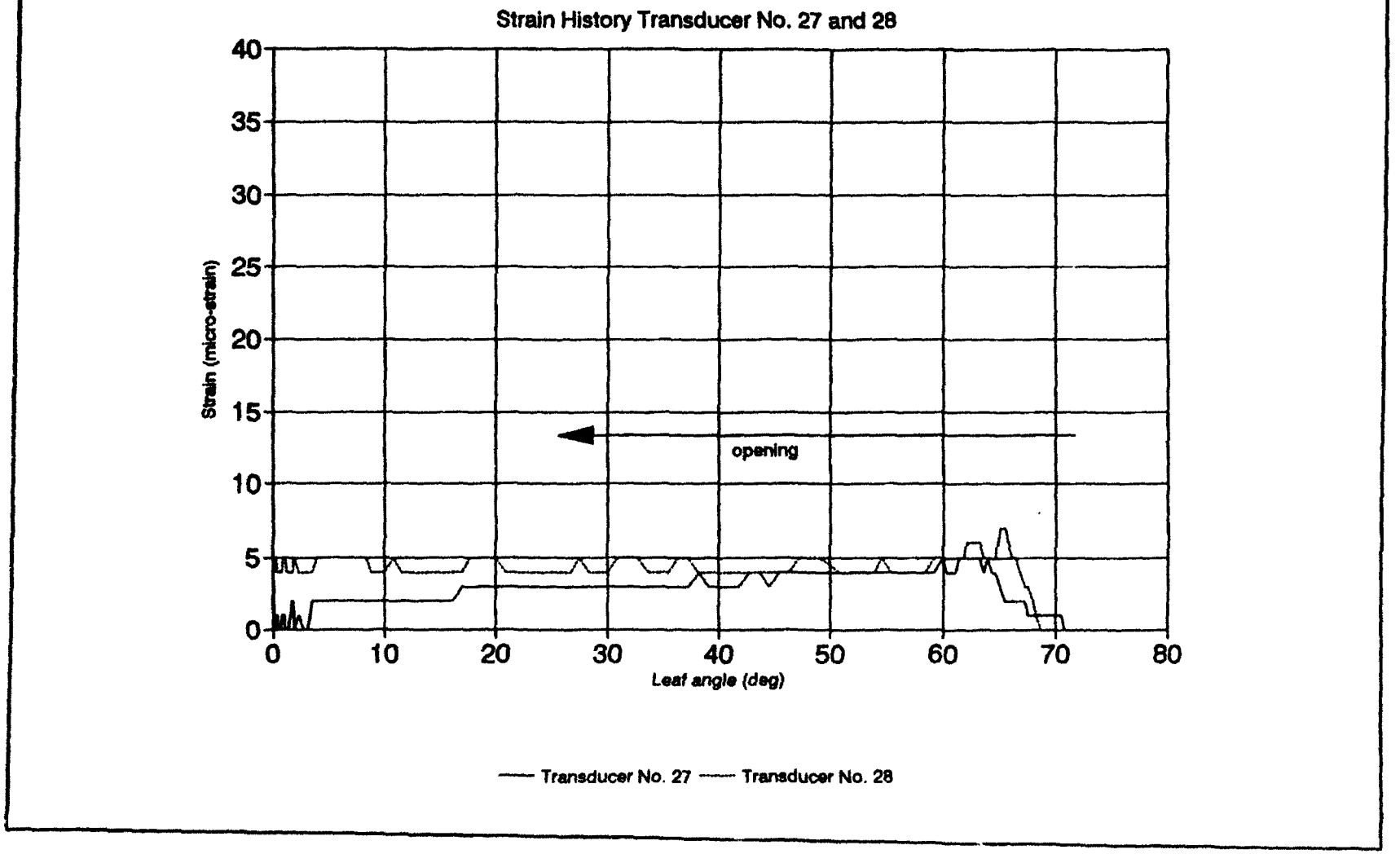

Figure B11. Gate operation opening test strain: G5 miter end

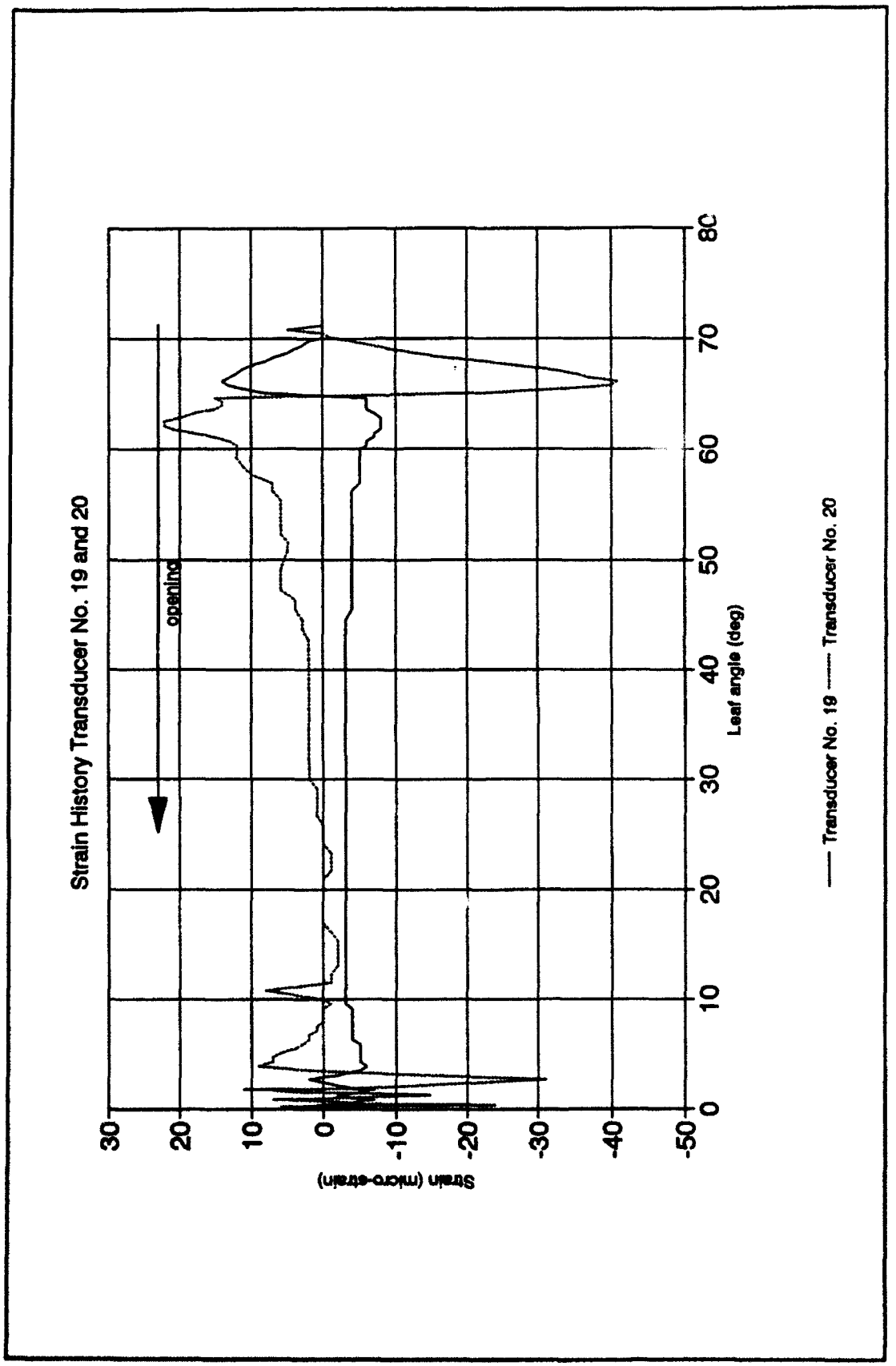

Figure B12. Gate operation opening test strain: diaphragm 3

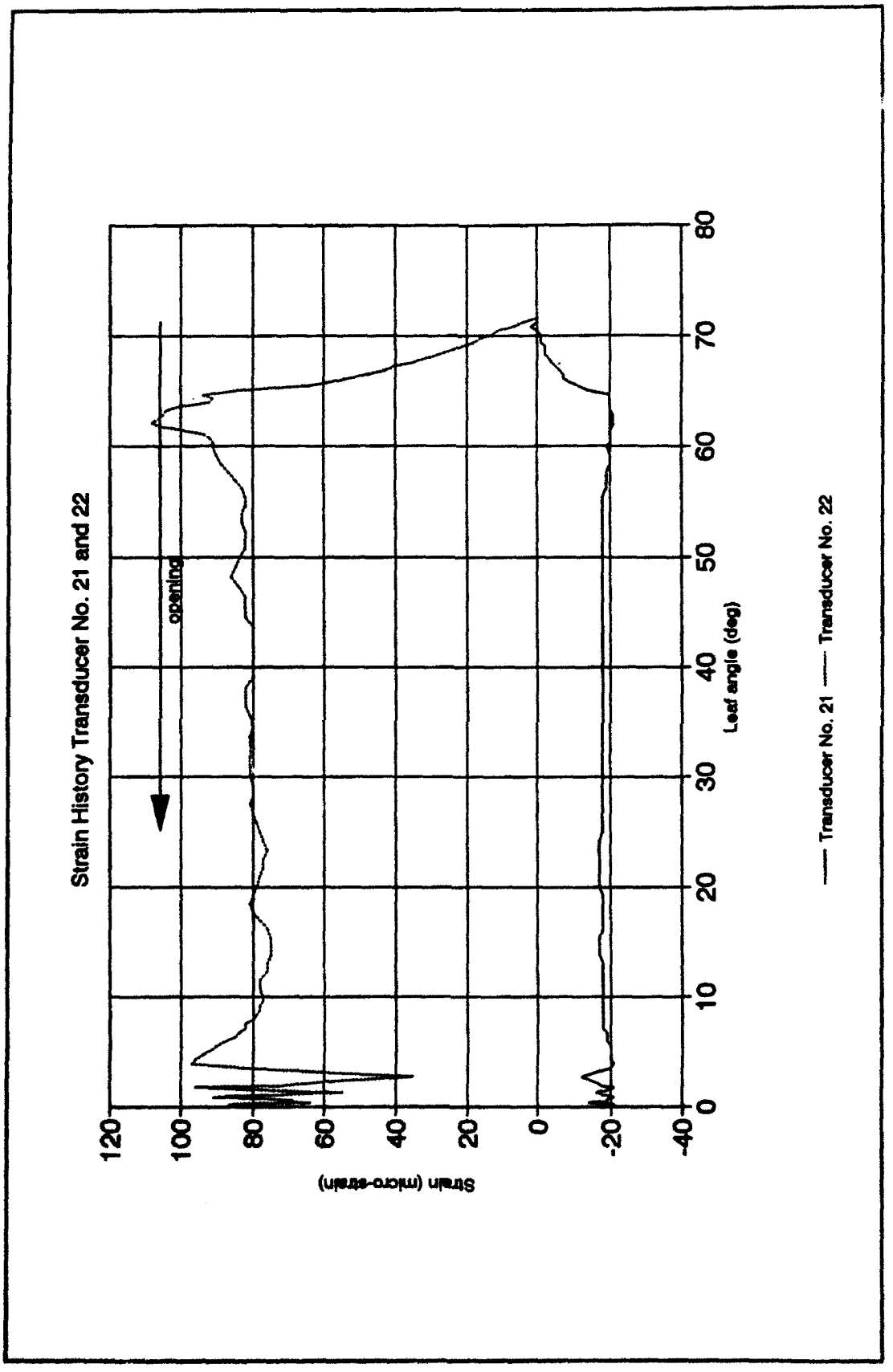

Figure B13. Gate operation opening test strain: diaphragm 2

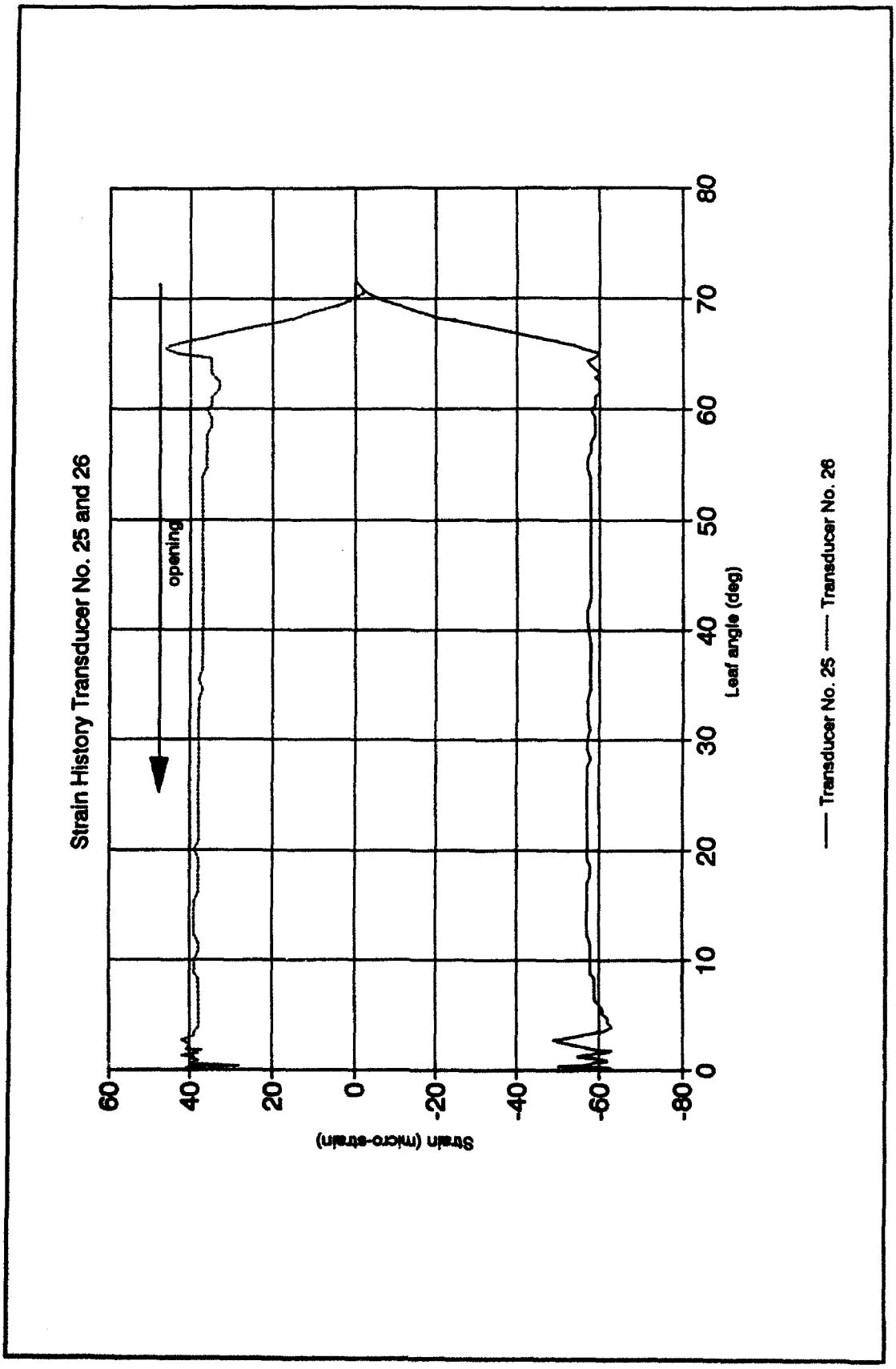

Figure B14. Gate operation opening test strain: diaphragm 1

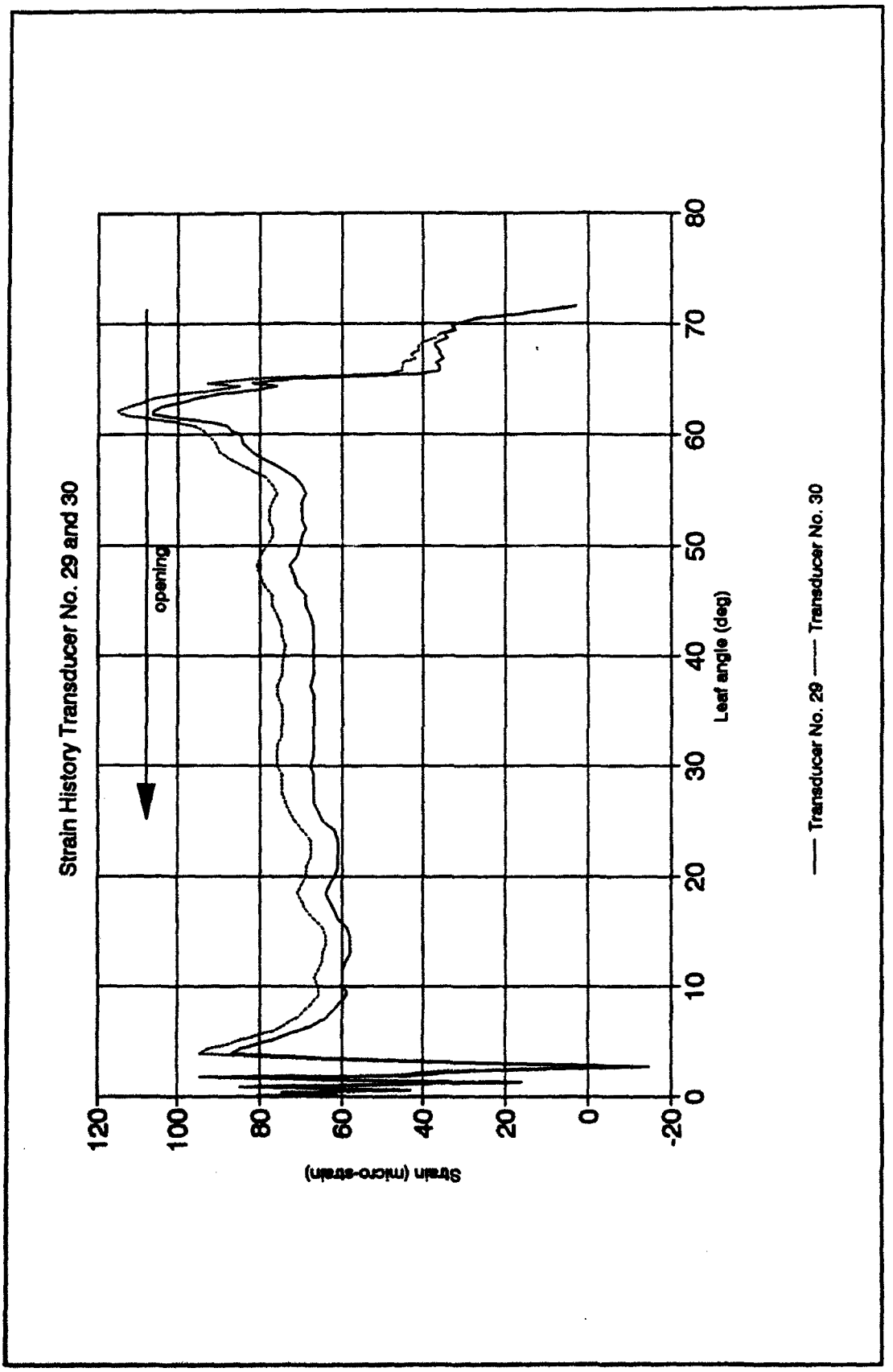

Figure B15. Gate operation opening test strain: diagonal 2

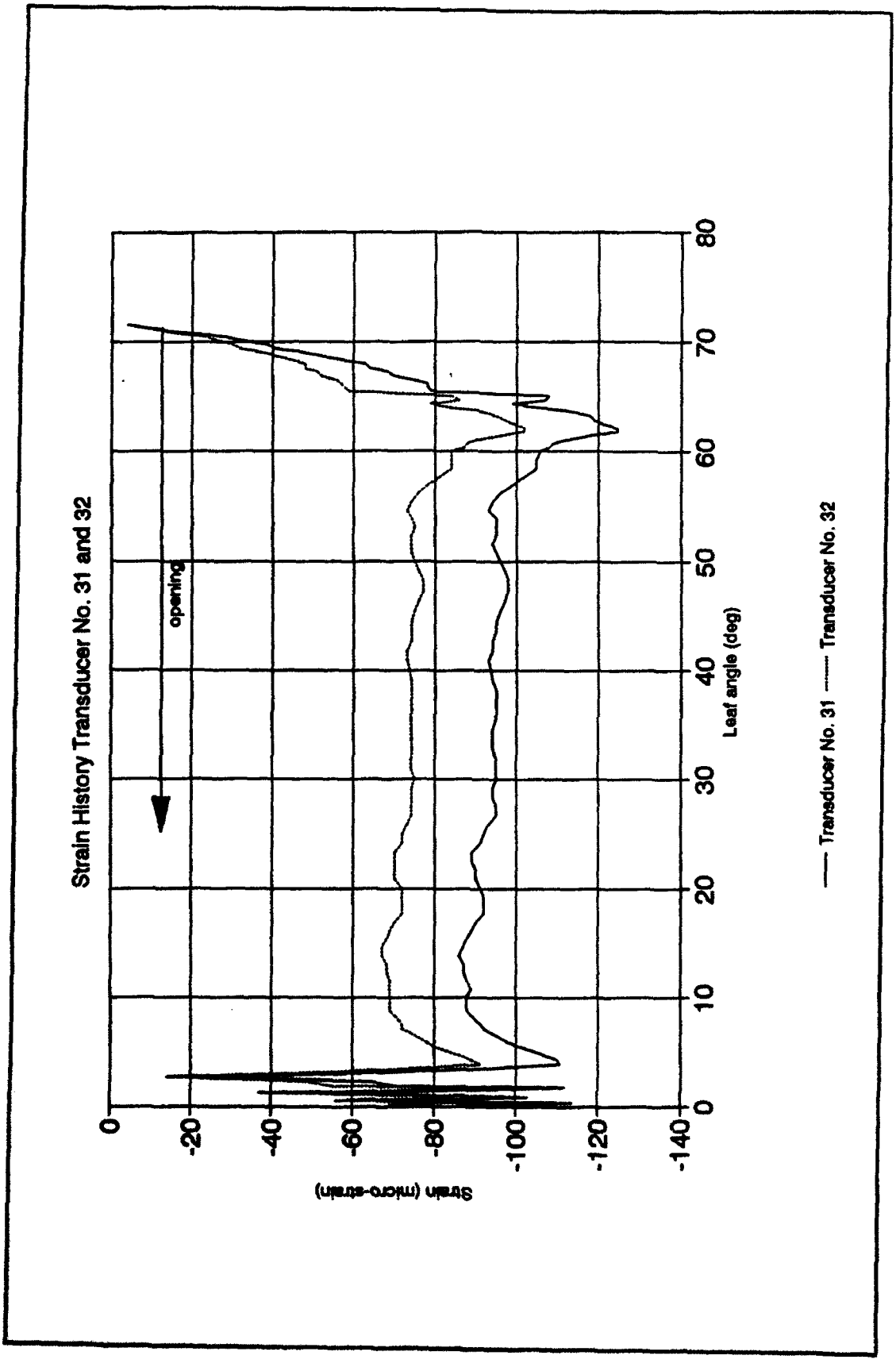

Figure B16. Gate operation opening test strain: diagonal 1

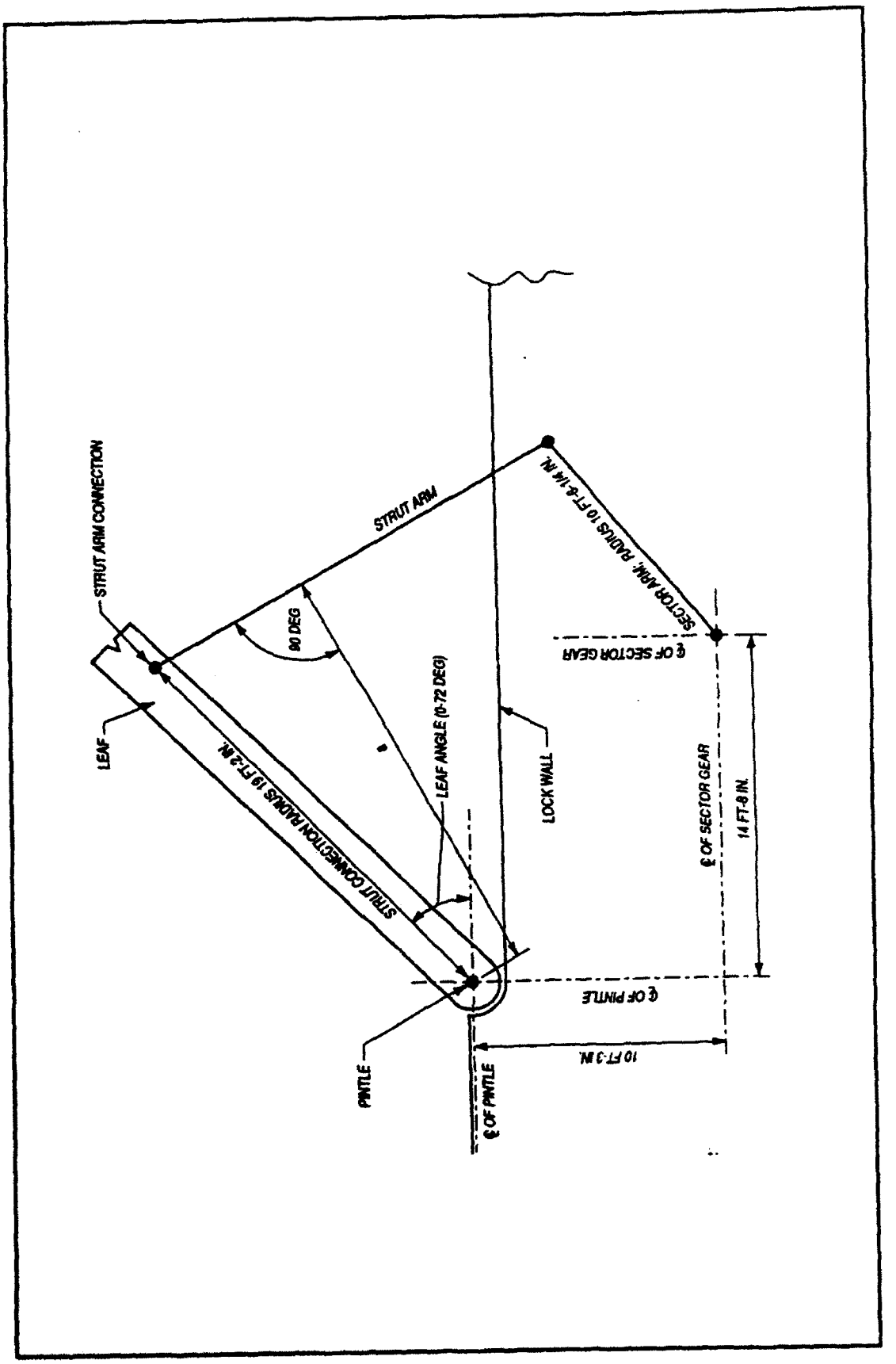

Figure B17. Modified Ohio River linkage geometry

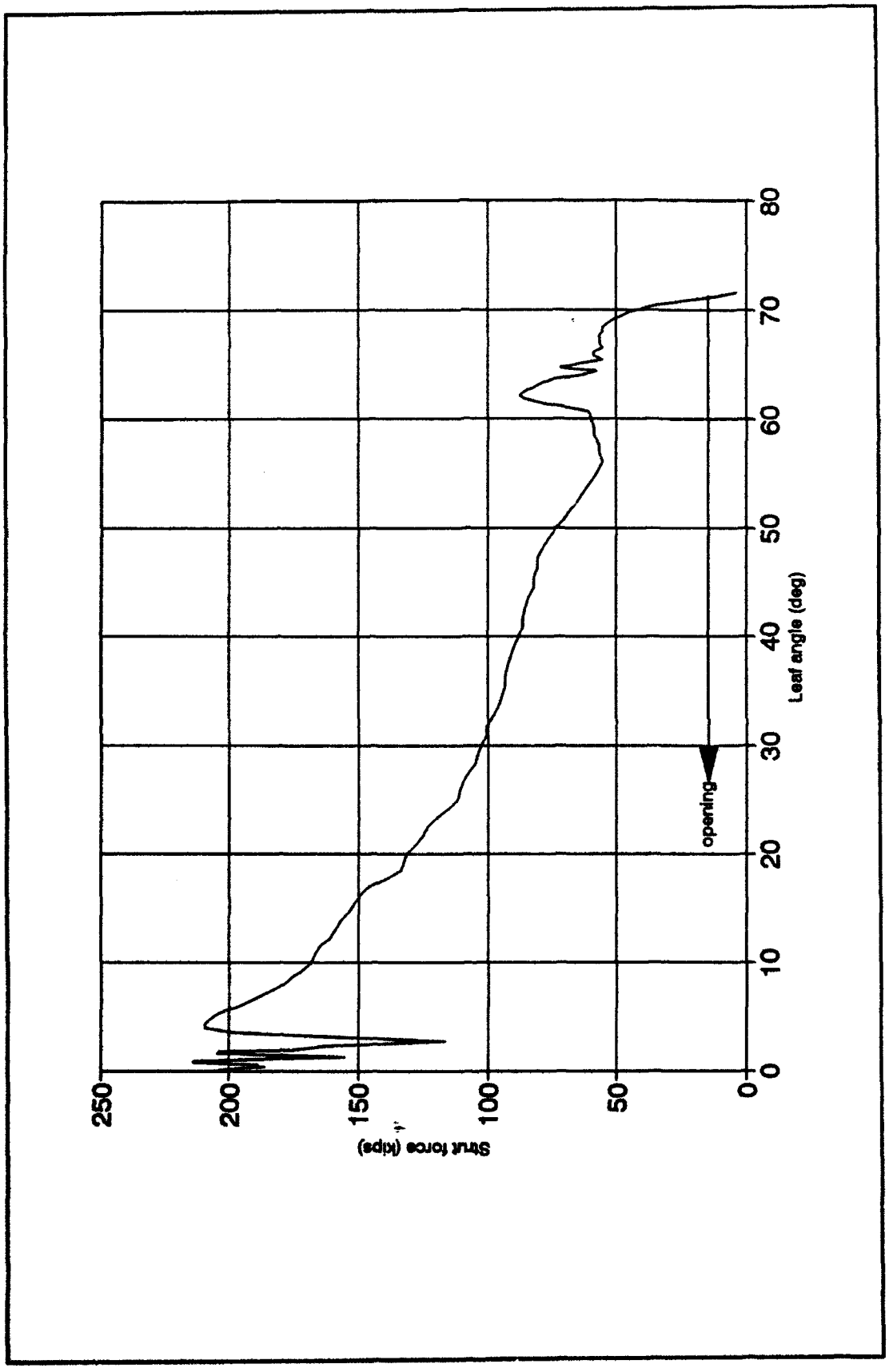

Figure B18. Gate operation opening test: operating strut force

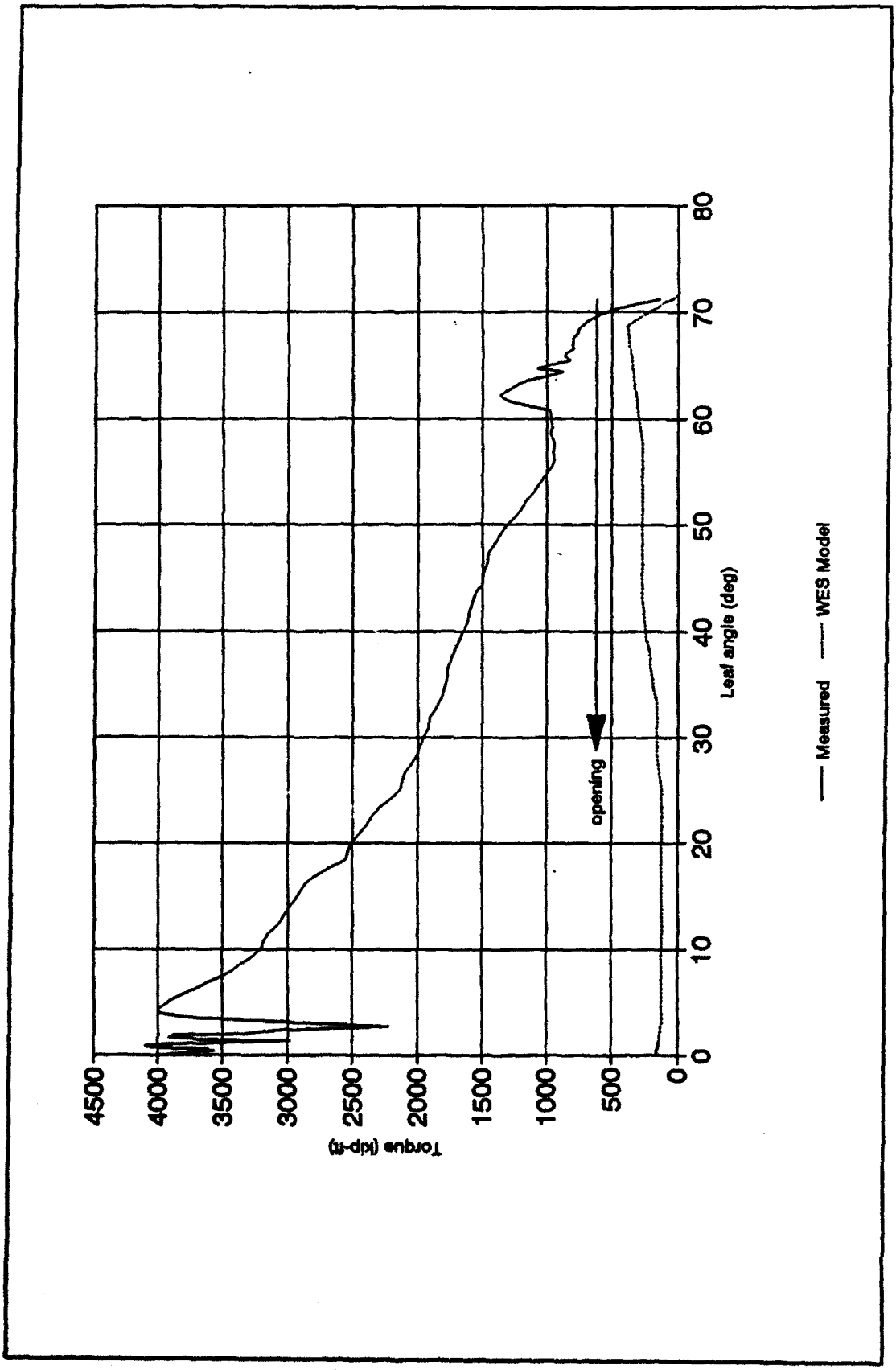

Figure B19. Gate operation opening test: pintle torque

Appendix C
Gate Operation Closing Test Data

Field Data

This appendix provides data obtained for the gate operation closing test. Figures C1-C16 graphically display the measured strain data as function of the leaf angle with respect to the lock wall. In Figures C1-C16, the data presented are labeled by the number of the corresponding transducer from which the data were recorded (See Figure 3 for location and numbering of transducers).

Pintle Torque Comparison with Model Studies

Figure C17 shows the operating strut force as a function of leaf angle calculated according to Equation B2 (negative force indicates compression in the operating strut). Figure C18 shows the comparison of the measured T, and that determined based on the WES model studies. (T was determined as described in Appendix B.) As opposed to the comparison for the opening test (see Figure B19), Figure C18 shows a very good comparison between the measured and WES model torque. Although there are some minor differences in magnitudes of T, the general trend in T through the range of leaf motion is very similar. A possible explanation for the significantly better comparison in T for closing is that, during opening, the presumed obstruction or silt buildup had been moved away from the bottom of the leaf. On closing (just after opening) the bottom of the leaf was clear of the obstruction.

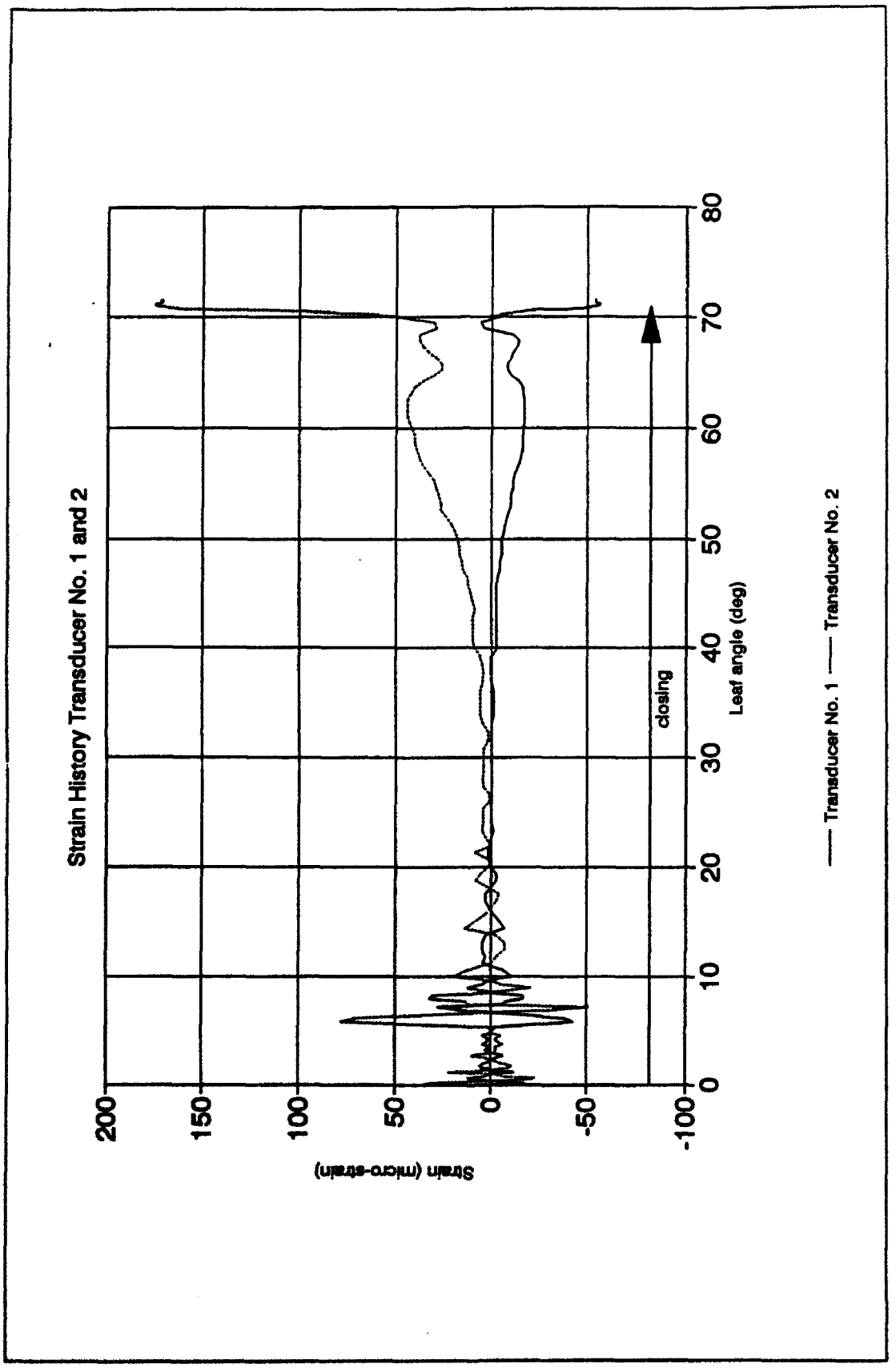

Figure C1. Gate operation closing test strain: G1 midspan

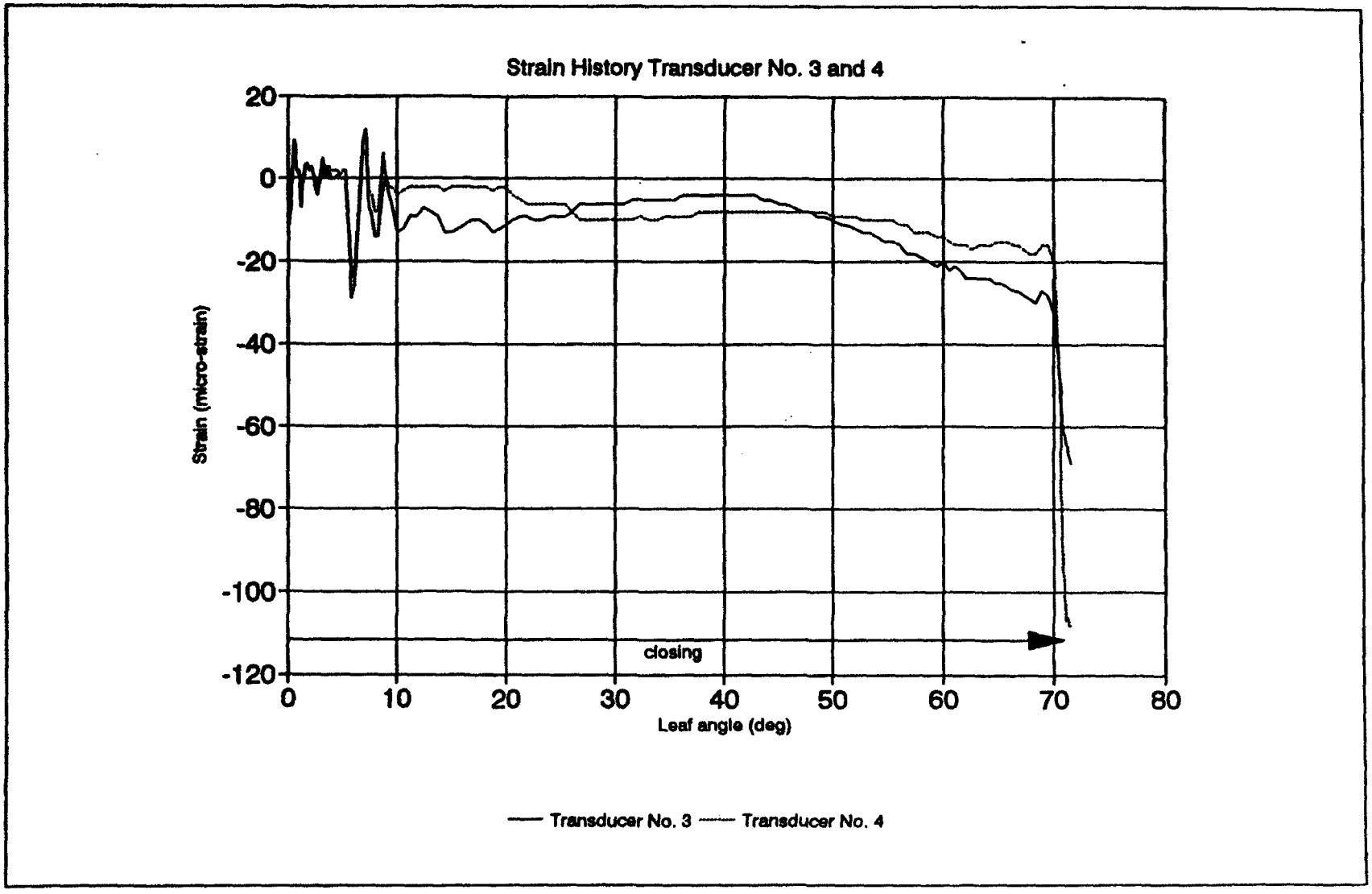

Figure C2. Gate operation closing test strain: operating strut

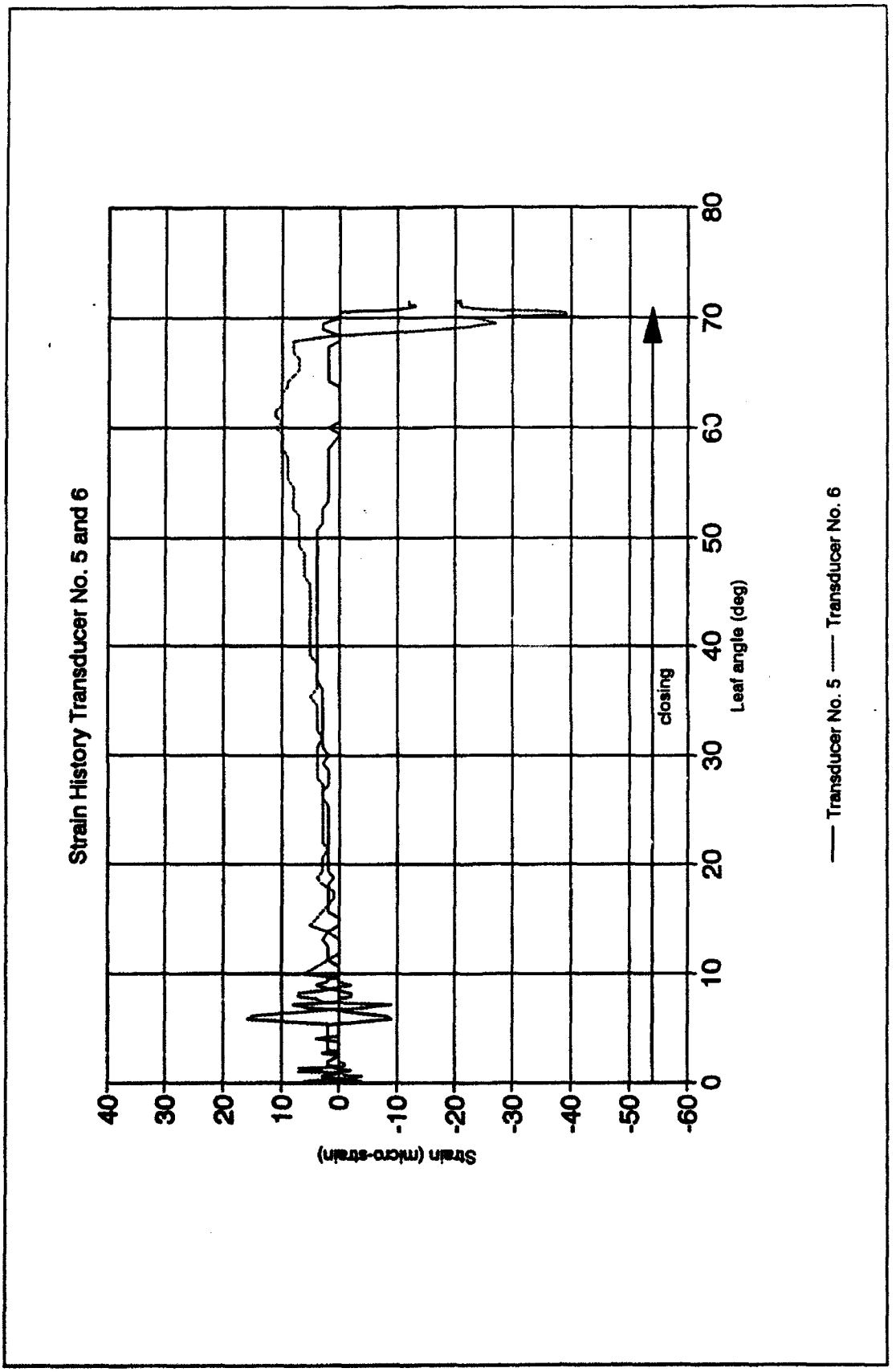

Figure C3. Gate operation closing test strain: G3 quoin end

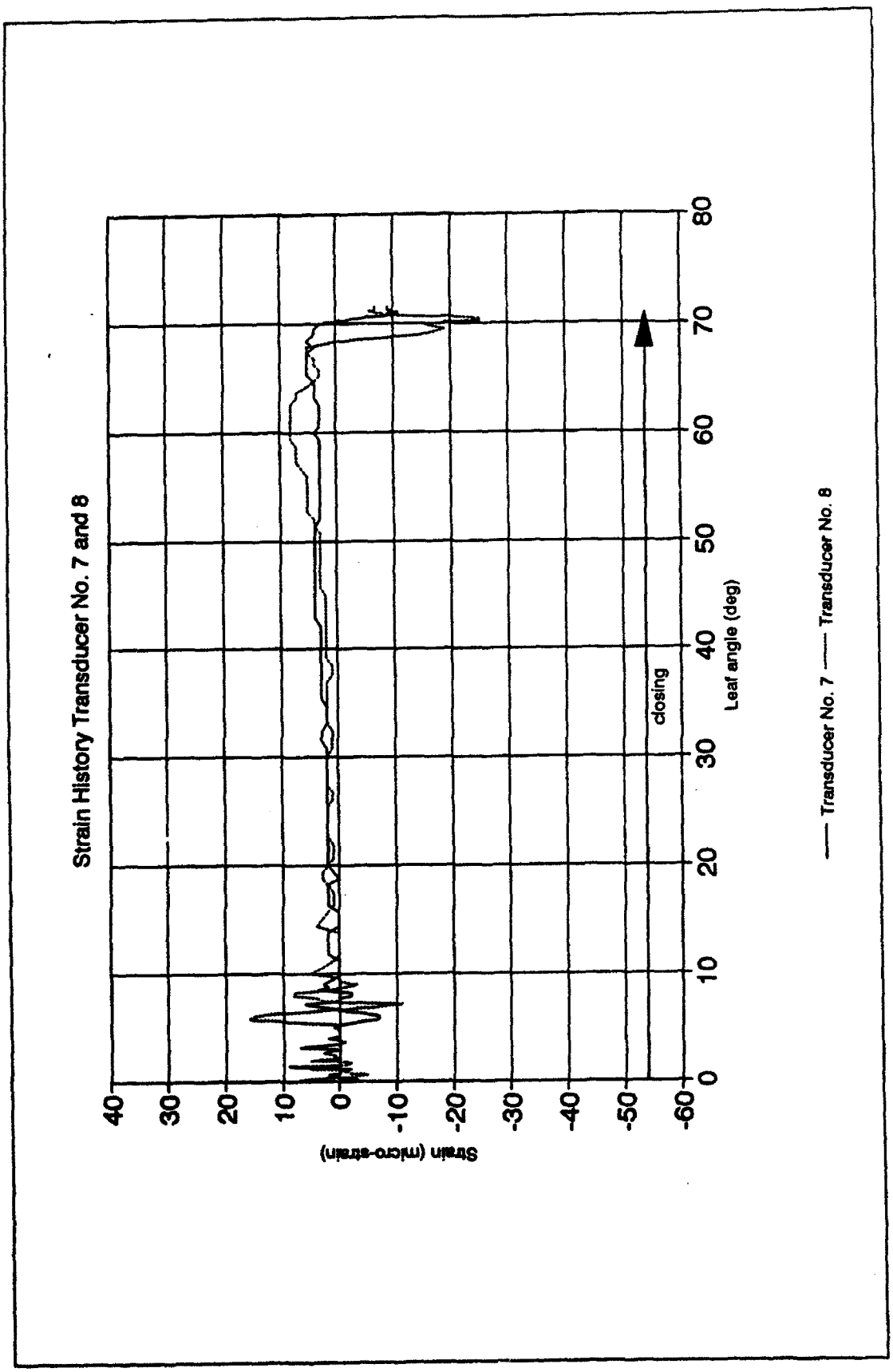

Figure C4. Gate operation closing test strain: G3 midspan

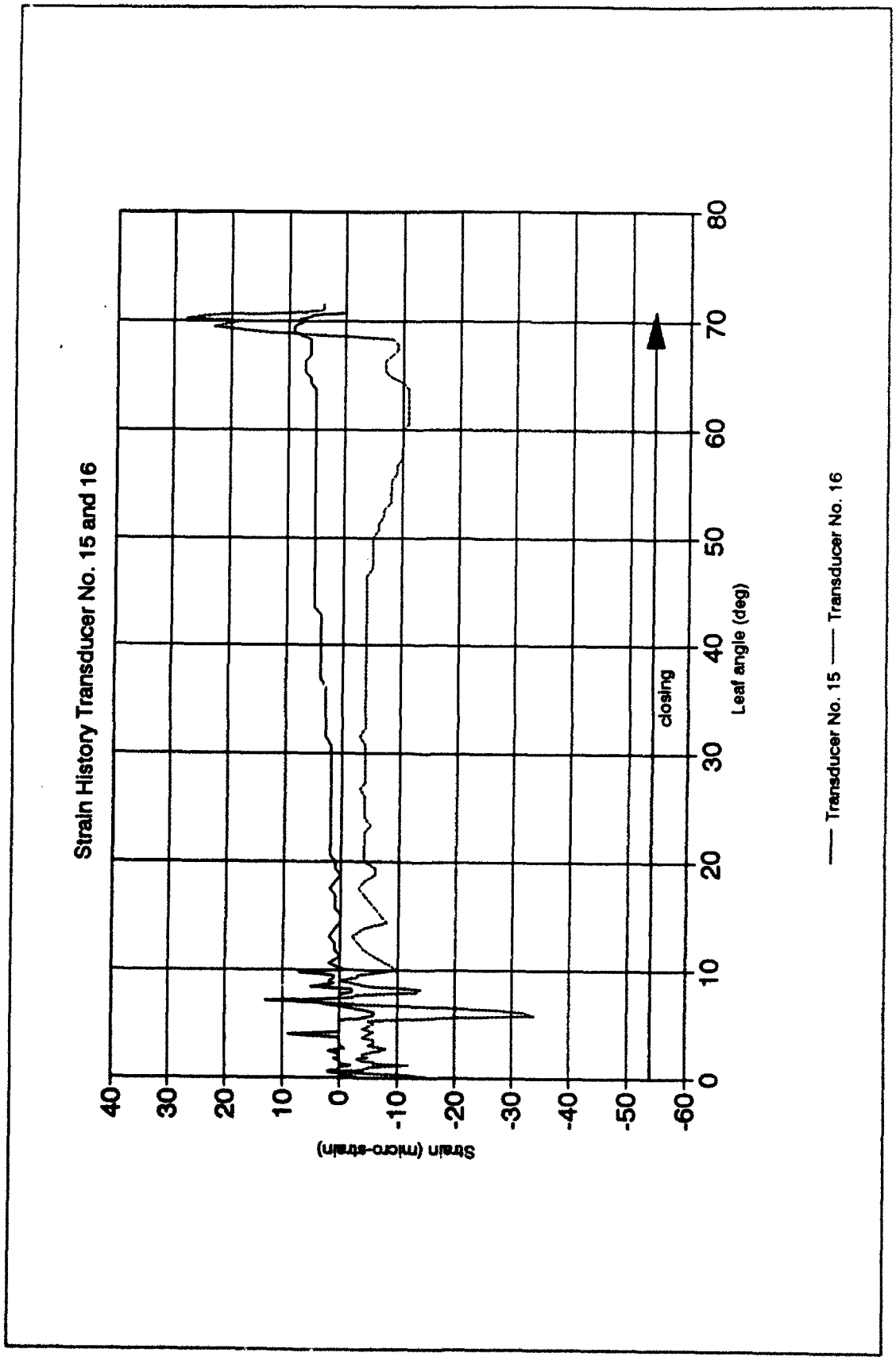

Figure C5. Gate operation closing test strain: G3 miter end

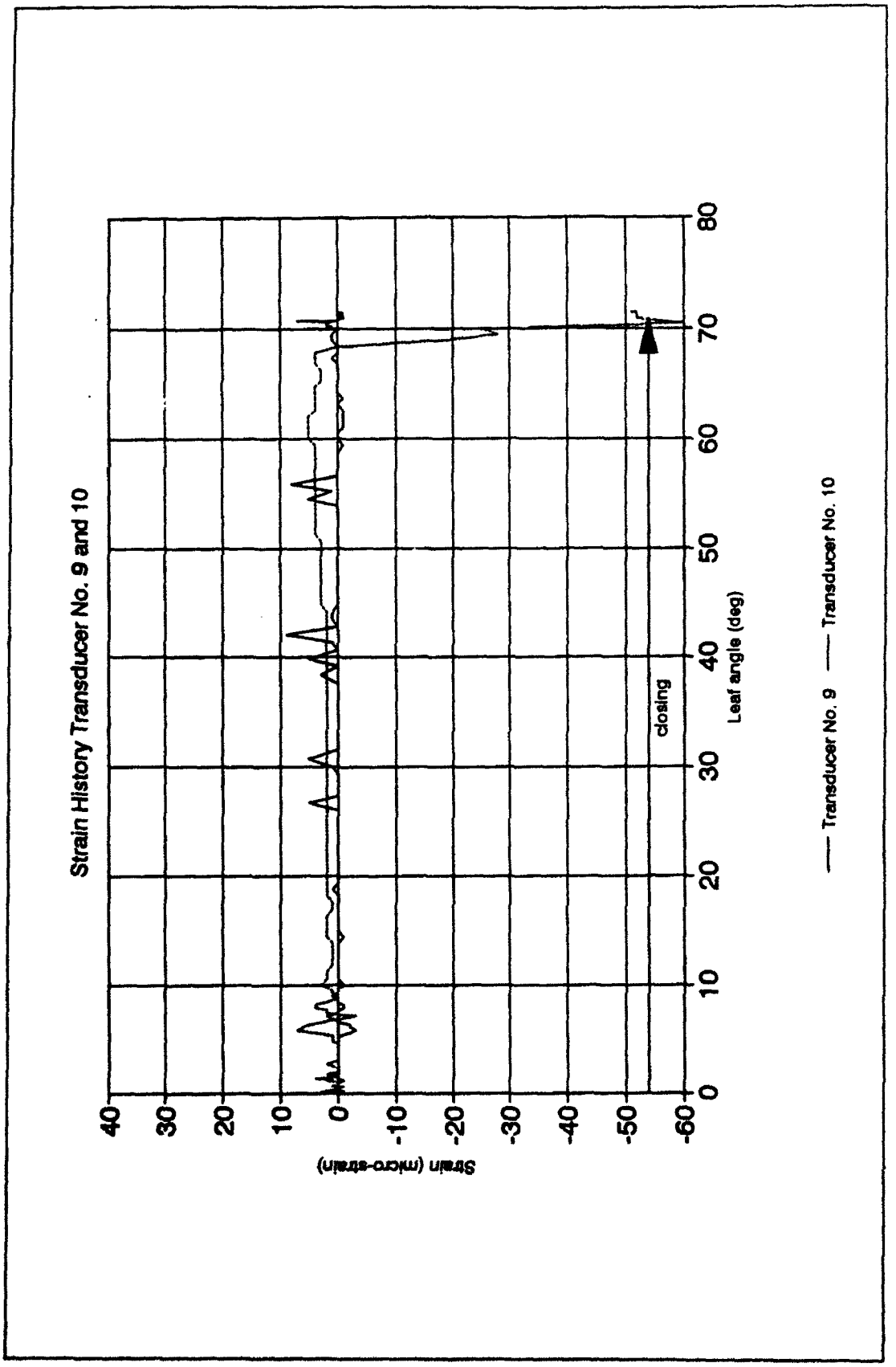

Figure C6. Gate operation closing test strain: G4 quoin end

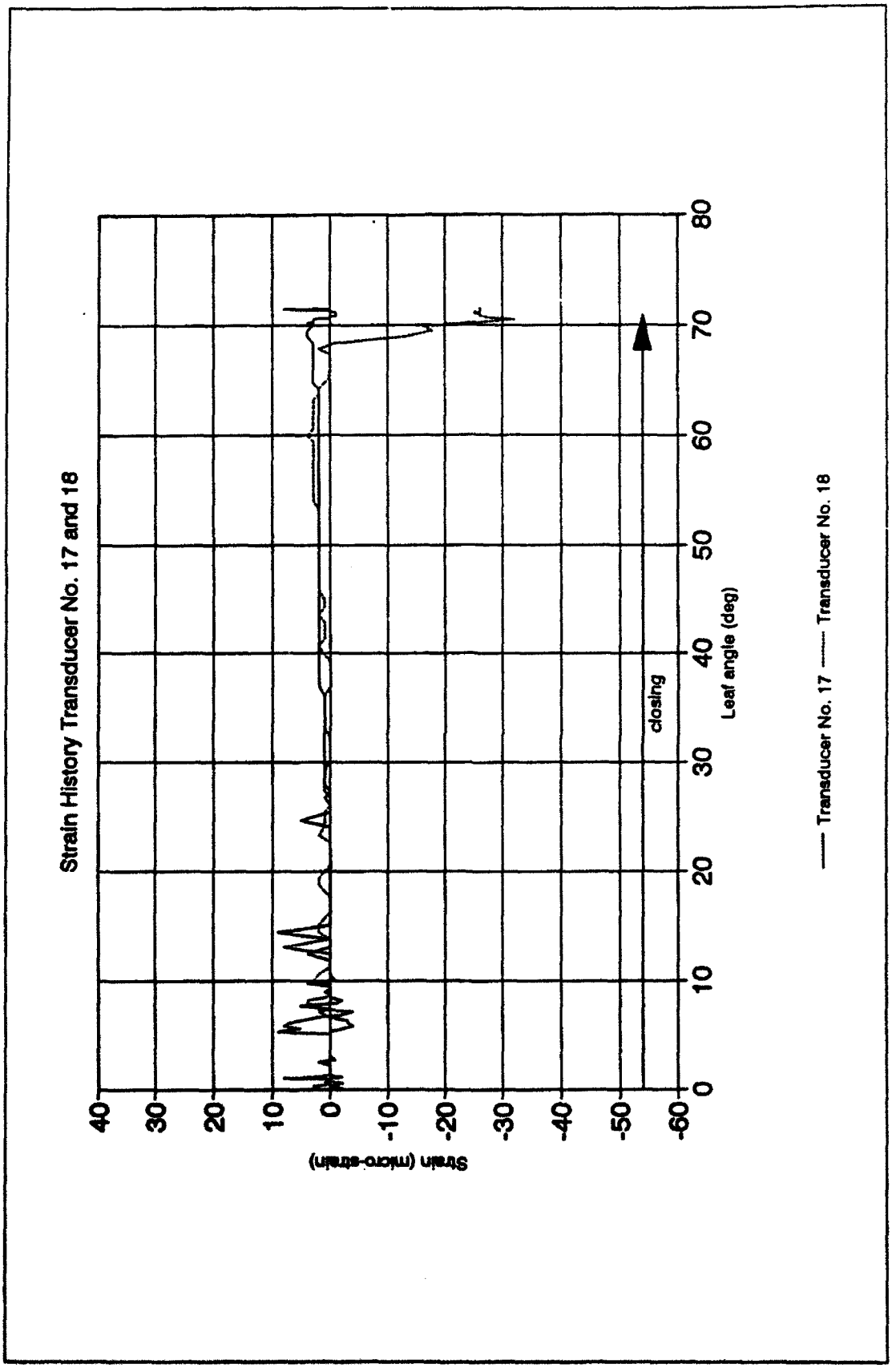

Figure C7. Gate operation closing test strain: G4 midspan

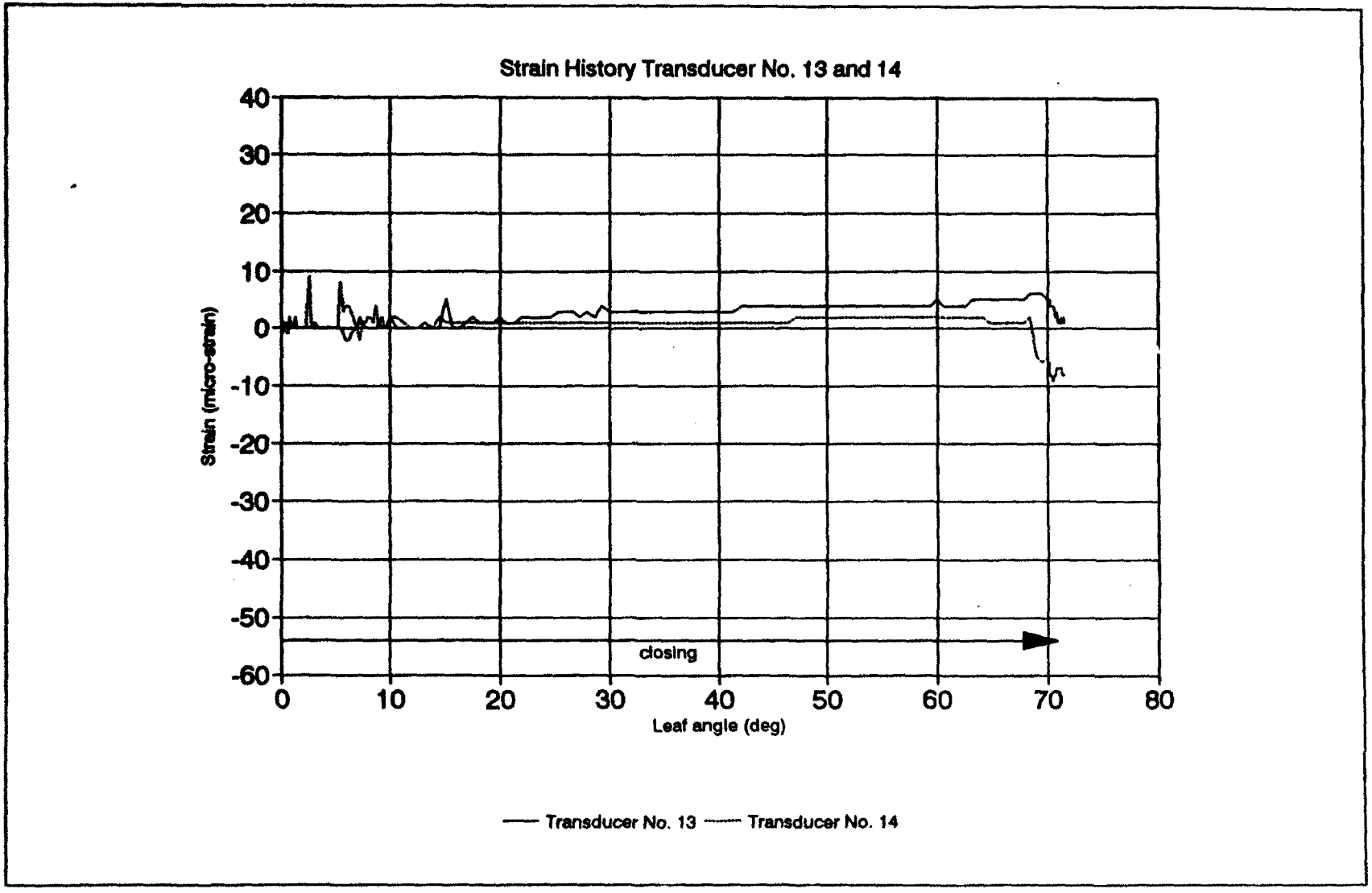

Figure C8. Gate operation closing test strain: G4 miter end

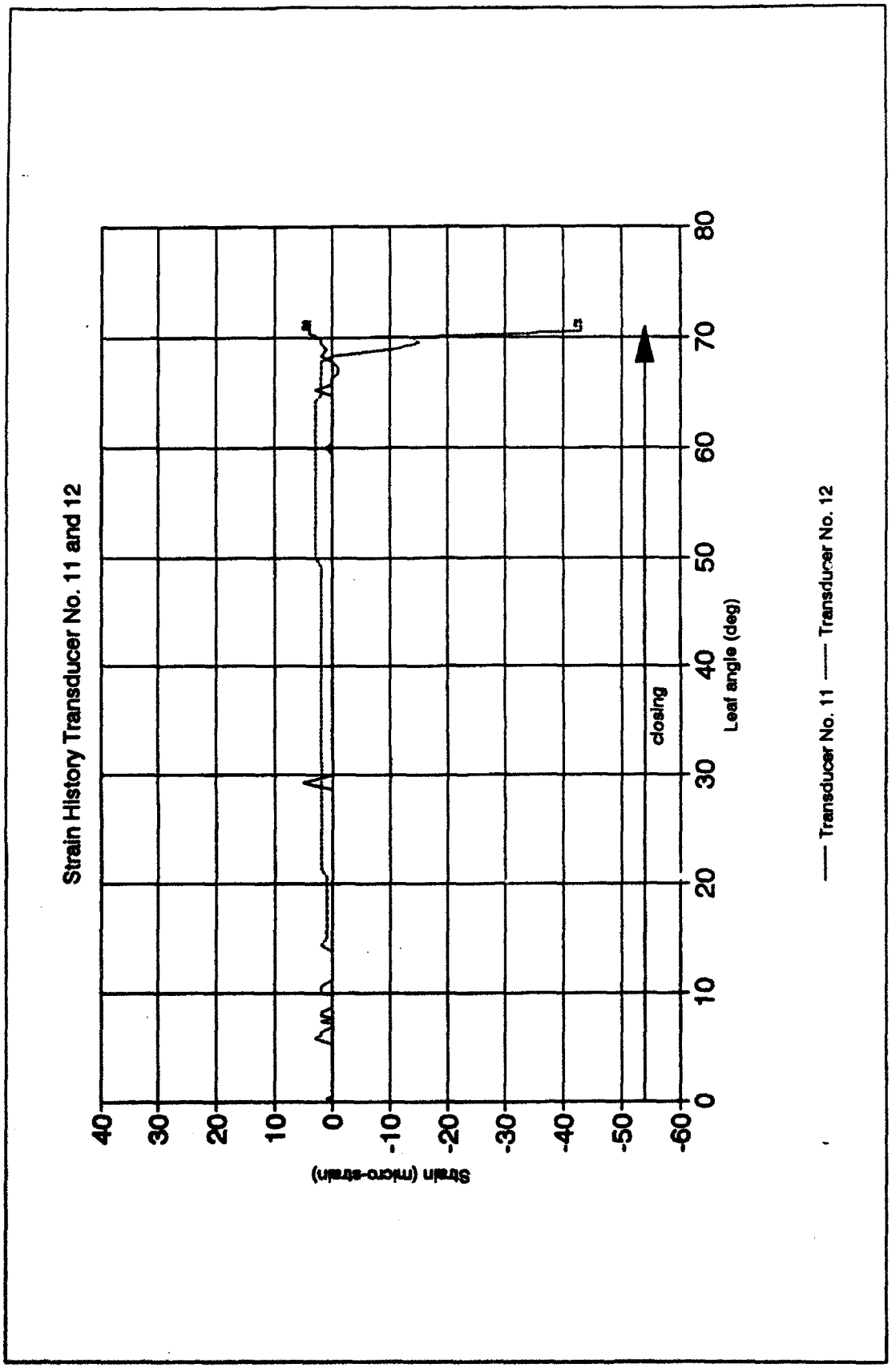

Figure C9. Gate operation closing test strain: G5 quoin end

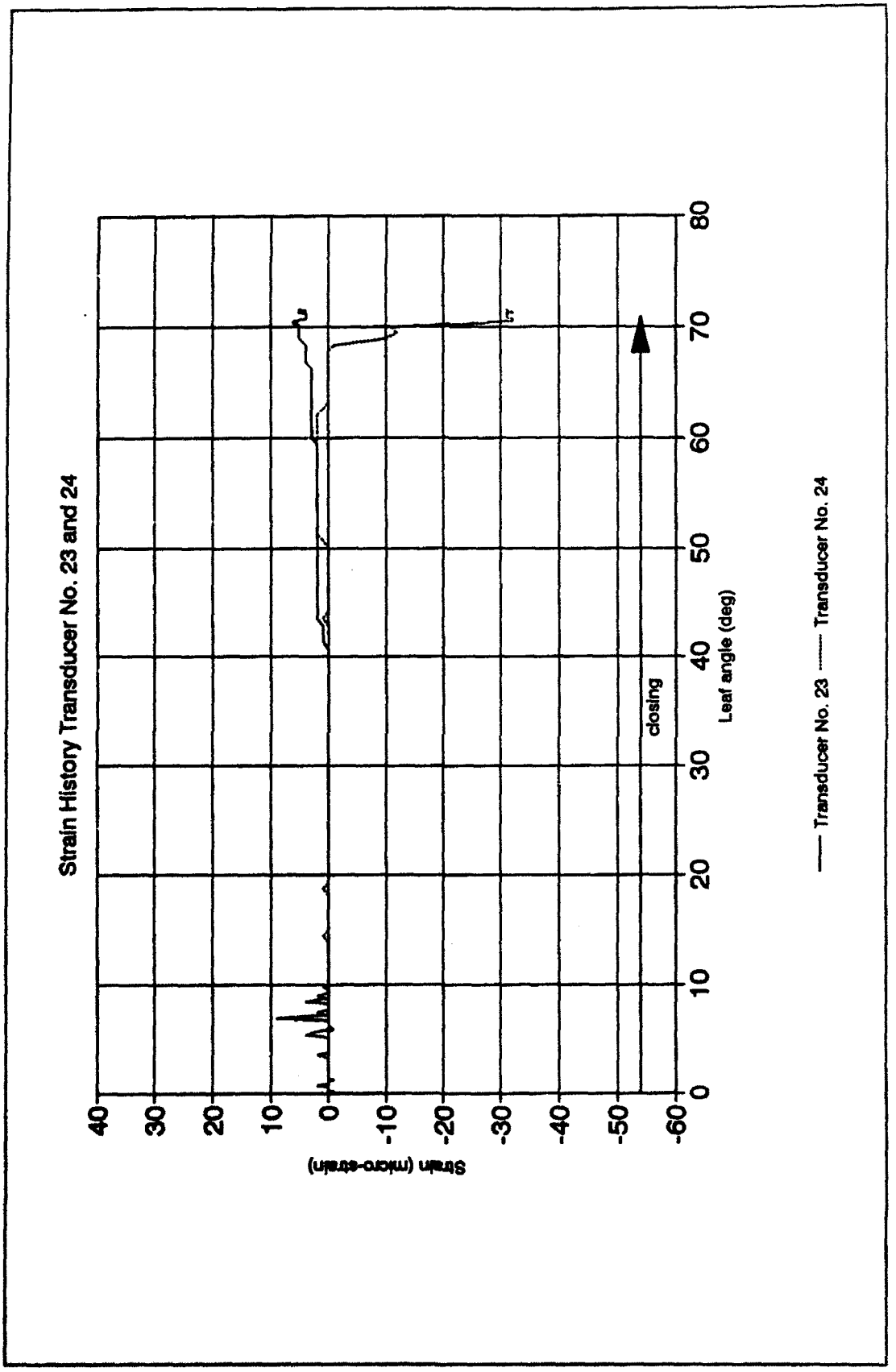

Figure C10. Gate operation closing test strain: G5 midspan

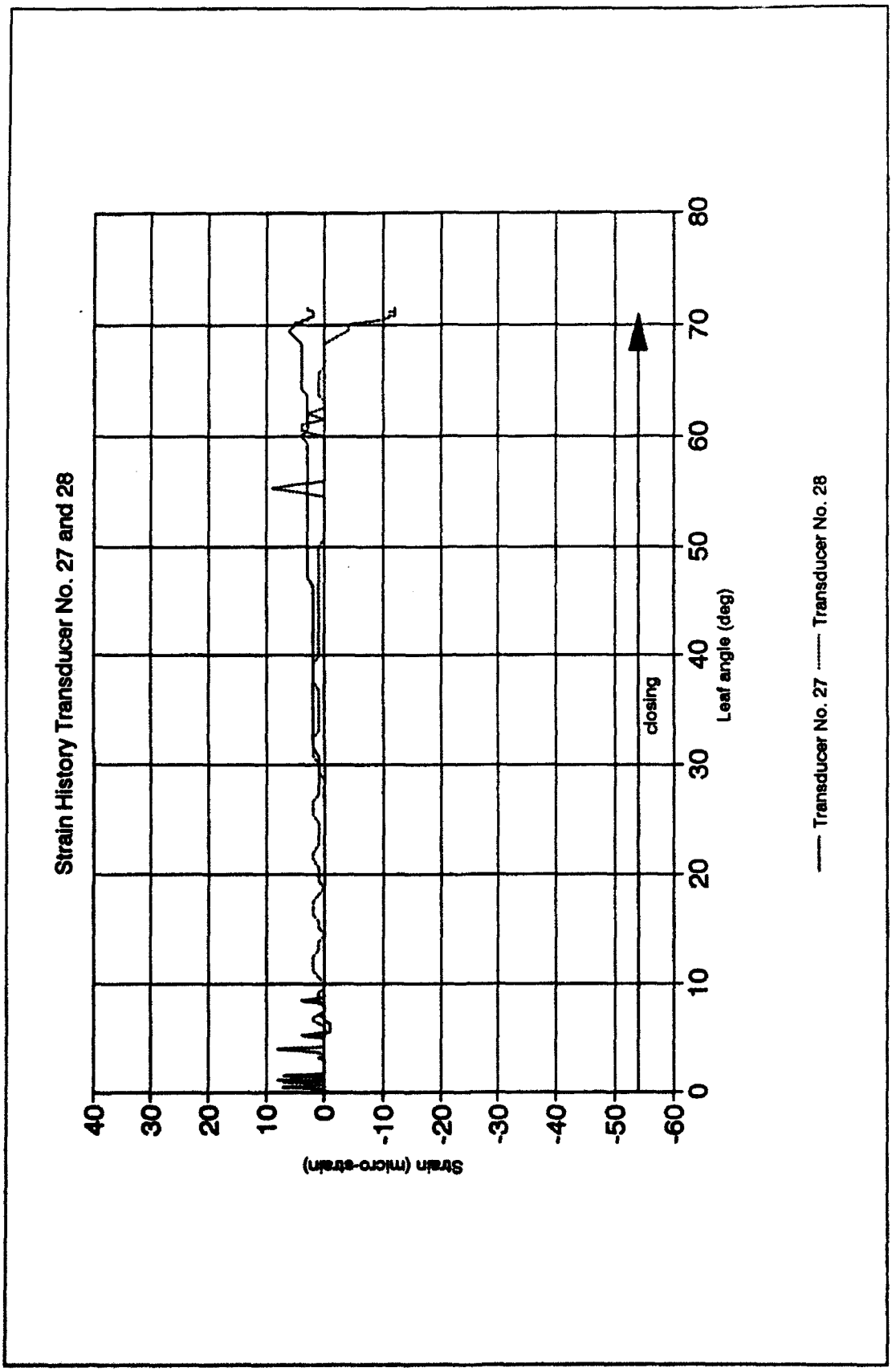

Figure C11. Gate operation closing test strain: G5 miter end

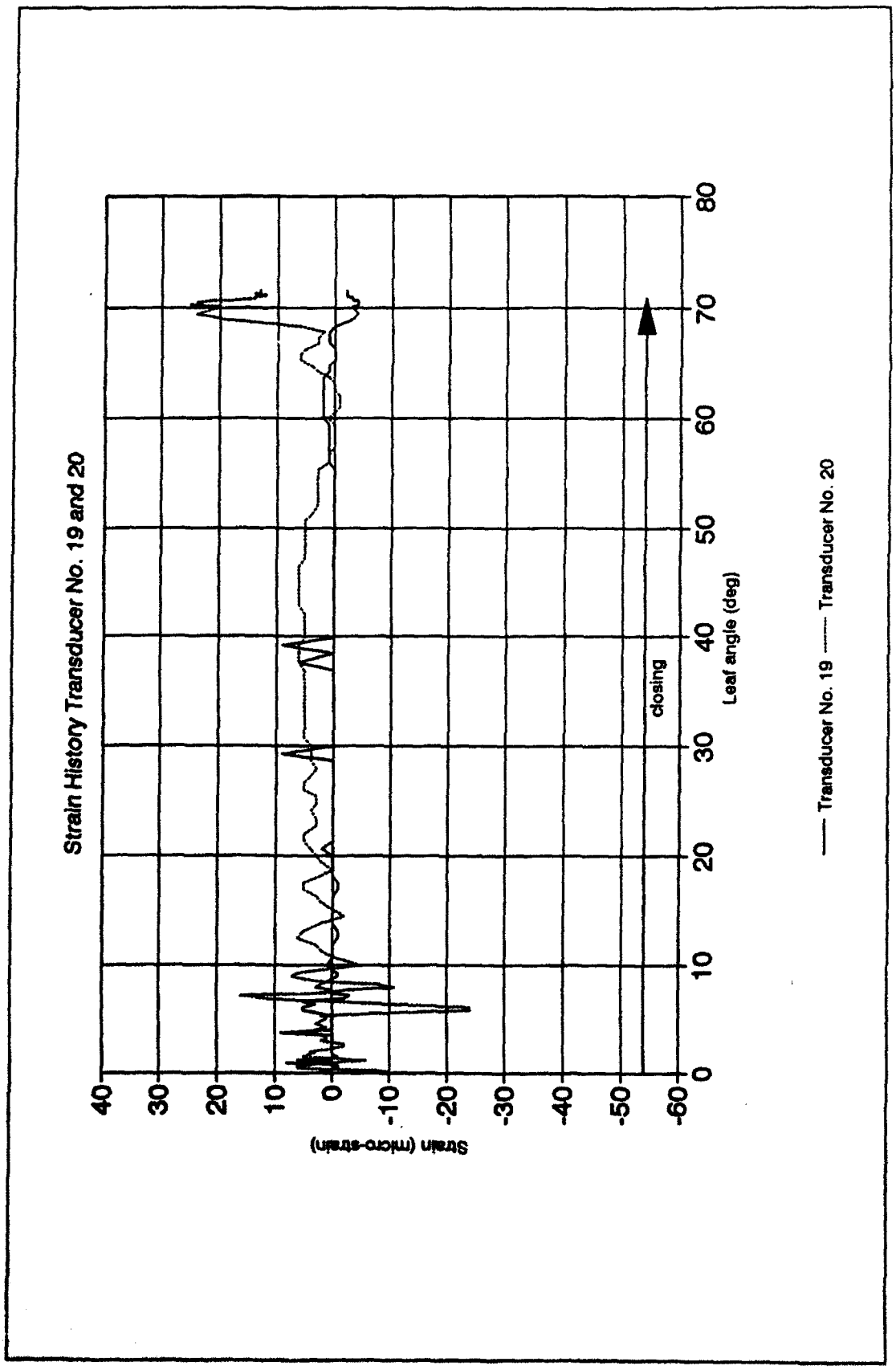

Figure C12. Gate operation closing test strain: diaphragm 3

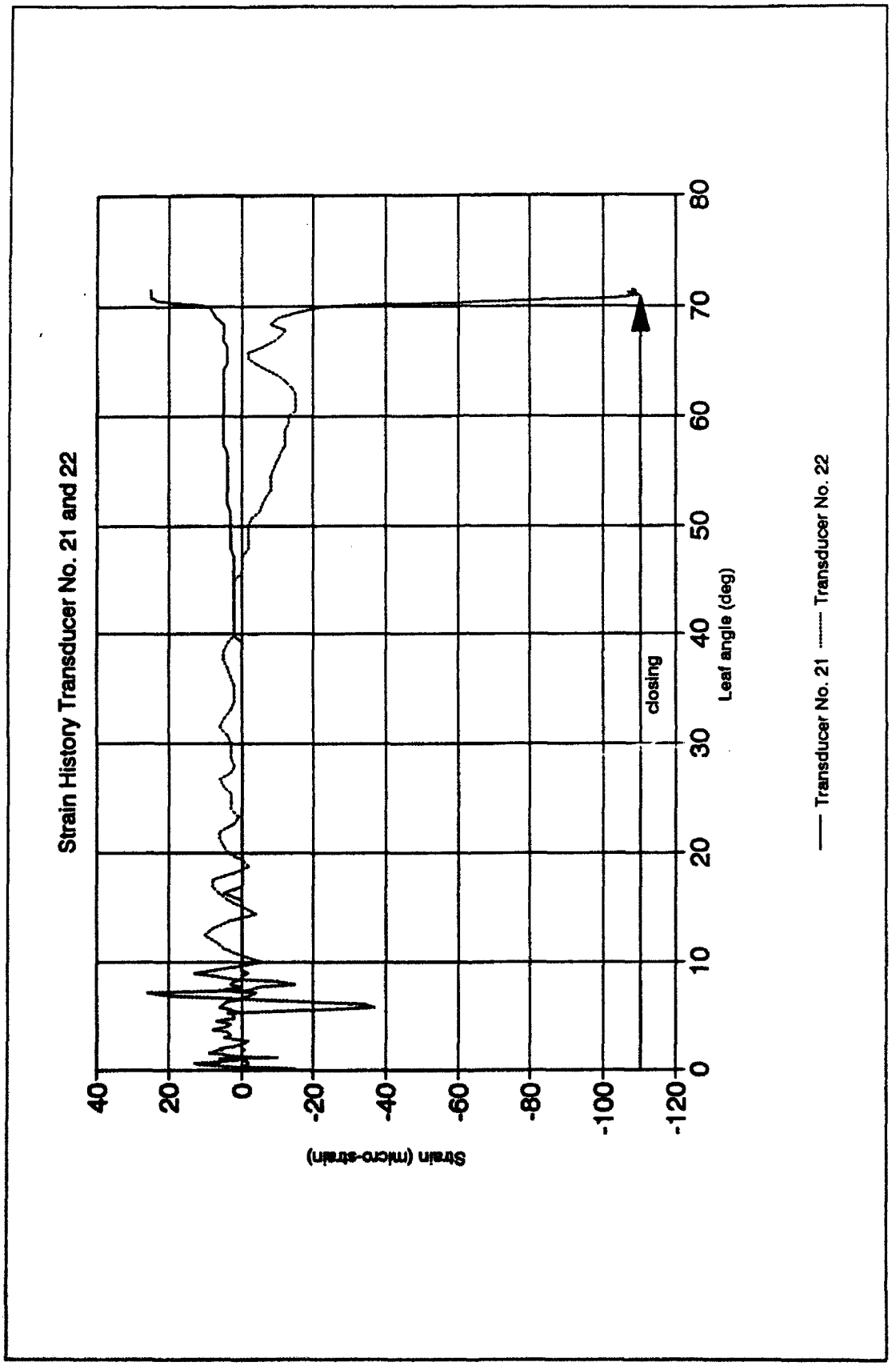

Figure C13. Gate operation closing test strain: diaphragm 2

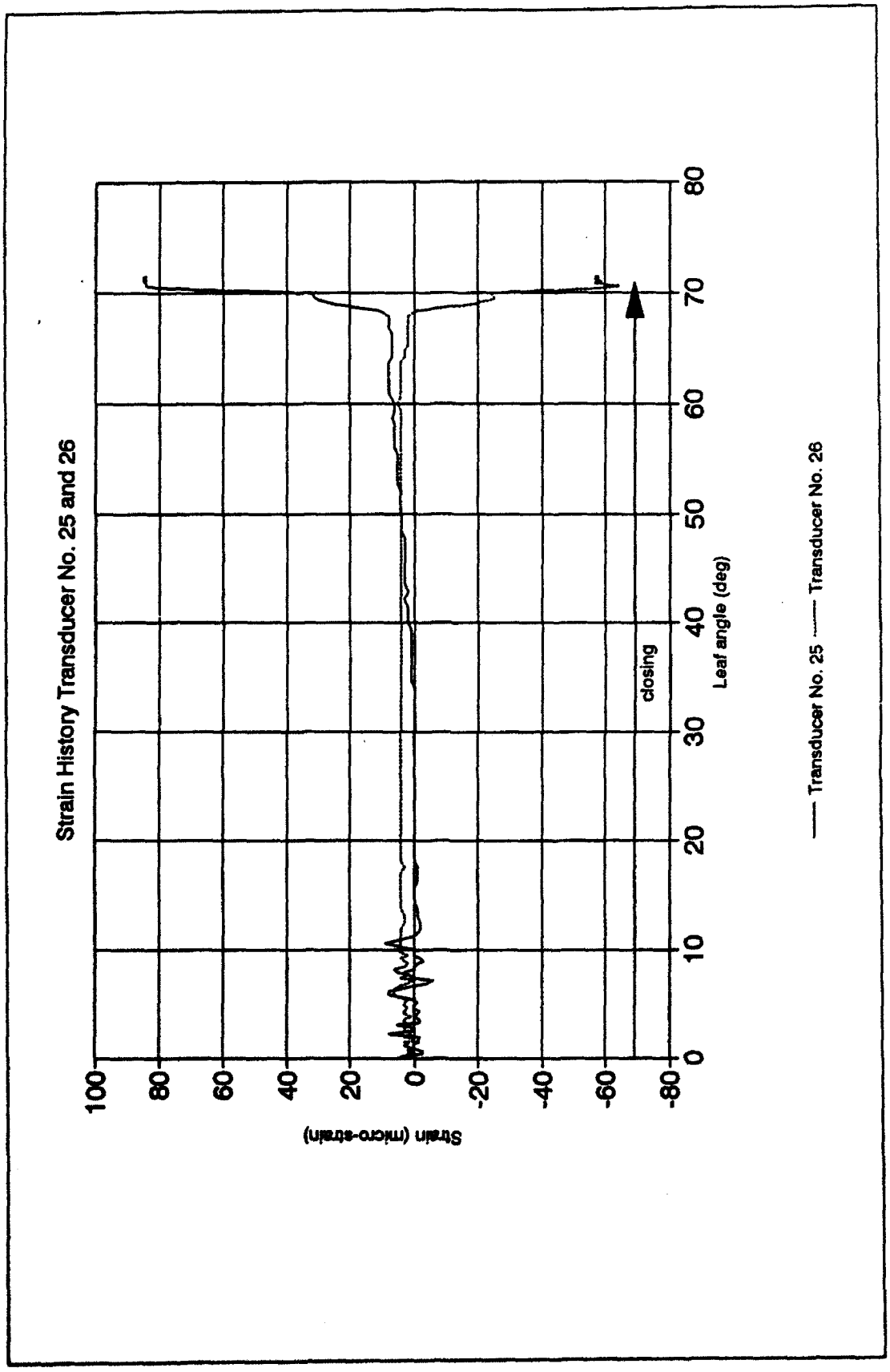

Figure C14. Gate operation closing test strain: diaphragm 1

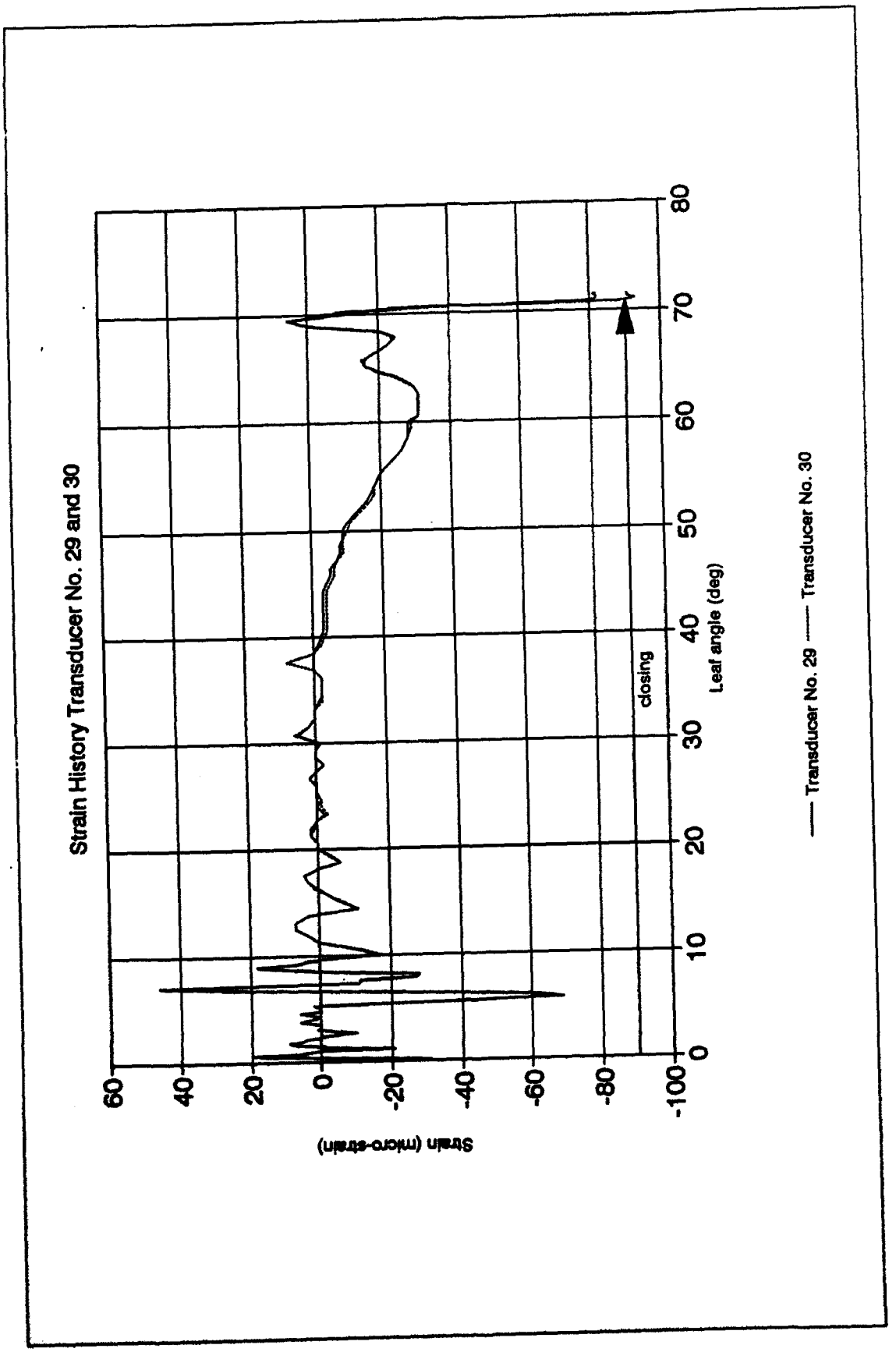

Figure C15. Gate operation closing test strain: diagonal 2

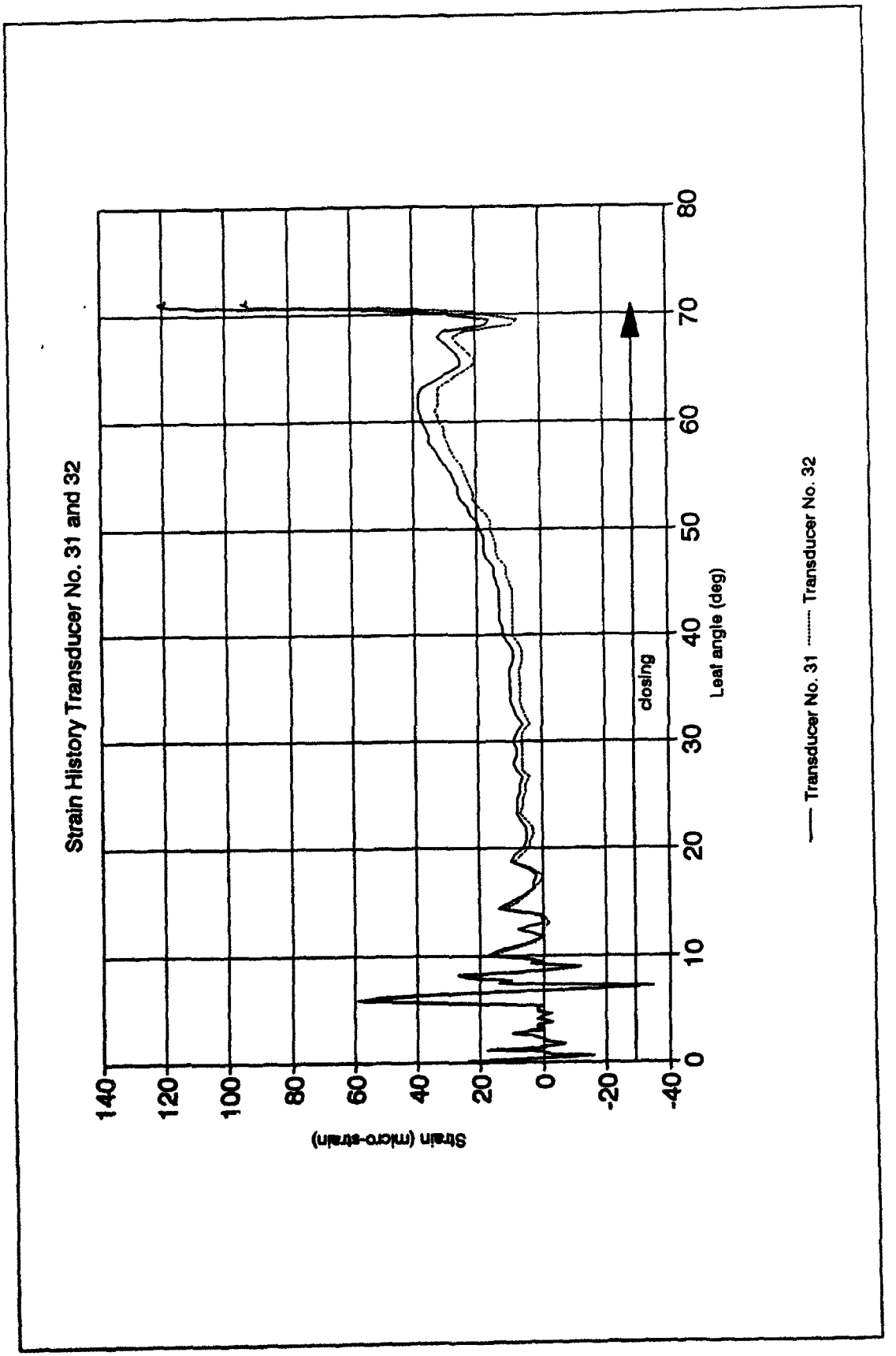

Figure C16. Gate operation closing test strain: diagonal 1

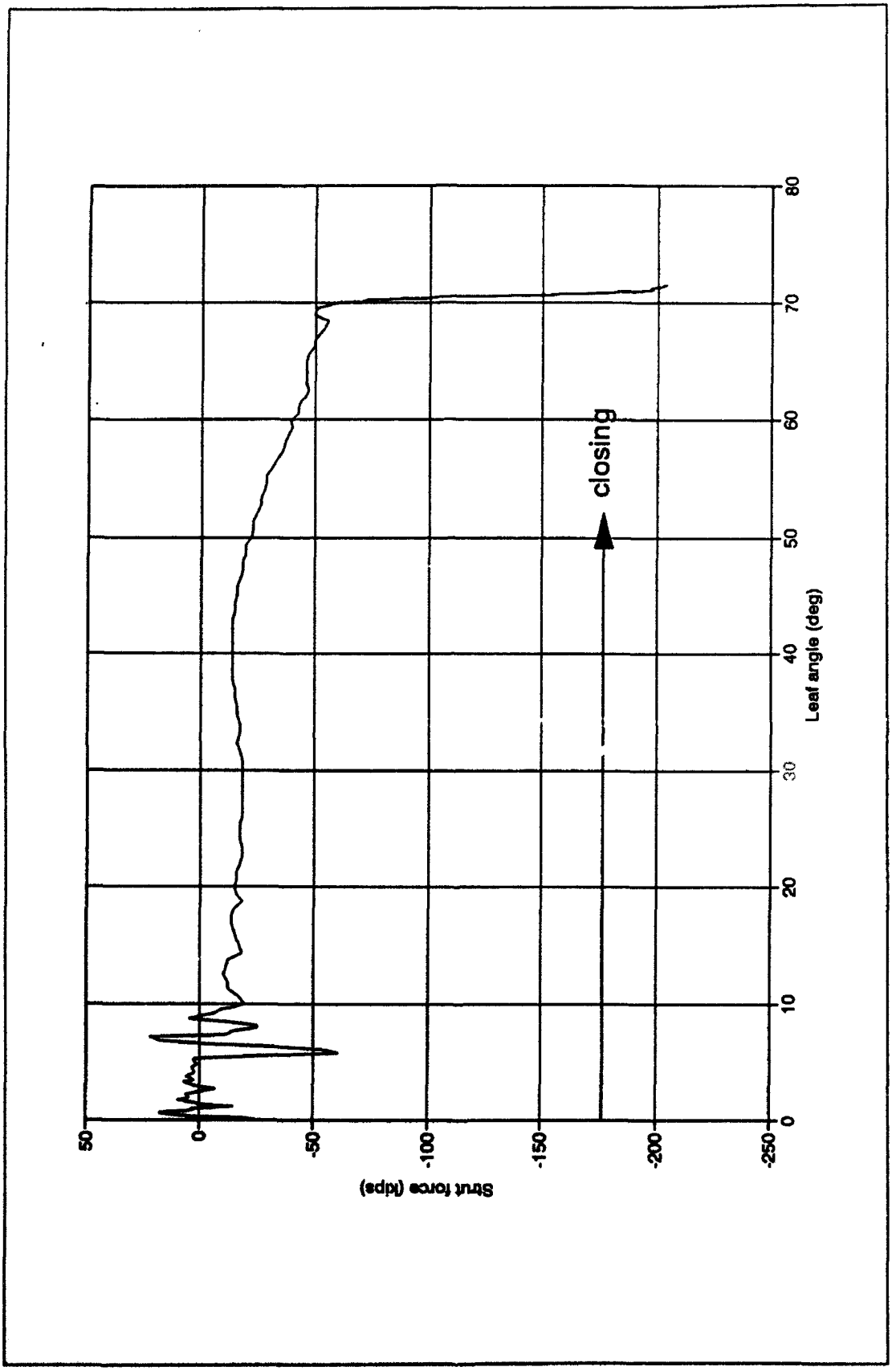

Figure C17. Gate operation closing test: operating strut force

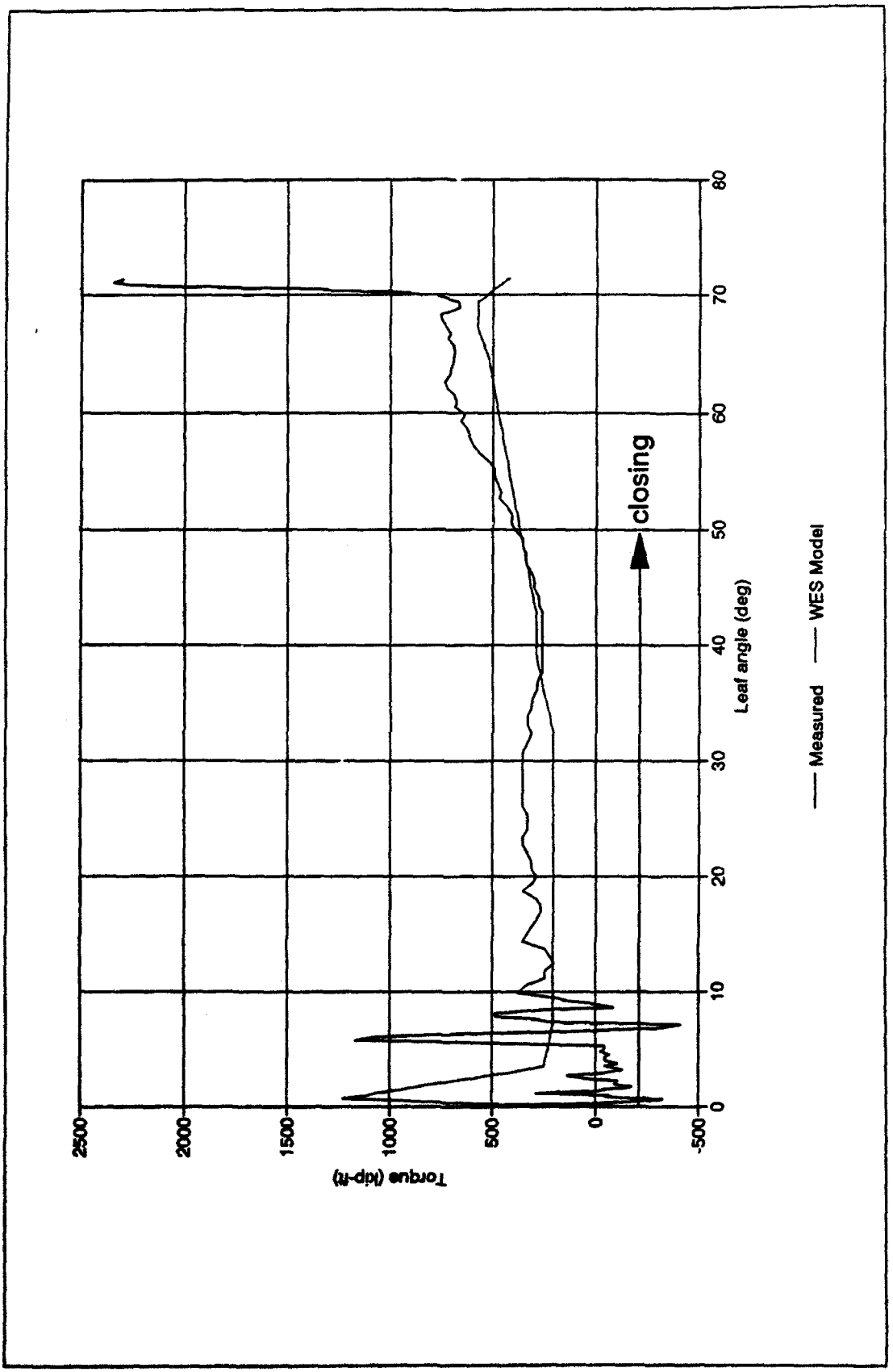

Figure C18. Gate operation closing test: pintle torque

REPORT DOCUMENTATION PAGE

Form Approved
OMB No 0704-0188

Public reporting burden for this collection of information is estimated to average 1 hour per response, including the time for reviewing instructions, searching existing data sources, gathering and maintaining the data needed, and completing and reviewing the collection of information. Send comments regarding this burden estimate or any other aspect of this collection of information, including suggestions for reducing this burden, to Washington Headquarters Services, Directorate for information Operations and Reports, 1215 Jefferson Davis Highway, Suite 1204, Arlington, VA 22202-4302, and to the Office of Management and Budget, Paperwork Reduction Project (0704-0188), Washington, DC 20503

1. AGENCY USE ONLY (Leave blank)	2. REPORT DATE	3. REPORT TYPE AND DATES COVERED
	August 1993	Report 4 of a series

4. TITLE AND SUBTITLE
Computer-Aided, Field-Verified Structural Evaluation;
Report 4, Field Test and Analysis Correlation at Red River Lock and Dam No. 1

5. FUNDING NUMBERS

6. AUTHOR(S)
Brett C. Commander, Jeff X. Schulz,
George G. Goble, Eric Hansen, Cameron P. Chasten

7. PERFORMING ORGANIZATION NAME(S) AND ADDRESS(ES)
Bridge Diagnostics, Inc.
5398 Manhattan Circle, Suite 280, Boulder, CO 80303;
U.S. Army Engineer Waterways Experiment Station
Information Technology Laboratory
3909 Halls Ferry Road, Vicksburg, MS 39180-6199

8. PERFORMING ORGANIZATION REPORT NUMBER
Technical Report
ITL-92-12

9. SPONSORING / MONITORING AGENCY NAME(S) AND ADDRESS(ES)
U.S. Army Corps of Engineers
Washington, DC 20314-1000

10. SPONSORING / MONITORING AGENCY REPORT NUMBER

11. SUPPLEMENTARY NOTES
Available from National Technical Information Service, 5285 Port Royal Road, Springfield, VA 22161

12a. DISTRIBUTION / AVAILABILITY STATEMENT
Approved for public release; distribution is unlimited.

12b. DISTRIBUTION CODE

13. ABSTRACT *(Maximum 200 words)*

The project entitled "Computer-Aided, Field-Verified Structural Evaluation" is an effort in which analytical and experimental methods are combined to form a unique structural evaluation system. As part of this project, this technical report describes experimental and analytical studies that were conducted for a horizontally framed miter gate leaf at Red River Lock and Dam No. 1 located in Catahoula Parish, Louisiana.

Strain was measured at various locations on the leaf while the leaf was subjected to two loading conditions consisting of hydrostatic head differential and gate leaf operation. Due to a low level of head differential at the time of testing, the miter ends of some girders were not supported by corresponding girders on the opposite leaf throughout the range of loading. This resulted in a boundary condition at the miter end that was not consistent with design assumptions, and an accurate model to represent behavior for the low range of loading was not achieved. However, the value of systematically comparing experimental and analytical data was demonstrated. Through examination of the experimental data and comparison with analytical data, the inconsistent boundary condition was identified and its effect on structural behavior was determined. In addition to discussion of the head differential loading, operating forces measured during the gate leaf operation tests are compared with predictions based on scale model studies conducted at the U.S. Army Engineer Waterways Experiment Station in 1964.

14. SUBJECT TERMS

Analytical model	Miter gate leaf
Eccentricity	Strain
Grid	Stress

15. NUMBER OF PAGES
80

16. PRICE CODE

17. SECURITY CLASSIFICATION OF REPORT	18. SECURITY CLASSIFICATION OF THIS PAGE	19. SECURITY CLASSIFICATION OF ABSTRACT	20. LIMITATION OF ABSTRACT
UNCLASSIFIED	UNCLASSIFIED		